ALMA MATER STUDIORUM – UNIVERSITÀ DI BOLOGNA

PhD Program in Cellular Molecular and Industrial Biology

Program n. 2: Functional Biology of Cellular and Molecular systems

XXII Cycle

Scientific area code BIO/11

MOLECULAR ARCHITECTURE OF FUR BINDING TO IRON-INDUCED AND -REPRESSED GENES IN *Helicobacter pylori*

PhD candidate: Francesca Agriesti

PhD Program Coordinator:

Prof. **Vincenzo Scarlato**

Tutors:

Prof. **Vincenzo Scarlato**

Dott. **Alberto Danielli**

FINAL EXAM 2010

ABSTRACT

The ferric uptake regulator protein Fur regulates iron-dependent gene expression in bacteria. In the human pathogen *Helicobacter pylori*, Fur has been shown to regulate iron-induced and iron-repressed genes. Herein we investigate the molecular mechanisms that control this differential iron-responsive Fur regulation. Hydroxyl radical footprinting showed that Fur has different binding architectures, which characterize distinct operator typologies. On operators recognized with higher affinity by *holo*-Fur, the protein binds to a continuous AT-rich stretch of about 20 bp, displaying an extended protection pattern. This is indicative of protein wrapping around the DNA helix. DNA binding interference assays with the minor groove binding drug distamycin A, point out that the recognition of the *holo*-operators occurs through the minor groove of the DNA.

By contrast, on the *apo*-operators, Fur binds primarily to thymine dimers within a newly identified $TCATT_{n10}TT$ consensus element, indicative of Fur binding to one side of the DNA, in the major groove of the double helix. Reconstitution of the $TCATT_{n10}TT$ motif within a *holo*-operator results in a feature binding swap from an *holo*-Fur- to an *apo*-Fur-recognized operator, affecting both affinity and binding architecture of Fur, and conferring *apo*-Fur repression features *in vivo*.

Size exclusion chromatography indicated that Fur is a dimer in solution. However, in the presence of divalent metal ions the protein is able to multimerize. Accordingly, apo-Fur binds DNA as a dimer in gel shift assays, while in presence of iron, higher order complexes are formed. Stoichiometric Ferguson analysis indicates that these complexes correspond to one or two Fur tetramers, each bound to an operator element.

Together these data suggest that the *apo*- and *holo*-Fur repression mechanisms apparently rely on two distinctive modes of operator-recognition, involving respectively the readout of a specific nucleotide consensus motif in the major groove for *apo*-operators, and the recognition of AT-rich stretches in the minor groove for *holo*-operators, whereas the iron-responsive binding affinity is controlled through metal-dependent shaping of the protein structure in order to match preferentially the major or the minor groove.

CONTENTS

INTRODUCTION

1. *Helicobacter pylori*

1.1 Epidemiology and infection

Helicobacter pylori is a gram-negative, spiral shaped, microaerophilic bacterial pathogen (Fig. 1), which colonizes the mucosal layer overlying the gastric epithelium of the human stomach. Isolated in 1982 by Robin Warren and Barry Marshall, it is recognized as the principal causative agent of chronic active gastritis (Blaser, 1990), as well as gastric and peptic ulcer diseases (Nomura *et al.*, 1994), and is associated with the development of B-cell mucosa-associated lymphoid tissue lymphoma and gastric adenocarcinoma (Peek *et al.*, 2002, Du *et al.*, 2002, Parsonnet *et al.*, 1994).

Fig. 1 Electron micrograph of *Helicobacter pylori*. *H.pylori* in vivo and under optimum in vitro conditions is an S-shaped bacterium with 1 to 3 turns, 0.5 ×5 µm in length, with a tuft of 5 to 7 polar sheathed flagella. Field emission SEM, bar = 0.5 µm. Image form (Mobley *et al.*, 2001).

While the infection is chronic and often asymptomatic, this bacterium infects over 50% of the world's population (Dunn *et al.*, 1997). The sheer number of infected individuals leads to a significant number of *H. pylori*-associated diseases cases each

year, worldwide. Moreover, since colonization usually occurs early in childhood and remains throughout the person's life if the infection is not treated with antibiotics (Blaser, 1990, de Reuse *et al.*, 2007), the chronicity increases the likelihood of disease. For these reasons *H. pylori* is considered an important public health problem with serious economic consequences and the World Health Organization has classified the organism as a class 1 carcinogen in 1994 (Bouvard *et al.*, 2009).

After initial infection, *H. pylori* rapidly reaches to the gastric mucosa layer in close contact with epithelial cells (Josenhans *et al.*, 2007). There, the bacterium is continuously faced with harsh physiological conditions such as mild to strong acidity, fluctuating nutrient, availability and osmolarity, oxygen tension and a vigorous host immune response. Therefore, *H. pylori* produces a number of factors to cope with changes in the micro-environment and the host response (van Vliet *et al.*, 2001a). Several factors that facilitate its survival, such as flagellins (Suerbaum *et al.*, 1993) and urease (Cussac *et al.*, 1992), and that are associated with pathogenesis, like the *cag* pathogenicity island (Covacci *et al.*, 1993) and the vacuolating toxin (Telford *et al.*, 1994, Cover *et al.*, 1994), have been extensively studied, and significant advances regarding the regulation of these factors have been made (Akada *et al.*, 2000, Joyce *et al.*, 2001).

H. pylori infections can be successfully cured with antibiotic treatment, associated with a proton pump inhibitor (Megraud *et al.*, 2003). Unfortunately, the available antimicrobial therapies are beginning to lose efficacy principally because of insurgence of antibiotic resistance, which frequently emerges de novo in *H. pylori*. Altered expression of gene products sensitive to antibiotic treatment seems to be especially important for resistance to penicillins and especially nitrimidazoles, the most common form of resistance encountered in *H. pylori* (Gerrits *et al.*, 2006). However, because it would be unrealistic to use antimicrobial therapies to eradicate an infection that affects 50% of the world population, it remains necessary to explore and identify both bacterial and host markers to diagnose individuals at high risk for the most severe infection outcomes, as well as to develop new effective therapeutic strategies. For these reasons, *H. pylori* remains a bacterial pathogen of major medical importance. This was acknowledged by the Nobel Price for Medicine in 2005 to Warren and Marshal who first discovered the bacterium (Marshall *et al.*, 1984).

1.2 Genome and regulatory functions

The complete genomic sequence of four *H. pylori* strains derived from unrelated clinical isolated are currently available [Hp 26695, (Tomb *et al.*, 1997); Hp J99, (Alm *et al.*, 1999); HpAG1, (Oh *et al.*, 2006) and HpG27, (Baltrus *et al.*, 2009)]. Although *H. pylori* was believed to exhibit a large degree of genomic and allelic diversity, the overall genomic organization, gene order and predicted gene products of these strains were found to be remarkably similar (Alm *et al.*, 1999).

The *H. pylori* genome is 1600 kb long and contains approximately 1500 open reading frames (ORFs) of which 60% were similar to genes of known function and could, therefore, be designated a putative identification, 18% showed similarity to genes that are conserved throughout other bacteria but do not have a known function and 23% were specific to *H. pylori* (Alm *et al.*, 1999, Scarlato *et al.*, 2001).

One of the most striking features of the *H.pylori* genome is the singular paucity of transcription factor and regulatory protein predicted (Scarlato *et al.*, 2001, Tomb *et al.*, 1997). Analysis of genome led to the identification of only 32 gene products classified as having a possible regulatory function of which only 17 are predicted to have a role in the regulation of transcription (Fig. 2). This is approximately half the number of those reported for *H. influenzae,* which has a genome of comparable size to *H. pylori* and less than a quarter to those predicted for *E. coli*. In addition, only one-third of the number of two-component regulatory systems of *E. coli* are present in *H. pylori* which possesses only four sensor proteins and seven response regulators (Tomb *et al.*, 1997).

The low abundance of regulators is consistent with a small genome, where transcription factors have been lost due the absence of selective pressure (Madan Babu *et al.*, 2006), reflecting the reductive evolution of this pathogen, which has been attributed to a constrained gastric habitat and the absence of other competitive microrganisms in this hostile environment (de Reuse *et al.*, 2007).

There is, however, evidence that *H. pylori* uses other mechanisms of regulation. These include slipped-strand mispairing within genes (Josenhans *et al.*, 2007) and in putative promoter regions (Alm *et al.*, 1999) and methylation by its nine type II methyltransferases (Marais *et al.*, 1999). Until this moment, little was known regarding posttranscriptional or translational control in *H. pylori*, even if evidence from two-

dimensional gel electrophoresis analysis has suggested that these exist (Laub *et al.*, 2000). However, a recent work reported a map of the primary trascriptome of *H. pylori* that reveals an unexpected complex RNA output from this small and compact genome. Accordingly, 60 small RNAs including the ε-subdivision counterpart of the regulatory 6S RNA and associated RNA products and potential regulators of *cis*- and *trans*-encoded target messenger RNAs has been identified (Sharma *et al.*, 2010).

Finally, the *H. pylori* genome does not have extensive operon structure. For example, the flagellar regulon is not contained in operons in this organism, which further confounds the apparent lack of regulation.

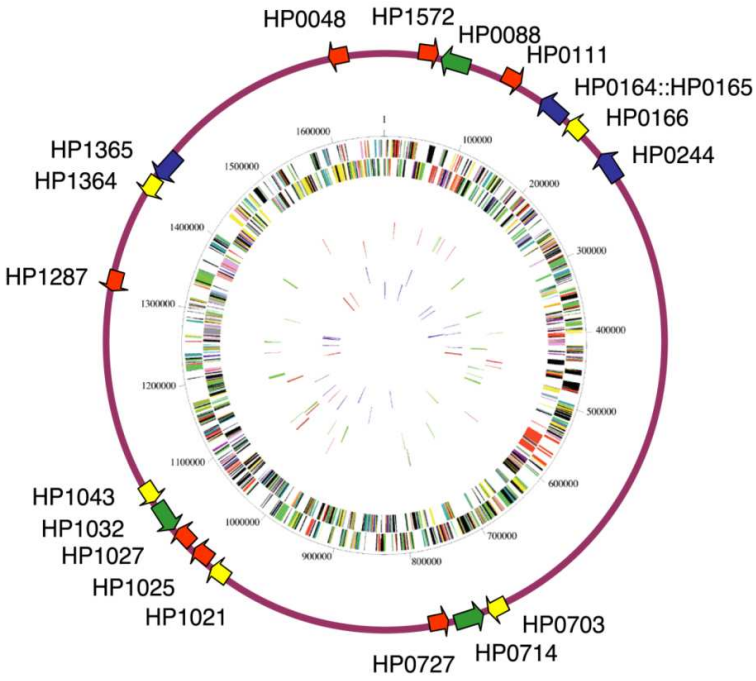

Fig. 2 Schematic representation of *H. pylori* genome and map position of regulatory genes (Scarlato *et al.*, 2001, Tomb *et al.*, 1997). Outer concentric circle: predicted coding regions on the plus strand; second concentric circle: predicted coding regions on the minus strand. Symbols: green arrow boxes, sigma factors (3); blue arrow boxes, sensor kinase (3); yellow arrow boxes, response regulator (5); red arrow boxes, transcriptional regulator (7).

Thus, despite the limited number of proteins putatively involved in regulation of transcription functions (as deduced from genome), *H. pylori* seems to use complex and fascinating mechanisms to control transcription. The key issue is how the few regulatory proteins of *H. pylori* can exploit their functions in order to regulate different sets of genes in a coordinate manner. Globally, the coordinated expression of the genetic repertoire is controlled by the transcriptional regulatory network (TRN), which controls the decision making of the bacterium in response to changes in the environment (Balazsi *et al.*, 2005). Recent evidence points to a very shallow of *H. pylori* TNR in which the few regulators are encompassed in four main modules which process the physiological responses needed to colonize the gastric niche: respectively, heat and stress response, motility and chemiotaxis, acid acclimation and metal ion homeostasis (Danielli *et al.*, 2010). For example, a tightly controlled metal trafficking is at the basis of the activation mechanism of the Ni^{2+}-dependent urease and the [Ni^{2+}-Fe^{2+}] hydrogenase (Mehta *et al.*, 2003). These two enzymes are central players in the infectious process: urease allows buffering of the acidic micro-environment surrounding the bacterium through the conversion of exogenous urea to ammonium and bicarbonate (Sachs *et al.*, 2003, Tsuda *et al.*, 1994), while hydrogenase allows infection through breakdown of hydrogen, an energy-yielding substrate that is freely available in the stomach (Maier *et al.*, 1996, Olson *et al.*, 2002).

2. METAL ION HOMEOSTASIS

2.1 General Features

Ions play an important role in the metabolism of all organisms as reflected by the wide variety of chemical reactions in which they take part. Ions are cofactors of enzymes, catalyzing basic functions such as electron transport, redox reactions, and energy metabolism; and they also are essential for maintaining the osmotic pressure of cells. Because both ion limitation and ion overload delay growth and can cause cell death, ion homeostasis is of critical importance to all living organisms. In bacteria, this is achieved by balancing their uptake, efflux, utilization, and storage (Fig. 3).

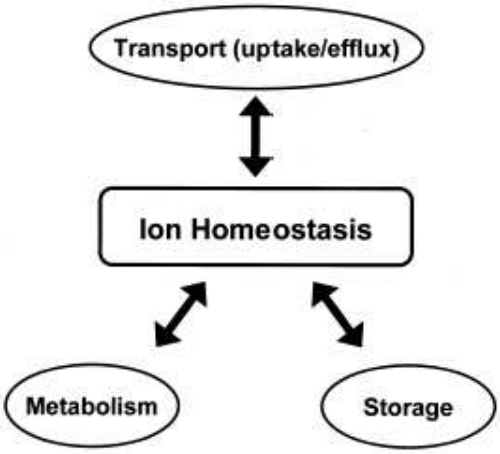

Fig. 3 Schematic representation of the mechanisms involved in maintaining ion homeostasis.

Maintaining ion homeostasis requires both sensor systems to detect the cytoplasmic ion concentration and effector systems to restore normal cell conditions, or to cope with stress caused by ion imbalance. For most ions, the cell can affect

homeostasis through regulation of the expression or the activity of its uptake and efflux systems. Since import of many cations appears to be relatively nonspecific, the corresponding regulatory mechanisms are probably based mainly on ion-specific efflux pumps. For some ions the existence of cytoplasmic storage proteins allows for more complex homeostasis mechanisms. Ion storage proteins remove excess ions from the cytoplasm and keep them in a nonreactive form, which can be accessed when the ion becomes scarce (van Vliet *et al.*, 2001a).

The ion-responsive regulatory systems of bacteria usually consist of a single regulatory protein that combines sensor and effector functions in one molecule. It senses the cytoplasmic ion concentration and, when activated, can induce or repress transcription of the corresponding uptake, efflux, and/or storage systems (Silver *et al.*, 1996). This ensure that the cytosol have the proper complement of transition metal ions (Blencowe *et al.*, 2003).

2.2 Iron Homeostasis

Iron is an essential element for most bacteria, as many enzymes involved in cellular metabolism require iron as a co-factor. Accordingly, ferroprotoporphyrin (heme) groups are essential moieties of many enzymes involved in bacterial respiration, electron transport, and peroxide reduction. Iron-sulfur proteins participate in electron transport reactions, anaerobic respiration, amino acid metabolism, and energy metabolism. Finally, iron-containing non-heme, non-iron-sulfur proteins are required for DNA synthesis, protection from superoxide, and amino acid biosynthesis.
In addition, in bacteria, the level of iron determines the expression of several virulence factors (Braun, 2005, Litwin *et al.*, 1993).

Although iron is considered an abundant element in nature, under aerobic conditions, most iron exists in the insoluble Fe^{3+} form. Reduction of Fe^{3+} to Fe^{2+} is toxic to cells because Fe^{2+} has the ability to generate hydroxyl radicals by catalysing the Fenton reaction (Imlay *et al.*, 1988, Hantke, 2001). Several proteins, such as albumin, ferritin, lactoferrin and transferrin, present in humans, reduce this toxicity by sequestering free Fe^{2+} and oxidizing it to insoluble Fe^{3+}, which is not readily available to support bacterial growth (Weinberg, 1978).

Hence, the survival and growth of bacteria during infection depends on their ability to interact with and acquire iron from the host. Bacteria have evolved several mechanisms to help utilization of host iron-bound compounds directly, or to separate iron from other host sources. Under iron-limiting conditions, most bacteria produce small iron-chelating molecules called siderophores, which can solubilize iron in the environment and present it to specific receptors for transport into the bacteria (Braun *et al.*, 1998, Braun *et al.*, 1999).

Unlike many other organisms, *H. pylori* does not synthesize siderophores (van Vliet *et al.*, 2001a). This is confirmed by analysis of the *H. pylori* genome sequence, which does not contain homologs of siderophore synthesis genes (Berg *et al.*, 1997). Compared to the range of iron compounds that other bacterial pathogens like *E. coli* and *Salmonella enterica* serovar Typhimurium can utilize, the number used by *H. pylori* is limited. Feeding assays indicate that *H. pylori* uses only very few siderophores produced by other organisms (Berg *et al.*, 1997, Husson *et al.*, 1993, Illingworth *et al.*, 1993). This limitation regarding iron acquisition may have developed owing to the absence of competition for nutrients by other microorganisms and the relatively low number of iron compounds available in the human stomach. In fact, in the gastric mucosa, the iron is complexed into haemoglobin or cheated by transferring in serum or by lactoferrin. As the conditions in the gastric lumen and mucosa are predicted to stabilize the soluble ferrous iron, it is likely that, in contrast with many other bacterial pathogens, ferrous iron uptake plays an important role for *H. pylori*.

The genome sequence of *H. pylori* suggests that this bacterium possesses several iron acquisition systems including both ferrous (Fe^{2+}) and ferric uptake systems (Alm *et al.*, 1999, Tomb *et al.*, 1997). In addition, it is known that *H. pylori* is capable to uptake iron from human lactoferrin and haem (Husson *et al.*, 1993, Dhaenens *et al.*, 1999, Worst *et al.*, 1999). Importantly, it seems that *H. pylori* infection is associated with a decrease in human serum ferritin concentration that might be induced by the uptake of ferritin in the stomach by *H. pylori* (Berg *et al.*, 2001). Accordingly, *H. pylori* infections have been also epidemiologically linked with disorders in iron metabolism and iron deficiency anemia, especially in adolescent and pregnant women (Muhsen *et al.*, 2008).

Furthermore, *H. pylori* possesses also iron storage and iron detoxification systems. This allows the cell to be protected from iron toxicity and also provides for an

iron deposit, which is available when iron is scarce. Bacterial iron storage proteins can be divided into two classes: ferritins and bacterioferritins and *H. pylori* contains one ferritin, the 19-kDa prokaryotic ferritin (Pfr) protein (HP0653), and one putative bacterioferritin, the HP-NAP protein (HP0243).

2.3 Regulation of Iron Homeostasis

Bacteria regulate their iron-uptake and iron-storage systems in response to the cytoplasmic Fe^{2+} concentration in order to reduce the generation of toxic radicals that will damage biological macromolecules (Braun *et al.*, 1999). When this concentration becomes too high, bacteria switch off their high-affinity iron uptake systems.

On the other hand, continuous uptake of iron creates the need for removal of iron from the cytoplasm and storage of excess iron. The shielding role of soluble metal-storage protein is often essential to this task. These proteins, from one site protect the cell from the toxic effects of intracellular free metal ions and, from the other site, should release the metal ions to metallo-enzymes and/or specific metallo-chaperones vehiculating the metals to the correct metal binding pockets of the enzymes, in order to trigger their enzymatic activity.

Thus the iron homeostasis is tightly controlled, both at the protein level, through incorporation of free metal ions into metallo-proteins, and more importantly at the transcriptional level, through the regulated expression of genes encoding metal-trafficking proteins, including storage and uptake proteins. In many bacteria, this transcriptional regulation is mediated by the ferric uptake regulator Fur (Crosa, 1997, Escolar *et al.*, 1999).

In contrast, this process in eukaryotic organisms occurs mainly at level of translation through the binding of a regulatory protein to specific mRNA transcripts (Schneider *et al.*, 2000).

3. THE TRANSCRIPTIONAL REGULATOR FUR

3.1 Overview

The ferric uptake regulator Fur is a widespread bacterial protein that regulates the expression of iron-uptake and iron-storage systems in response to intracellular iron. The Fur protein has been best characterized in *E. coli* (Bagg *et al.*, 1987, de Lorenzo *et al.*, 1987, Hantke, 1981), and Fur homologous have been found in both Gram-negative bacteria and Gram-positive bacteria (Bsat *et al.*, 1998, Xiong *et al.*, 2000).

Fur is a key regulator of iron metabolism, but in different organisms it clearly plays a role in numerous other aspects of physiology (Escolar *et al.*, 1999). In particular, in *H. pylori*, the relative paucity of transcriptional regulators, combined with the necessity to respond to environmental stresses (see Chapter 1.2), may have resulted in *H. pylori* Fur (*Hp*Fur) being involved in the regulation of other adaptive responses. (Ernst *et al.*, 2005a). Thus, other than regulation of iron metabolism, *Hp*Fur has also been implicated in the regulation of acid resistance (Bijlsma *et al.*, 2002, Bury-Mone *et al.*, 2004, van Vliet *et al.*, 2004), nitrogen metabolism (van Vliet *et al.*, 2001b, van Vliet *et al.*, 2003) and oxidative stress resistance (Dubrac *et al.*, 2000). Further, Fur-mediated regulation is also required for gastric colonization by *H. pylori*, as demonstrated in a mouse model of infection (Bury-Mone *et al.*, 2004, Gancz *et al.*, 2006).

Therefore, due to Fur involvement in the regulation of many other processes in the cell, it is tempting to also consider Fur like a global regulator rather than a simple transcriptional regulator (Escolar *et al.*, 1999). The importance of Fur as global regulator is reflected by more than 200 identified target gene loci in *H. pylori* genome, as shown in a genome-wide location analysis (Danielli *et al.*, 2006).

In the classical Fur regulation paradigm, Fur acts as transcriptional repressor in the presence of iron, which acts as co-repressor, promoting the binding affinity of Fur to AT-rich DNA elements, termed Fur-boxes, encompassed in the core promoters of iron-regulated genes (Escolar *et al.*, 1997, Escolar *et al.*, 1999). Thus, Fur binding to the Fur-boxes, occludes the promoter from being recognized by the vegetative RNA polymerase (RNAP) holoenzyme, resulting in transcriptional repression of target genes.

However, under low iron conditions the iron-free Fur (*apo*-Fur) has a reduced affinity for the Fur-boxes allowing the RNAP free access to the promoters of the downstream genes. Classical Fur-regulated promoters are repressed under iron replete conditions and derepressed under iron starvation conditions.

Fur represents the founding member of a family of regulators composed by several subclasses of bacterial metalloproteins. These proteins differ in function and have different DNA-binding sites but are all involved in metal-dependent control of gene expression. However, the Fur family includes members that sense metals in the cell as well as other signals than metal ions, including the sensors of zinc starvation Zur (Gaballa *et al.*, 1998, Patzer *et al.*, 1998), the manganese-uptake regulator Mur (Diaz-Mireles *et al.*, 2004), the nickel-selective regulator Nur (Ahn *et al.*, 2006) and a hydrogen peroxide stress-sending repressor, PerR, from *Bacillus subtilis* (Bsat *et al.*, 1998). PerR is capable of binding Fe^{2+} or Mn2+ to a metalloregulatory site which represses the expression of genes that control a response to H_2O_2 and oxidative stress, through a singular mechanism in which the iron-binding site now functioning as a metal-based sensor of peroxides (Lee *et al.*, 2006b).

3.2 Structure-function relationship: mechanisms of iron sensing and allosteric activation

The *H. pylori fur* gene was originally isolated as coding sequence able to partially complement an *E. coli* Δ*fur* knockout strain (Bereswill *et al.*, 1999, Bereswill *et al.*, 1998). The deduced polypeptide sequence predicts a protein of ~ 17 kDa mass, containing 150 residues, with high homology to *E. coli* Fur (*Ec*Fur). Accordingly, antibodies directed against *Ec*Fur cross-react with the *Hp*Fur protein (Bereswill *et al.*, 1999). It also shares extensive sequence and secondary structure homology to the broad family of Fur-like metallo-regulators found in Gram-negative and Gram-positive bacteria, including *Pseudomonas aeruginosa* Fur (*Pa*Fur), *B. subtilis* PerR (*Bs*PerR), *Mycobacterium tubercolosis* Zur (*Mt*Zur) (reviewed Lee *et al.*, 2007b). Biochemical and spectroscopic studies indicated that Fur proteins assume a homodimeric tertiary structure (Pecqueur *et al.*, 2006, Pohl *et al.*, 2003) and are able to multimerize also in the absence of target DNA (Delany *et al.*, 2002a, Vitale *et al.*, 2009). Evidence

gathered from the first, and currently sole, complete crystal structure of *Pa*Fur, suggests that each monomer contains two winged HTH motifs, encompassed in the N-terminal DNA-binding domain, and a dimerization domain, encoded by the C-terminal half of the polypeptide sequence. More in details, the DNA-binding domain is composed of four helices followed by two-stranded antiparallel β-sheet, while the dimerization domain of each *Pa*Fur monomer consists of an α/β-domain in which three β-strand are covering in one long α-helix (Fig. 4). Both structural elements are involved in the formation of a functional protein dimer (Pohl *et al.*, 2003).

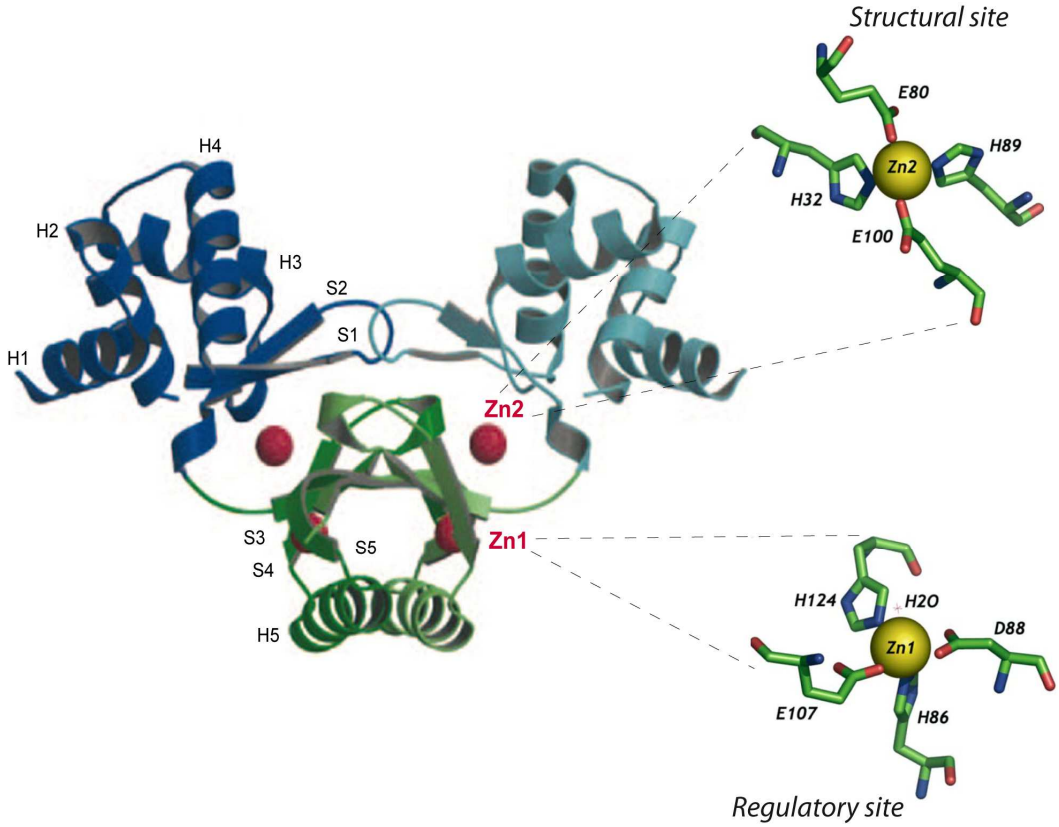

Fig. 4 Ribbon diagram of the crystal structure of the *Pseudomonas aeruginosa* Fur. A Fur dimer with secondary structural elements annotated, are shown in the left panel. The DNA-binding domains are depicted in blue and the dimerization domain in green. The symmetry-related second monomer is shown in light blue and green. In the crystal structure two functional metal binding sites were identified: structural site and regulatory site (right panel). Adapted from (Pohl *et al.*, 2003, Pennella *et al.*, 2005).

Although the crystal structure of *Hp*Fur is not available, sequence alignments of *Hp*Fur along with *Pa*Fur and other several Fur proteins revealed significant differences in protein structure, one of which consists in an additional N-terminal helix in *Hp*Fur protein that may be involved in DNA recognition, as will be discussed below. (Fig. 5)

Extensive studies in *Ec*Fur, *Pa*Fur, *Bs*Fur, as well as *Hp*Fur indicated that each Fur monomer contains at least two related metal-binding sites: a structural zinc binding site (Zn^2) and a regulatory binding site (Zn^1), in which the Zn^{2+} ion is readily exchange by the regulatory ion Fe^{2+} (or also Mn^{2+}) (Pennella *et al.*, 2005, Pohl *et al.*, 2003) . The regulatory site, responsible for activation of DNA binding activity, is coordinated by the side chain of residues His-86, Asp-88, Glu-107, His-124, located exclusively in the dimerization domain. The structural site connects the DNA-binding domain and the dimerization domain and comprises the side chains of His32, Glu80, His89 and Glu100 in a tetrahedral geometry (Fig. 4 and Fig. 5).

In *Hp*Fur, metal chelation with EDTA disrupts the Zn^{2+}-substituted dimeric form into a monomer, while reconstitution of the dimer requires reducing agents and metal ions such as Zn^{2+} or Cd^{2+} (Vitale *et al.*, 2009). This strongly suggests that the structural Zn binding site is important for the multimerization of the protein. In contrast to *Pa*Fur, where the structural site contains a zinc ion coordinated in tetrahedral geometry by two histidine and two glutamate residues (see above and Fig. 4 and Fig. 5), in *Hp*Fur the structural zinc ion is coordinated by two CXXC motifs (specifically Cys102/Cys105 and Cys142/Cys145), conserved also in *Mt*Zur and *Bs*PerR (Vitale *et al.*, 2009). The coordination of the structural zinc ion in a ZnCys4 motif is closer to *Bs*PerR (Lee *et al.*, 2006b), than to *Ec*Fur where the Zn^{2+} ion is coordinated by two cysteines, one histidine and one aspartate (Jacquamet *et al.*, 1998). In this light, it is noteworthy to recall that *Bs*PerR is involved in regulation of redox genes in *B. subtilis* (Fuangthong *et al.*, 2002), using the ferrous ion coordinated at the regulatory site as reducer of hydrogen peroxide, thereby catalyzing the oxidation of residues important for the DNA binding activity of the regulator (Lee *et al.*, 2006b, Jacquamet *et al.*, 2009). This mechanism explains the capacity of *Bs*PerR to sense and transduce the hydrogen peroxide signal in a transcriptional output. This opens the intriguing hypothesis that also *Hp*Fur may work similarly, combining both iron- as redox-sensing regulatory features.

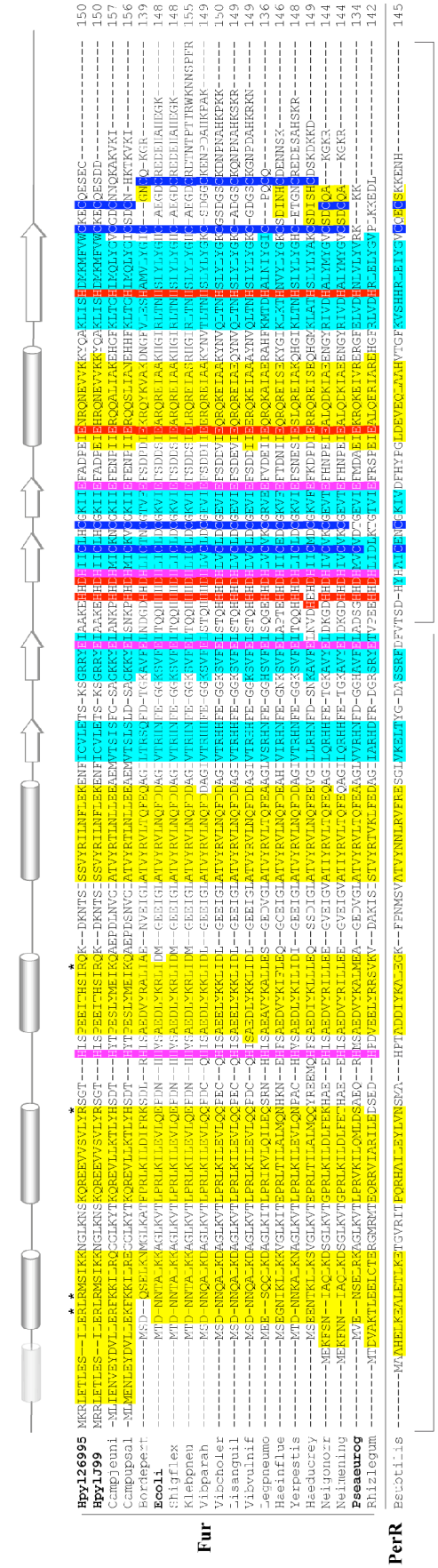

Fig. 5 Sequence alignment of 20 proteins from the SWISSPROTEIN database annotated as homologous to the ferric uptake regulator (Fur) of *E. coli* compared to PerR of *B. subtilis*. Residues highlighted in yellow and sky-blue indicate conserved α-helix (cylinder) and β-sheet (arrow). Light cylinder indicates additional α-helix found in *H.pylori* Fur. The metal binding sites annotated are based on the crystal structure of *Pa*Fur (Pohl *et al.*, 2003) and biochemical characterization of *Hp*Fur (Vitale *et al.*, 2009) and *Bs*PerR (Lee *et al.*, 2006a)

3.3 Recognition of DNA: Fur box consensus sequence and Fur-DNA interactions

The mode of interaction of Fur with DNA has been controversial to date (Baichoo *et al.*, 2002a, Escolar *et al.*, 1999, Lavrrar *et al.*, 2003). Fur binds with high affinity to AT-rich DNA sequences known as a Fur boxes. The classical Fur box has been described as 19 bp inverted repeat GATAATGATnATCATTATC (Fig. 6A).

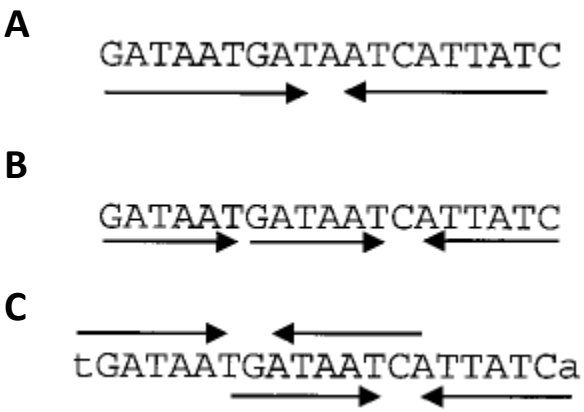

FIG. 6. Comparison of models to explain the Fur box consensus sequence. (A) The Fur box is classically defined as a 19-bp inverted repeat sequence(de Lorenzo *et al.*, 1987), originally envisioned to bind a single Fur dimer. (B) An alternative view proposes that Fur binds to repeated arrays of three or more copies of the hexamer GATAAT (Escolar *et al.*, 1998a, Escolar *et al.*, 1999). According to this model, the classic Fur box is three GATAAT motifs in a head-to-head-to-tail (6-6-1-6) array. (C) Further studies propose that the 19-bp Fur box results from two overlapping heptamer inverted repeats $[(7\text{-}1\text{-}7)_2]$ that together define a 21-bp sequence (Baichoo *et al.*, 2002a).

Since Fur is a dimer in solution, it was originally proposed that one dimer would bind to each Fur box according to a model in which Fur contacts the major groove of DNA and the protein symmetry axis is perpendicular to the DNA axis (Fig. 7A; (Pohl *et al.*, 2003).

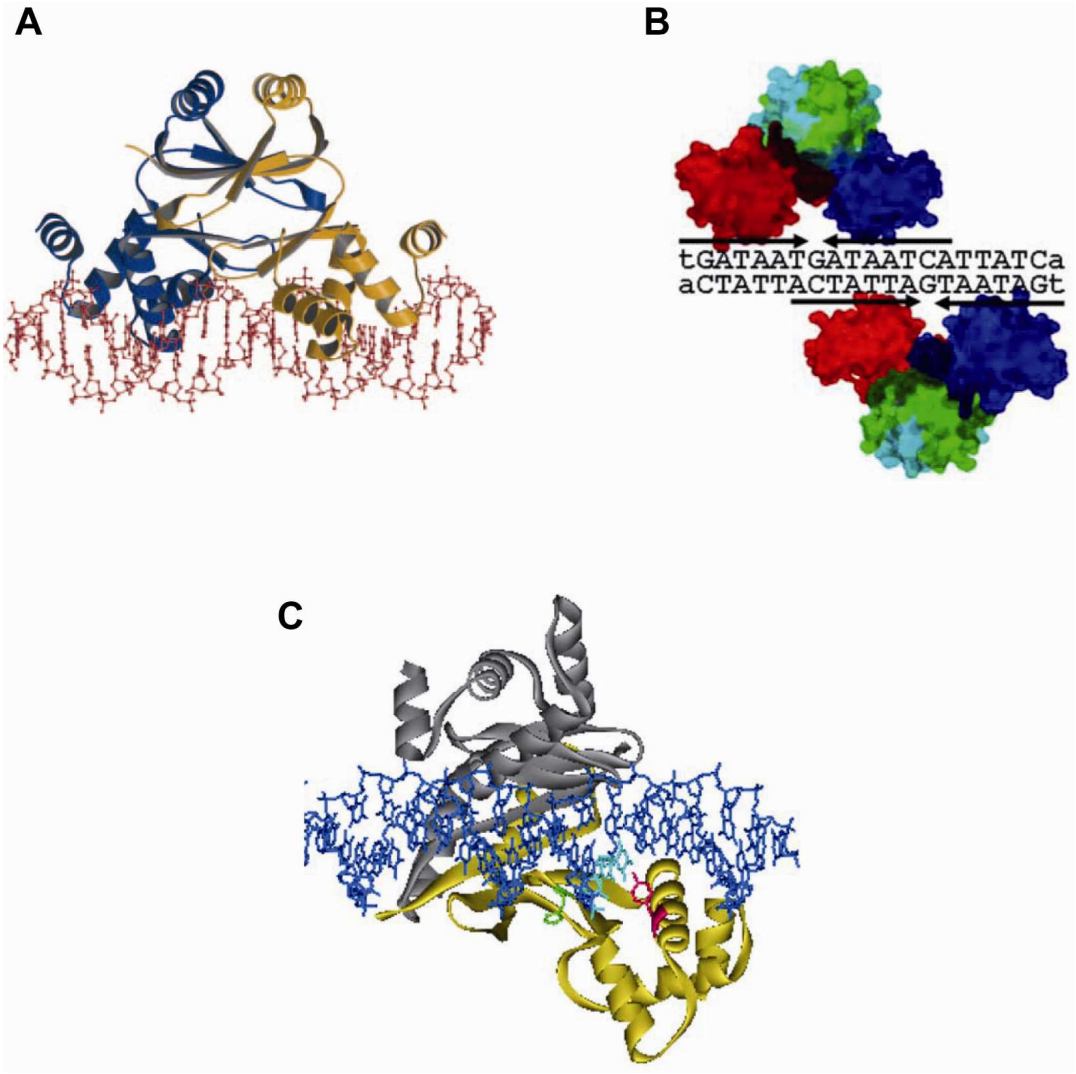

FIG. 7. Interaction of Fur with DNA. **(A)** Model of one Fur dimer bound to canonical B-DNA. Note that the twofold symmetry of the protein dimer follows the pseudo twofold symmetry of the DNA sequence (Pohl *et al.*, 2003). **(B)** Model of the interaction of *Bs*Fur with DNA. In this revised model of two overlapping 7-1-7 motif (arrows), two Fur dimers bind the two 7-1-7 motifs from opposite side of the DNA (Baichoo *et al.*, 2002a). The N-terminal DNA-binding domains are in red and blue, the C-terminal dimerization domains are in green. **(C)** Model derived from biochemical characterization of *Ec*Fur-DNA interactions. In this new model, the protein symmetry axis formed an angle of ca. 50° with the DNA axis (Tiss *et al.*, 2005).

However, this model was not easily reconciled with the typically observed 31 bp footprint, since a Fur dimer would not be expected to protect more than 20 bp in a DNase I protection assay. In addition, Fur proteins tend to polymerize at many operator sites to generate footprints that are not simple multiple of the 31 bp protected region. (Escolar *et al.*, 2000). Indeed, Fur binds cooperatively at some promoter regions and generates helical arrays spiralling around the DNA duplex (Lavrrar *et al.*, 2002, Le Cam *et al.*, 1994).

These observations motivated detailed studies using synthetic oligonucleotides. As a result, Escolar *et al.* (1998a) proposed a reinterpretation of 19 bp Fur box as a head-to-head-to-tail repeat of simple hexamer GATAAT (Fig. 6B). Accordingly to this model, Fur would bind tightly to repeated arrays of examers as long as they contained a minimum of GATAAT motifs. However, this interpretation is not easy to reconcile with the dimeric state of Fur and it is not clear whether each hexamer motif represents the proposed binding sites for one monomer or one dimer (Escolar *et al.*, 1999).

Compilation and analysis of Fur regulated genes from *B. subtilis* led to a revised proposal (Baichoo *et al.*, 2002a). A multiple sequence alignment of all identified fur-regulated genes led to a consensus Fur box containing a heptameric inverted repeat (7-1-7) of TGATAATNATTATCA. Two such motifs, offset by 6bp, generate a 21-bp sequence containing the classical 19-bp Fur box (Fig. 6C). According to this model, the classical 19-bp Fur box is recognized by two Fur dimmers, each interacting with one of two overlapping 7-1-7 motifs from opposite faces of the DNA duplex (Fig. 7B).

Recently, the characterization of the DNA-binding site in the *Ec*Fur by UV crosslinking and mass spectrometry, has shown that Tyr55 of *Ec*Fur, contacts two thymines in position 18 and 19 of the consensus Fur box (Tiss *et al.*, 2005). This evidence has suggested a conformational model of the Fur-DNA complex in which the protein wraps helically around the DNA and its symmetry axis formed an angle of 50° with the DNA axis (Fig. 7C). Furthermore, the binding of two dimers was as plausible in this model as it was in the model in Fig. 7B.

The presence of 19 bp Fur box consensus sequences is correlated with iron-repressible genes in numerous bacteria (Baichoo *et al.*, 2002b, Grifantini *et al.*, 2003, Panina *et al.*, 2001). In addition, Fur homologue from many different bacteria can at least partially complement an *E. coli fur* mutant, providing further evidence that DNA-binding specificity is conserved among many Fur family members. Indeed, simply

searching bacterial genomes for close matches to the 19 bp Fur consensus identifies numerous candidates for iron-regulated genes. In the case of *B. subtilis*, approximately one-half of the Fur regulon could be identified by this simple expedient (Baichoo *et al.*, 2002b) and a similar correlation was reported for *Neisseria meningitidis* (Grifantini *et al.*, 2003). This approach misses weaker sites and sites that match the shorter 7-1-7 consensus (and presumably bind only one dimer). In addition, recent evidence suggests that in some cases Fur and Fur-like proteins may recognize distinctly different classes of DNA-binding sites (Lee *et al.*, 2007b).

4. FUR REGULATION

The first genes to be linked to Fur control were identified as being transcriptionally repressed by iron, constitutively derepressed in *fur* mutants, and bound by the Fur protein in the core promoter region.

However, while Fur was first characterized as an autoregulatory transcriptional repressor under iron-replete conditions (*holo*-repressor), it has subsequently been shown to function as an activator and even to repress certain genes in the absence of the iron cofactor (*apo*-repressor). These diverse types of Fur regulation are discussed in further detail below.

4.1 *holo*-Fur regulation

The best-described means of Fur regulation is hallmarked by the iron-bound form of Fur (*holo*-Fur) which displays iron-dependent DNA binding ability to conserved sequences (Fur boxes), located in the promoters of iron-regulated genes, with iron functioning as repressive cofactor. Fur binding blocks the binding of RNA polymerase, thus preventing transcription of these target genes (Escolar *et al.*, 1997, Escolar *et al.*, 1998b). This type of regulation is here termed *holo*-Fur repression (see Fig. 8).

A greater understanding of the mechanism of Fur regulation came with the first description of a DNA binding consensus sequence for *E. coli* Fur (see Chapter 3.4 and Fig. 6A). This consensus sequence became the gold standard for comparison of types of Fur regulation across bacterial species and facilitated the understanding of exactly how Fur functions as a regulator. Although the Fur box of *E. coli* is used as the standard to which other Fur binding sequences are compared, it is not clearly conserved in all organisms that exhibit Fur regulation. Accordingly, in *H. pylori*, the *Ec*Fur box is not well conserved and a proper consensus is currently ill-defined. However, sequence alignments of several genes regulated by *holo*-Fur, indicated that the binding sequence occurs in AT-rich regions oftentimes with repeats of AAT, arranged in the consensus Fur box NNNNNAATAATNNTNANN (Merrell *et al.*, 2003). This consensus sequence is significantly different from that for *E. coli* and is certainly less conserved,

even among *H. pylori* Fur-regulated genes, than the *E. coli* sequence. While it is currently unclear, it may be that the requirement for Fur binding is less reliant on a recognition sequence and more related to the overall structural configuration of the target promoter sequence in *H. pylori.* This notion is further supported by the fact that *Hp*Fur is only partially able to complement an *E. coli fur* mutant (Bereswill *et al.*, 2000) and that an *E. coli* Fur titration assay (FURTA-Ec) was not very successful at identifying Fur-regulated genes in *H. pylori* (Bereswill *et al.*, 1999, Bereswill *et al.*, 1998) until the system was modified to heterologous expression of the *H. pylori* Fur homologue (Fassbinder *et al.*, 2000).

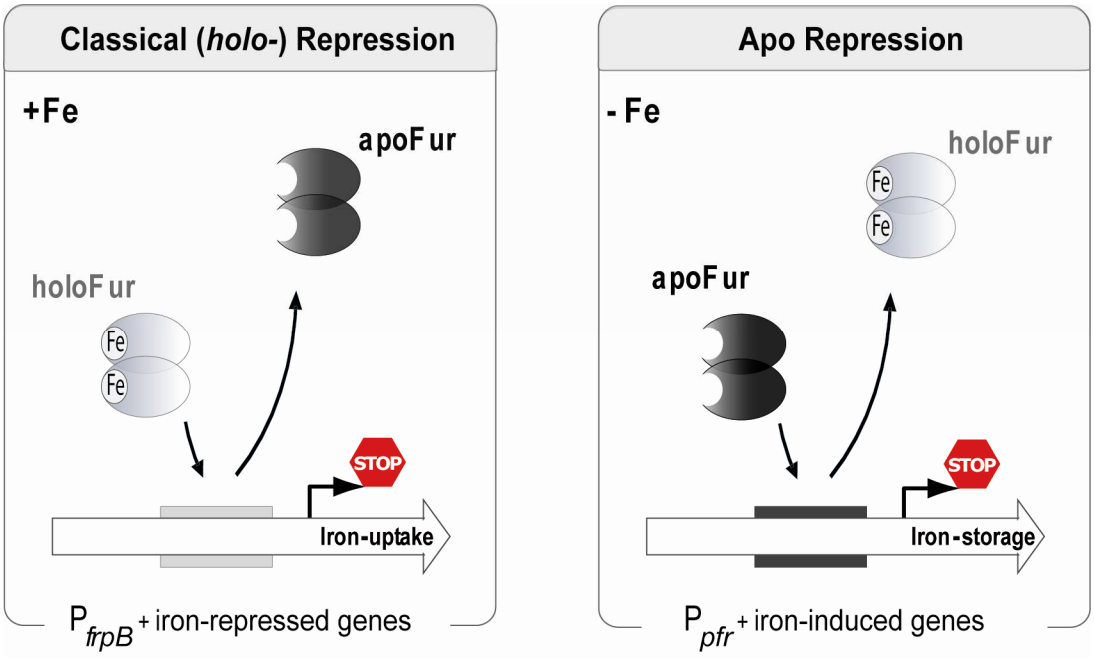

Fig. 8 Basic features of *holo*- and *apo*-Fur repression. (Left) Classical *holo*-Fur repression. As iron becomes increasingly available in the bacterial cell, the iron cofactor binds to Fur protein and the iron-bound Fur dimers represses transcription by binding the Fur box in their target promoters and block the binding of RNA polymerase. (Right) *apo*-Fur repression. Under iron depletion conditions, Fur is in its *apo*-form and binds to the Fur boxes of its target promoters. The binding blocks the RNA polymerase, hence transcription is repressed.

Even though all of the specifics are not known, *holo*-Fur repression in *H. pylori* has been well documented, and binding to several gene targets has been confirmed through DNase I footprinting analysis. Indeed, the predicted Fur regulon in *H. pylori* is quite extensive (Danielli *et al.*, 2006, Ernst *et al.*, 2005a, Merrell *et al.*, 2003). The regulon includes mainly iron uptake genes, like *frpB* (Delany *et al.*, 2001a, Delany *et al.*, 2001b), *exbB* (Delany *et al.*, 2005), *fecA* (Danielli *et al.*, 2009, van Vliet *et al.*, 2002), *ceuE* and *feoB* (van Vliet *et al.*, 2002), that are repressed under iron replete conditions in order to prevent the harmful effects of iron overload. In this way a fine control of iron homeostasis is maintained (see Chapter 2.3).
In addition, *holo*-Fur regulon includes also other genes involved in functions like acid resistance (van Vliet *et al.*, 2003), colonization and virulence (Danielli *et al.*, 2006). Thus, is not surprising that *fur* has been shown to be important for efficient colonization of the mouse gastric mucosa by *H. pylori* (Bury-Mone *et al.*, 2004, Gancz *et al.*, 2006).

It seems that iron-bound Fur-regulated genes in *H. pylori* have one to three Fur binding sites within their promoters. The sites with the highest affinity span the -10 and/or -35 promoter element; the lower affinity Fur binding sites are located further upstream from the primary Fur box (Delany *et al.*, 2005, Delany *et al.*, 2001a, Delany *et al.*, 2001b). This high-affinity orientation supports the current hypothesis of Fur competing with RNA polymerase for binding to target promoters. Indeed, what we know about Fe-bound Fur regulation in *H. pylori* agrees with what is seen for many other organisms and is the most common mechanism of Fur regulation.

4.2 *apo*-Fur Regulation

Soon it became clear that Fur regulation in *H. pylori*, goes beyond the classical, well-documented *holo*-Fur regulation. Accordingly, a mechanism of iron-sensitive repression has also been demonstrated. It involves iron-free Fur (*apo*-Fur) binding to target promoters, in absence of its iron cofactor (*apo*-Fur), to prevent the binding of RNA polymerase. This phenomenon is here termed *apo*-Fur regulation and involves repression of iron storage genes under iron limited conditions (Fig. 8) (Delany *et al.*, 2001b). While the *holo*-Fur repression is conserved across a wide range of bacterial

species, the ability of Fur to repress gene expression in its *apo*-form remains unique to *H. pylori*. Because the *apo*-Fur regulation has not been described for other bacterial species and because Fur clearly plays a role in global gene regulation in response to environmental stimuli, and enhances the fitness of *H. pylori* as pathogen, go on with the study of Fur in *H. pylori* is of particular interest.

The *apo*-Fur regulon consists of an entirely different set of genes than the *holo*-Fur regulon and is predicted to contain approximately 16 genes (Ernst *et al.*, 2005a), though few genes have definitively been shown to be regulated in this manner.

Expression of the iron storage protein Pfr is regulated by *apo*-Fur; *pfr* expression is promptly derepressed under Fe^{2+} replete conditions but is constitutively expressed in a *fur* mutant (Bereswill *et al.*, 2000). Distinctively, *Hp*Fur acts as a transcriptional repressor also in this case, with iron acting as inducer, instead of as co-repressor (Delany *et al.*, 2001b). Specifically, Fur binds an operator overlapping the -10 element of the *pfr* promoter with higher affinity in the absence of iron ions.
From a bacterial standpoint, repression of the iron storage protein Pfr under iron-limited conditions makes biological sense, as the expression of a storage protein in the absence of a molecule to be stored would be a waste of energy.

Another confirmed *apo*-Fur target is *sodB,* encoding superoxide dismutase. Binding of Fur to *sodB* in the absence of iron was demonstrated via electrophoretic mobility shift assays and DNase I footprinting analysis, which have shown that the *sodB* promoter has only one Fur binding region, spanning the -10 and -35 promoter elements (Ernst *et al.*, 2005b). Recently, it has been demonstrated that a strain-specific substitution of a single nucleotide flanking this operator results in loss of *sodB* metal-responsive and Fur-dependent regulation (Carpenter *et al.*, 2009a). Interestingly, comparison of *pfr* and *sodB* Fur boxes shows very little sequence homology between them. Additionally, there is little homology with the known *H. pylori holo*-Fur boxes and even less homology with the *E. coli* consensus Fur binding sequence (Delany *et al.*, 2001b, Ernst *et al.*, 2005b).

The ability of Fur to bind to distinct sites in the presence or absence of iron may also play a role in the autoregulation of *fur* gene by an “anti-repression” mechanism (Delany *et al.*, 2003).

4.3 Autoregulation of Fur

While some organisms have additional regulatory proteins to regulate Fur expression (De Lorenzo *et al.*, 1988, Delany *et al.*, 2005), autoregulation of Fur is the most conserved mechanism of *fur* regulation. Fur represses its own expression under iron-replete conditions. Biologically speaking, it makes sense to link the expression of Fur to the level of available iron, given the dangers of iron toxicity (see Chapter 2). Fur can be thought of as a rheostat that senses the available iron and responds by regulating its own expression accordingly (Delany *et al.*, 2002a, Delany *et al.*, 2003).

In general Fur autoregulation is the straightforward classical holo-Fur repression. However, in some organisms, Fur autoregulation appears to be more complex. For example, in *Lysteria monocytogenes*, *fur* is upregulated under iron-limited conditions, and the Fur protein is able to bind to and protect the Fur box region of its own promoter in the absence of the metal cofactor (Ledala *et al.*, 2007). In contrast to this and *holo*-Fur autoregulation, *Vibrio vulnificus* Fur has been shown to bind to and activate *fur* expression in the absence of iron (Lee *et al.*, 2007a).

Fur autoregulation in *H. pylori* may very well be the most complex Fur autoregulatory circuit known to date, since it combines both the classical *holo*-Fur repression and the *apo*-Fur anti-repression that is also exhibited in *V. vulnificus*. Initial studies by Delany and colleagues revealed three Fur binding regions in the *H. pylori fur* promoter (Delany *et al.*, 2002a). The first two operators are likely to be involved in repression of the *fur* promoter, as they encompass both the -10 and -35 promoter elements, but the role of the third and farthest-upstream operator was initially unclear (Delany *et al.*, 2002a). In their subsequent work, the authors showed that the third operator region was indeed important for Fur autoregulation and that it functions as a site for *apo*-Fur anti-repression (as subsequently shown for *V. vulnificus*). Additionally, operator I is involved in both *holo*-Fur repression and *apo*-Fur anti-repression of expression through binding Fur in its respective forms (Delany *et al.*, 2003). Which form binds is driven by the prevalence of iron, as both forms bind to this operator with equal affinities. The current model of *H. pylori* Fur autoregulation also suggests that if the concentration of Fur dips below a certain level, then Fur binding to operator I is lost, allowing this site to act as an UP element for RNA polymerase (Delany *et al.*, 2003). Given that this organism utilizes Fur in both its *holo*- and *apo*- forms, it is

perhaps not surprising that Fur autoregulation in *H. pylori* is a complex mixture of *holo*-Fur repression and *apo*-Fur anti-repression. Additionally, with few regulatory proteins relative to its genome size, *H. pylori* would likely have evolved to utilize every regulatory mechanism it has to ensure proper homeostasis.

4.4 Fur Activation

The complexity of *fur* autoregulation in *H. pylori* points to yet another regulatory function of Fur; Fur can act as a positive regulator. The first indication that Fur may act as a positive regulator came from microarray analyses where a number of genes were suggested to be Fur induced (Danielli *et al.,* 2006, Ernst *et al.*, 2005a).

However, the process of Fur activation in *H.pylori* is currently little understood, except with *nifS* which encodes a [Fe-S] cluster synthesis protein. Footprinting analyses have identified two Fur boxes located far upstream of the transcriptional start site in *nifS* promoter, associated with a direct positive regulation mechanism (Alamuri *et al.*, 2006).

While, for both *holo*- and *apo*-Fur repression, the Fur boxes are located near the transcriptional start site, the Fur boxes for Fur-activated genes are all located far upstream from the transcriptional start site. This suggests that Fur activation does not occur in the same manner as a Fur repression. Even so, formal demonstration of transcriptional activation mediated by *Hp*Fur and the molecular bases behind this mechanism have not been provided yet, leaving important questions open whether and how *Hp*Fur can function in vivo as authentic transcriptional activator, either in its *apo*- or *holo*-form.

In fact, in many bacteria positive Fur regulation has been proven to be indirect, mediated by the presence of small regulatory sRNAs, acting post-transcriptionally on the decay and translation of target mRNAs (Masse *et al.*, 2007). Similar mechanisms are not known in *H. pylori*, but natural antisense transcripts (NATs) and putative small non-coding RNAs, have been reported (Xiao *et al.*, 2009a, Xiao *et al.*, 2009b). Recently, 60 new sRNA, including 6S RNA, and potential regulators of *cis*- and *trans*-encoded target messenger RNAs have been identified (Sharma *et al.*, 2010).

4.5 Focusing on *holo*- and *apo*-Fur repression: target genes and DNA-binding

As discussed above, Fur can act as either a repressor or an activator and function with or without its iron cofactor, in its *holo*- or *apo*-form. However, while the mechanism of *holo*-Fur repression is well understood, little is known about *apo*-Fur regulation for which the mechanism of action remains unclear.

However, the current data do not suggest a conserved binding sequence for *apo*-Fur binding. In addition, the structural features that distinguish those sites bound by Fur in the absence of iron (*apo*-Fur) versus the presence of its iron cofactor (*holo*-Fur) have not been elucidates.

In *H. pylori*, the *holo*- and *apo*-Fur repression have been first verified for *frpB* and *pfr* genes, which encode an outer-membrane protein and a non-haem iron containing ferritin, involved in iron-uptake and iron storage, respectively (Delany *et al.*, 2001a, Delany *et al.*, 2001b).

Delany et al, in 2001 (Delany *et al.*, 2001b), showed that iron affects the expression of these genes differentially. Accordingly, the *frpB* promoter (P_{frpB}) is iron-repressed in contrast to *pfr* promoter (P_{pfr}), whose expression is iron-induced, reflecting the unusual *apo*-Fur repression. Regardless of iron availability, both P_{frpB} and P_{pfr} promoters are constitutively de-repressed in Fur mutant, indicating that the Fur protein mediates both types of iron-dependent repression.

DNase I Footprinting analyses have also demonstrated that the *frpB* and *pfr* gene regulation is directly mediated by Fur, which binds to multiple operators on P_{frpB} and P_{pfr} promoters regions. Specifically, two Fur operators have been identified on P_{frpB} while three regions of protection have been described on P_{pfr}. The structural organization of P_{frpB} and P_{pfr} is represented schematically in Fig. 9.

On both promoters, the operator with the highest affinity for either *holo*- or *apo*-Fur (indicated as OPI), spans the -10 and -35 promoter elements, while the lower affinity Fur operators are located upstream from the primary Fur box. This high affinity orientation supports the current hypothesis of Fur competing with RNA polymerase for binding to target promoters.

The affinity of the Fur protein for these operator sequences is differentially affected by the iron in both promoters (Delany *et al.*, 2001b).

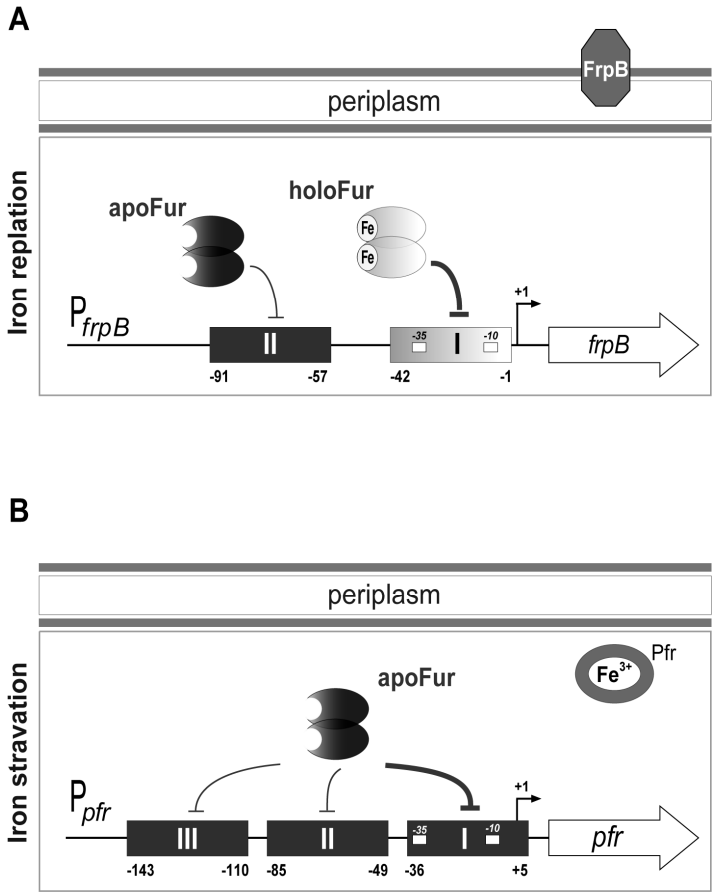

FIG. 9 Schematic representation of P_{frpB} (A) and P_{pfr} (B) promoter structure. Fur binding sites have been identified through DNase I footprinting analysis by Delany et al 2001. Light grey box (marked I) indicates the operator site recognized mainly by the *holo*-protein, while dark boxes (marked I, II and III) indicate operator sites with higher affinity for *apo*-Fur. For each operator the numbers refers to their positions respect to the transcriptional start site. On each promoter, the −10 and −35 regions and the transcriptional start site (bent arrow) are indicated, and the open reading frames are indicated by horizontal open arrows. Width of arrows is proportional to the affinity of Fur for the operator sites.

Accordingly, the affinity of Fur for the *frpB* operator I increases with Fe^{2+}. Thus, this operator is the site with highest affinity for *holo*-Fur. In contrast, the affinity for the

three *pfr* operators and the operator II on P_{frpB} decreases in presence of iron, which indicates that Fur has the highest affinity in its *apo*-form (Fig. 9).

Hence, the *H. pylori* Fur protein exploits different mechanisms of DNA binding that are operator dependent and results in differential effects of Fe^{2+} on the binding ability of the protein.

Based on this evidence, this study focuses on the characterization of the molecular determinants that underlie the iron-responsive Fur binding using the *frpB* and *pfr* gene promoters as a functional example for the *holo*- and *apo*-Fur-mediated repression.

Herein, we demonstrate the existence of a peculiar binding architecture, specifically associated to the operator typology recognized by either *holo*- or *apo*-Fur. Furthermore, we show that the binding of the *holo*- and *apo*-regulator is apparently mediated in *cis*, within the operator sequence, whereas iron modulates protein oligomerization on DNA. In addition, we elucidate the binding residues important for both *holo*- and *apo*-Fur binding, defining a peculiar consensus motif for the *apo*-protein, while highlighting the important role of the overall DNA structure for the *holo*-Fur binding. Thus two distinctive mechanism of recognition are proposed for the specific recognition of *apo*- and *holo*-Fur targets, respectively. The first occurs through the specific recognition of a peculiar consensus motif in the major groove and the second one relies on the specific recognition of the overall structure of DNA that is recognized by Fur trough binding into the minor groove of DNA.

RESULTS

5. Fur shows a distinctive binding architecture on *holo*- and *apo*-Fur recognized operators

5.1 Fur binding architecture on P_{frpB} and P_{pfr}

The ferric uptake regulator (Fur) protein is known to act as a Fe^{2+}-dependent transcriptional repressor of bacterial promoters (*holo*-Fur repression). However, in *Helicobacter pylori*, in addition to the classical Fur repression paradigm, Fur can mediate the regulation of iron-induced genes through a mechanism that has been termed *apo*-Fur repression.

The *holo*- and *apo*-Fur repression has been verified on the promoters of the *frpB* and *pfr* genes, respectively, and shown to be associated with different iron-dependent binding affinities of Fur for specific operators within the promoter regions of these genes.

Thus, the *Hp*Fur exploits different mechanisms of DNA binding that are operator dependent and results in differential effects of Fe^{2+} on the binding ability of the protein to DNA (Delany *et al.*, 2001b).

To further characterize the *holo*- and *apo*-Fur-DNA interactions, we performed hydroxyl radical (OH*) footprinting experiments with probes consisting of the promoter regions under study, P_{frpB} and P_{pfr}. The use of hydroxyl radicals as the cleaving agent in footprinting experiments, provides more detailed information about the bases directly involved in protein-DNA contacts, thereby contributing to reveal the mechanicistic features of protein-DNA interaction that other methods fail to provide (e.g. DNase I footprinting). Each promoter probe, end-labelled at either the coding or the non coding DNA strand, was incubated with increasing amounts of tag-removed recombinant purified Fur protein, in the presence of 150 μM $MnCl_2$ or 150 μM 2,2'-dipyridyl (a specific iron chelator) and subjected to OH* cleavage. Manganese was used as a co-factor instead of iron, as it is more stable and has been shown to function like Fe^{2+} under in vitro binding conditions (Escolar *et al.*, 1999, de Lorenzo *et al.*, 1987).

Representative results of OH* footprinting from the coding strand of the P_{frpB} and P_{pfr} promoter probes are shown in Fig. 10. Consistently, the nucleotides protect

from OH* cleavage fall within the operator regions previously identified in DNase I footprinting experiments (Delany *et al.*, 2001b).

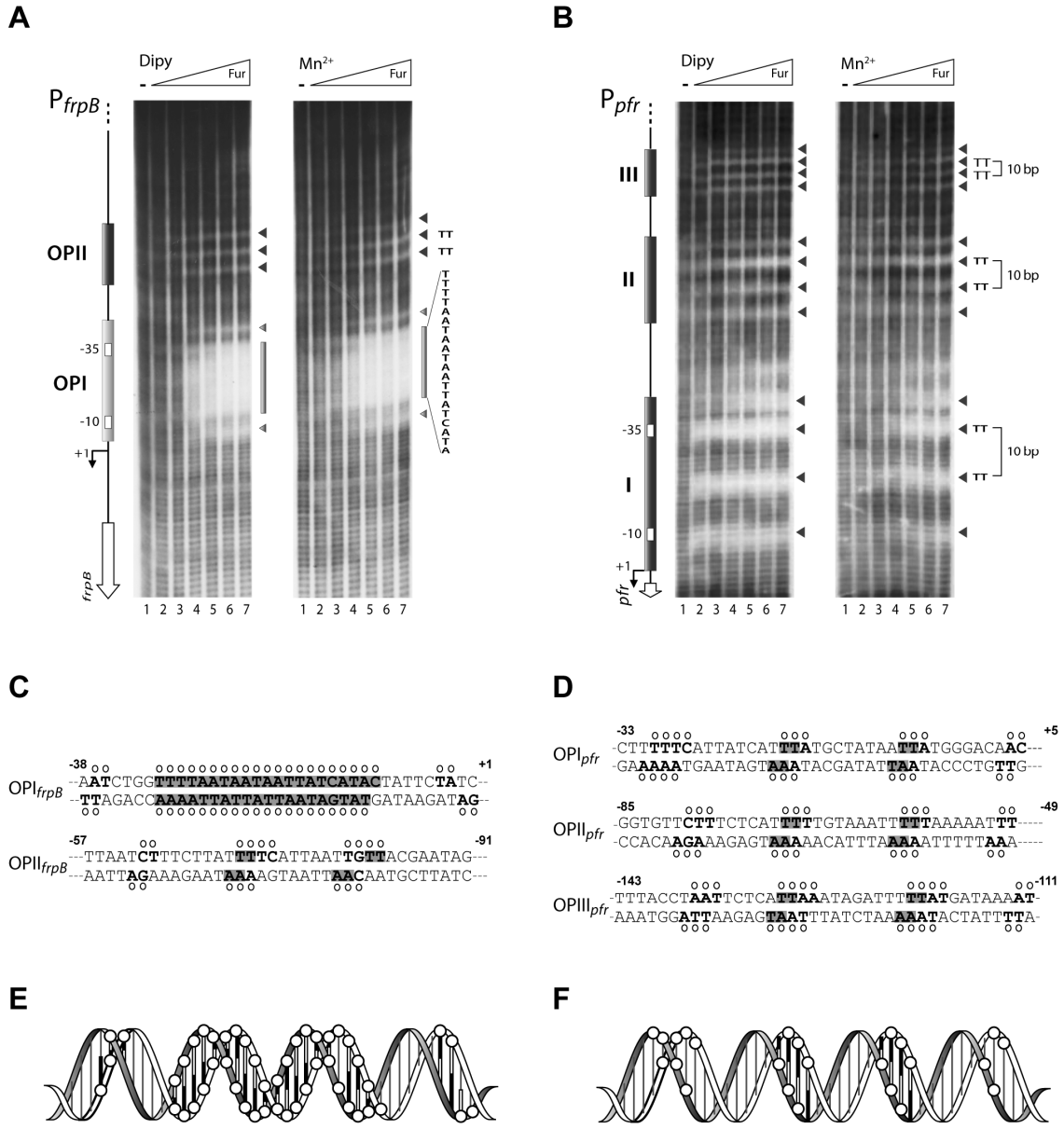

FIG. 10. Distinctive binding architecture of Fur to the P_{frpB} and P_{pfr} promoter regions. Specific DNA probes for P_{frpB} **(A)** and P_{pfr} **(B)** fragments, end labeled in their coding strands, were incubated with increasing amounts of recombinant Fur protein in presence of 150 µM 2,2'dipyridyl (marked Dipy, left panel) or in presence of 150 µM $MnCl_2$ (marked Mn^{2+}, right panel). Lanes 1 to 7; 0, 29, 61, 122, 244, 490, 980 nM Fur added, respectively. Left to each gel, light and dark grey boxes indicated the Fur binding sites, identified by DNase I footprinting

analysis, with highest affinity for *holo*- and *apo*-Fur, respectively (Delany *et al.*, 2001b). The open boxes on the right indicate the extended region of OH*protection, while the arrowheads indicate short protected areas from OH* cleavage. A G+A sequence reaction ladder for each promoter probe was run in parallel (data not shown) to map the protected bases. A bent arrow marks the transcriptional start site, the position of the -10 and -35 hexamers are symbolized by open rectangles, and the open reading frames are indicated by vertical open arrows to the left of each gel.
Summary of protection data on operators from P_{frpB} **(C)** and P_{pfr} **(D)**. For each operator, the numbers refer to the position with respect to the transcriptional start site (position1). Open circles indicate bases protected by Fur on the coding and non coding strand. Among them, the strong protected bases are shaded in grey. Representative helical projections of the hydroxyl-radical-protected residues on the OPI_{frpB} **(E)** and OPI_{pfr} **(F)** backbone. Hydroxyl-radical-protected residues are marked by open circles. Shaded and black bars in the DNA helix represent adenine and thymine bases respectively.

The OH* footprints highlighted important structural differences in the interaction of Fur with its operator regions. On the operator with the highest affinity for *holo*-Fur (i.e. OPI_{frpB}), the binding of Fur results in an extended footprint of 21 bp, mapping in an AT-rich region (Fig. 10A and 10C). Furthermore, at higher concentrations of Fur, two short additional stretches of protection, flanking symmetrically the core of the 21 bp protected region, appeared (Fig. 10A, lanes 6-7). Hence, OH* nicking revealed that Fur displays an extended protection pattern on an operator that is recognized with higher affinity by the *holo*-protein.

Similar results have been obtained from the non coding strand, which shows the identical extended footprint in the same region (data not shown, results are reported in Fig. 10C). This indicates protein wrapping around the DNA helix, as sketched in helical projections of the hydroxyl-radical-protected residues on a duplex DNA, modeled as a canonical B-form (Fig. 10E).

In striking contrast, the binding of Fur on operators with the highest affinity for the *apo*-protein (OPI, OPII, OPIII on P_{pfr} and OPII on P_{frpB}), results in a periodic pattern of four short protected regions of two/four nucleotides in length (Fig. 10B and 10D). The two central regions are separated by 10±1 bp, while the two flanking stretches are separated by 8±1 bp from the central core. Thus, the average periodicity of regions protected by Fur is close to 10 bp, and the protected areas on the non coding strands are offset form those of the coding strands by 1 nucleotide (data not shown, results are shown in Fig. 10D). Both these features are characteristic of protection of

the double helix on one face and that access of OH* nicking is permitted only on the other face of the helix (Tullius *et al.*, 1987). This indicates that Fur binds to one side of the DNA on these operators, as illustrated in Fig. 10F, in which OH*-protected bases are mapped onto a scheme of B-DNA.

Within the bases directly contacted by the *apo*-protein, Fur binds mainly to a couple of thymine dimers separated by a gap of 10bp (Fig. 10B). Fur binding to thymine dimers is consistent with results from previous work in *E. coli*, which pointed to two thymine dimers directly involved in Fur-DNA interactions (Tiss *et al.*, 2005). Moreover, it has been reported that the T residues could be an essential recognition element in direct contact with the Fur protein (Escolar *et al.*, 1998b).

Treatment with the metal ion, or iron chelator, affects differently Fur affinity toward the operators mapping in the P_{frpB} and P_{pfr} promoters (Fig. 10, panel A and B respectively). On OPI_{frpB}, in presence of Mn^{2+}, a protection is detected readily at 29 nM Fur (lane 2; Fig. 10A) whereas, in the absence of the metal ion, protection occurs at fourfold higher protein concentration (lane 4; Fig. 10A). In contrast, all three P_{pfr} operators ($OPI_{pfr,}$ $OPII_{pfr}$ and $OPIII_{pfr}$) and OPII on P_{frpB}, display an opposite behavior: the full protection occurs at lower protein concentration when the regulatory metal ion is chelated (compare lanes 2 and 7; Fig. 10B and 10A). This is consistent with what has been previously shown in DNase I footprinting analyses (Delany *et al.*, 2001b).

Notably, chelation of iron by the addition of 2,2'-dipyridyl resulted in a pattern of OH* protection that is indistinguishable form that observed after metal addition, suggesting that both operators are recognized by *holo*- as well as *apo*-Fur (Fig. 10A and Fig. 10B). Therefore, chelation of the regulatory metal has no effect on the specificity of Fur binding, but influences the affinity of the protein for DNA. This strongly suggests that the nucleotide sequence of each operator dictates the Fur binding architecture to DNA, irrespectively of the presence of the regulatory metal ion of the Fur protein.

Moreover, we verified if the multiple-operator promoter organization could affect Fur binding to single operators, due to possible co-operative effects. For this purpose, OH*footprinting assays were carried out on the single Fur operators isolated from the promoter context (see Material and Methods). The cloned operator regions OPI_{pfr}, $OPII_{pfr}$ $OPIII_{pfr}$ form P_{pfr} and OPI_{frpB} $OPII_{frpB}$ from P_{frpB}, were end labelled at either the coding or the non coding strand and subjected to OH* cleavage, with results

shown in Fig. 11. The results revealed protection patterns identical to those observed on the entire promoter regions: the same bases were protected by Fur (data not shown) and the binding architecture was maintained (compare Fig. 10A and B to Fig. 11A and B, respectively).

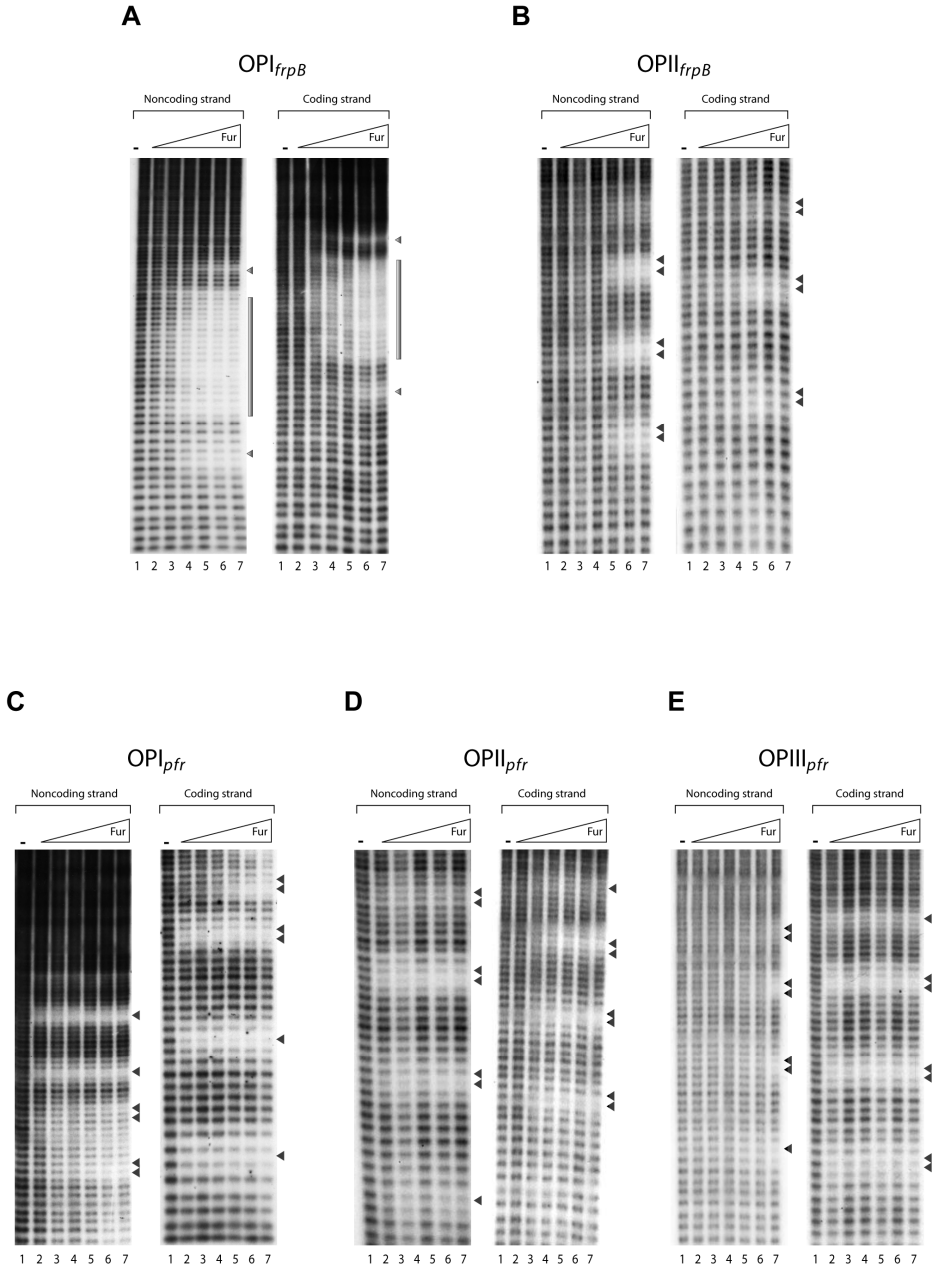

FIG. 11. Hydroxyl Radical footprinting on isolated DNA operators from P_{frpB} and P_{pfr}. Specific DNA probes for OPI$_{frpB}$ **(A)** OPII$_{frpB}$ **(B)** OPI$_{pfr}$ **(C)** OPII$_{pfr}$ **(D)** and OPIII$_{pfr}$ **(E)**, end labeled at their non coding and coding DNA strands, were incubated with increasing amounts of recombinant Fur protein and subjected to OH* cleavage. Lanes 1 to 7 contain 0, 29, 62, 122, 244, 490, 980

nM Fur, respectively. Symbols have been previously described in legend in Fig. 10. A G+A sequence reaction ladder for each promoter probe was run in parallel to map the protected bases (not shown).

Also in this case, while the presence/absence of metal divalent ions modulates the affinity of Fur for different operators, it did not influence the specificity and architecture of Fur binding (data not shown).

Taken together these results suggest that neither the metal ion cofactor, nor possible *in trans* effects due to the promoter structure, are responsible for the specific recognition of distinctive regulatory elements. Thus, the specific operator sequences dictate the binding architecture of Fur to DNA. Consequently, the molecular determinant responsible for the different mode of binding of Fur to DNA resides in *cis* within the operator sequences. Accordingly, two different operator typologies, here named *holo*- and the *apo*-operators, are characterized by a distinctive binding architecture of the protein, which are recognized with higher affinity by *holo*- and *apo*-Fur, respectively

5.2 Fur binding architecture on P_{fecA1} and P_{fecA2}

In order to verify whether the characteristic binding architecture of Fur on the *holo*- and *apo*-operators could represent a general rule for discriminating binding of Fur, we extended OH* footprinting analysis on other Fur regulated promoters, P_{fecA1} and P_{fecA2}, whose genes have been reported to be iron repressed in a Fur-dependent fashion (van Vliet *et al.*, 2002, Danielli *et al.*, 2009). Figure 12 shows the pattern of protection of Fur on the P_{fecA1} and P_{fecA2} promoters probes.

Once more, on operators recognized with higher affinity by the *holo*-protein (OPI_{fecA1} and $OPII_{fecA2}$), Fur binds a continuous AT-rich stretch of about 20 bp, displaying the extended protection pattern similarly to that observed previously on P_{frpB} OPI (compare Fig. 10A and Fig. 12A).

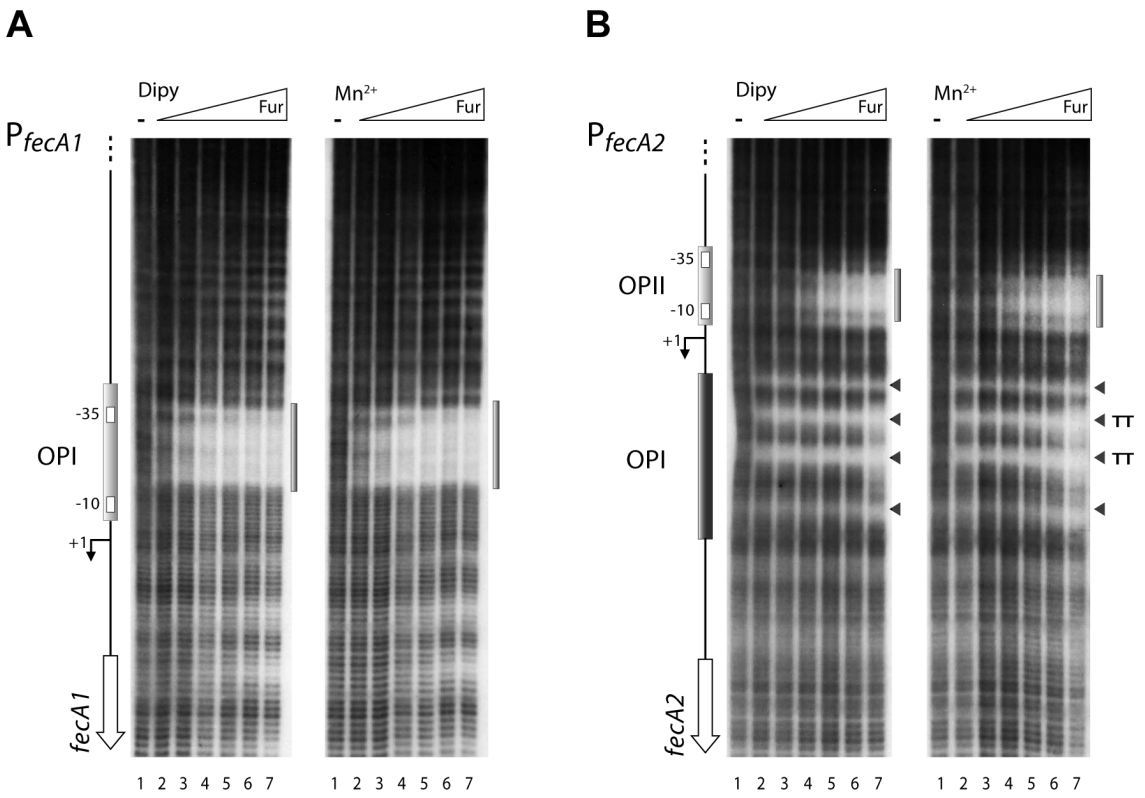

FIG. 12. Distinctive binding architecture of Fur to the P_{fecA1} and P_{fecA2} promoter regions. Specific DNA probes for P_{fecA1} **(A)** and P_{fecA2} **(B)** fragments, end labeled in their coding DNA strands, were incubated with increasing amounts of recombinant Fur protein in presence of 150 µM 2,2'dipyridyl (marked Dipy, left panel) or in presence of 150 µM $MnCl_2$ (marked Mn^{2+}, right panel). Lanes 1 to 7 contain 0, 29, 61, 122, 244, 490, 980 nM Fur, respectively. Left to each panel, light and dark grey boxes indicate the Fur binding sites, identified by DNase I footprinting analysis, with highest affinity for *holo*- and *apo*-Fur, respectively (Danielli *et al.*, 2009). The grey box on the right indicate the extended region of OH*protection, while the arrowheads indicate short protected areas from OH* cleavage. A G+A sequence reaction ladder for each promoter probe was run in parallel (data not shown) to map the protected bases. A bent arrow marks the transcriptional start site, the position of -10 and -35 promoter elements are symbolized by open rectangles, and the open reading frames are indicated by vertical open arrows to the left of each gel.

In addition, on OPI_{fecA2}, Fur exhibits a periodic pattern of four protected areas with a central couple of thymine dimers separated by 10 bp, whilst the affinity of the protein remains unaltered in the presence or absence of a metal regulatory ion (Fig. 12B).

These results validate a direct association between the peculiar binding architecture of Fur and the differential iron responsive binding of the *holo*- and the *apo*-protein to specific DNA operators.

6. TCATT$_{n10}$TT: Consensus motif for *apo*-Fur recognized operators

Currently, little is understood about the sequences important for *Hp*Fur binding to target promoters. One common feature among Fur boxes is the high number of A/T nucleotides relative to C/G nucleotides. Thus, it is perhaps not a surprise that the definition of a consensus box is somewhat hindered by the fact that the *H. pylori* genome is highly AT-rich (Tomb *et al.*, 1997). Accordingly, a consensus sequence is still ill-defined and this is true for both *holo*- and *apo*-Fur (Carpenter *et al.*, 2009b).

For *holo*-Fur binding, a consensus sequence was proposed, consisting of an AT-rich region encompassing two repeats of the AAT triplet (Merrell *et al.*, 2003). This consensus sequence is significantly different form that for *E. coli* (de Lorenzo *et al.*, 1987) and is certainly less conserved, even among *H. pylori* Fur-regulated genes, than the *E. coli* sequence (Carpenter *et al.*, 2009a). Instead, to date, there is no defined consensus sequence for *apo*-Fur binding.

To gain information on a putative consensus motif required for recognition by either *holo*- or *apo*-Fur, we performed sequence analysis of the differentially recognized operators, previously analyzed by OH* footprinting assays (Fig. 10 and 12). The sequence of three *holo*-Fur recognized operators (OPI$_{frpB}$, OPI$_{fecA1}$ and OPII$_{fecA2}$) and sequences of the four *apo*-Fur recognized operators (OPI$_{pfr}$, OPII$_{pfr}$, OPII$_{pfr}$ and OPI$_{fecA1}$) were aligned with the CLUSTAL W computer program. Alignments were subsequently submitted to the Web LOGO program to built a consensus logo sequence reported in Fig. 13 (Larkin *et al.*, 2007, Thompson *et al.*, 1994).

For the *holo*-recognized operators, this analysis revealed an AT-rich nucleotide stretch with multiple and contiguous AAT triplets, tentatively organized in a TAATAAT$_{n2}$ATTATTA inverted repeat (Fig. 13A). By contrast, sequence analysis of the *apo*-Fur recognized operators led to the identification of a peculiar consensus motif TCATT, separated by a gap of 10 bp from a thymine dimer (Fig. 13B). Interestingly, the TCATT$_{n10}$TT consensus motif encompasses the thymine dimers directly protected by Fur in OH*FP analyses (Fig. 10 and Fig. 12).

We conclude that the *holo*-Fur might recognize sequences within the *holo*-operator, which is an AT-rich inverted repeat, TAATAAT$_{n2}$ATTATTA, while the *apo*-Fur might recognize sequences within the newly identified *apo*-operator TCATT$_{n10}$TT.

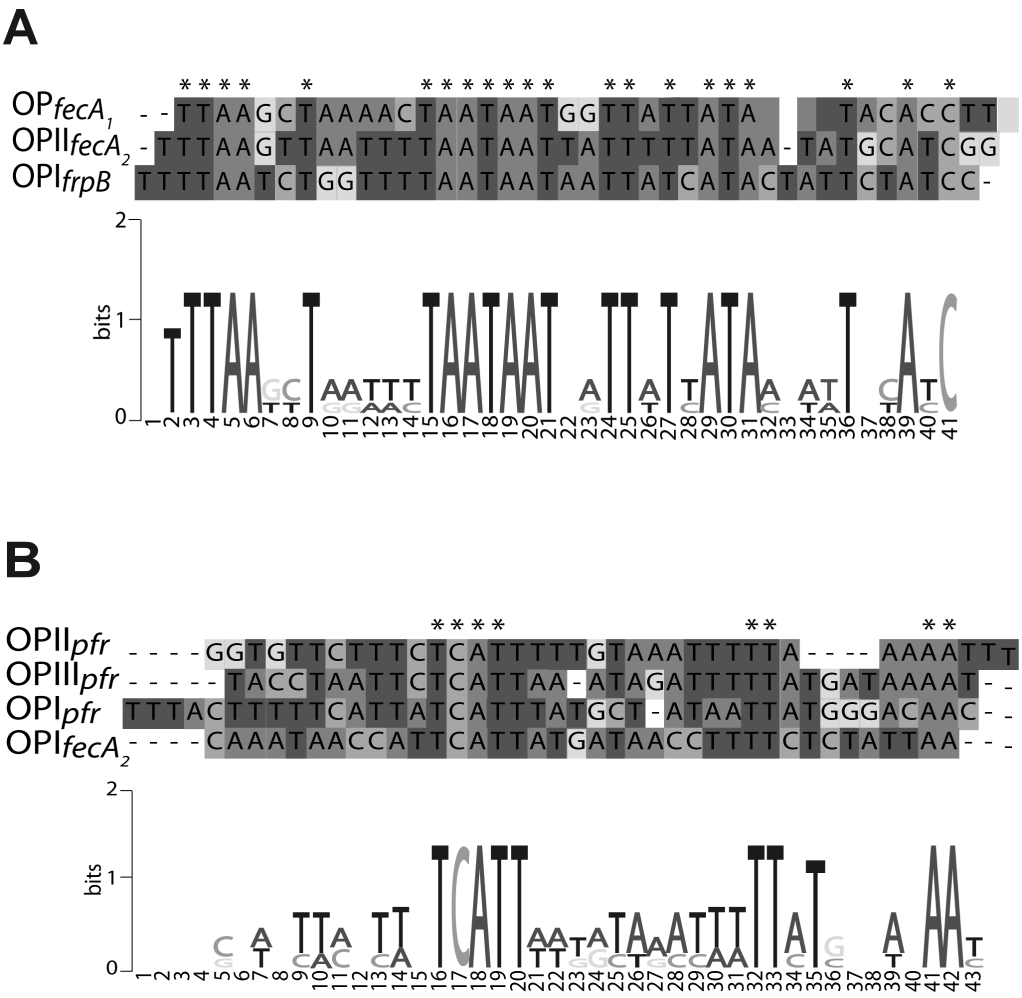

FIG. 13. Consensus motifs of the *H. pylori holo*- and *apo*-Fur recognized operators. Sequence alignment for *holo*-Fur controlled operators **(A)** and *apo*-Fur recognized operators **(B)** are aligned at the top of each panel. Asterisks above the sequence alignments indicate conserved bases. Alignments were used to generate a sequence logo, reported at the bottom of each panel. The height of each letter corresponds to its relative abundance at that position.

7. $TCATT_{n10}TT$ is the recognition element for Fur binding to an *apo*-Fur recognized operator

The $TCATT_{n10}TT$ motif has been proposed as consensus motif for the *apo*-Fur binding (See Chapter 6). In order to verify the functional role of this consensus motif, we decided to evaluate the binding affinity of the *apo*- and *holo*-Fur on the wild type and mutant *apo*-operator. To this aim, we carried out mutagenesis of *pfr* operator I (OPI_{pfr}), that is the operator with highest affinity for the *apo*-protein (Fig. 9; (Delany *et al.*, 2001b). We started with mutagenesis of the C base since it provides a discriminating element in the AT-rich background of the $TCATT_{n10}TT$ element. Sequence analysis of OPI_{pfr}, revealed the presence of another incomplete TCATT element upstream of the identified consensus motif. For this reason, we substituted the C base to A in one or both TCATT elements, generating the mutants $OPI_{pfrc11a}$ and $OPI_{pfrc11\text{-}17c}$, respectively (Fig. 14A).

The binding of Fur to wild type (OPI_{pfr}) and mutant *pfr* OPI operators ($OPI_{pfrc11a}$ and $OPI_{pfrc11\text{-}17a}$, respectively) was investigated by electrophoretic mobility shift assays (EMSA). EMSA was performed incubating probes encompassing the operators under study, which spans from positions -36 to +5 of the promoter regions of the *pfr* gene, with increasing amounts of purified Fur protein, in presence of 150 μM Fe^{2+} or 150 μM 2,2 dipyridyl. Fur-DNA complexes were resolved on native polyacrylamide gels, the intensity of discrete bands was quantified (with a phosphorimager), and the K_D was determined by plotting both free and bound DNA as function of the protein concentration.

Figure 14B shows the binding affinity curves to the wild type operator probe $OPI_{pfrwt.}$. In the absence of iron, 1.5 nM Fur was necessary to shift 50% of the probe (K_D), whereas the K_D of the Fur-DNA complexes formed in presence of iron was calculated as 6 nM. Therefore, the affinity of *apo*-Fur is fourfold higher than the affinity of *holo*-Fur for OPI_{pfrwt}. These results provide further evidence that the *pfr* operator I is the operator with the highest affinity for *apo*-protein, confirming previous DNase I (Delany *et al.*, 2001b) and OH* footprinting assays (Fig. 10). In addition, this data strengthen the idea that the molecular determinant responsible for the different,

metal-dependent mode of binding of Fur to DNA is carried *in cis*, within the operator sequence.

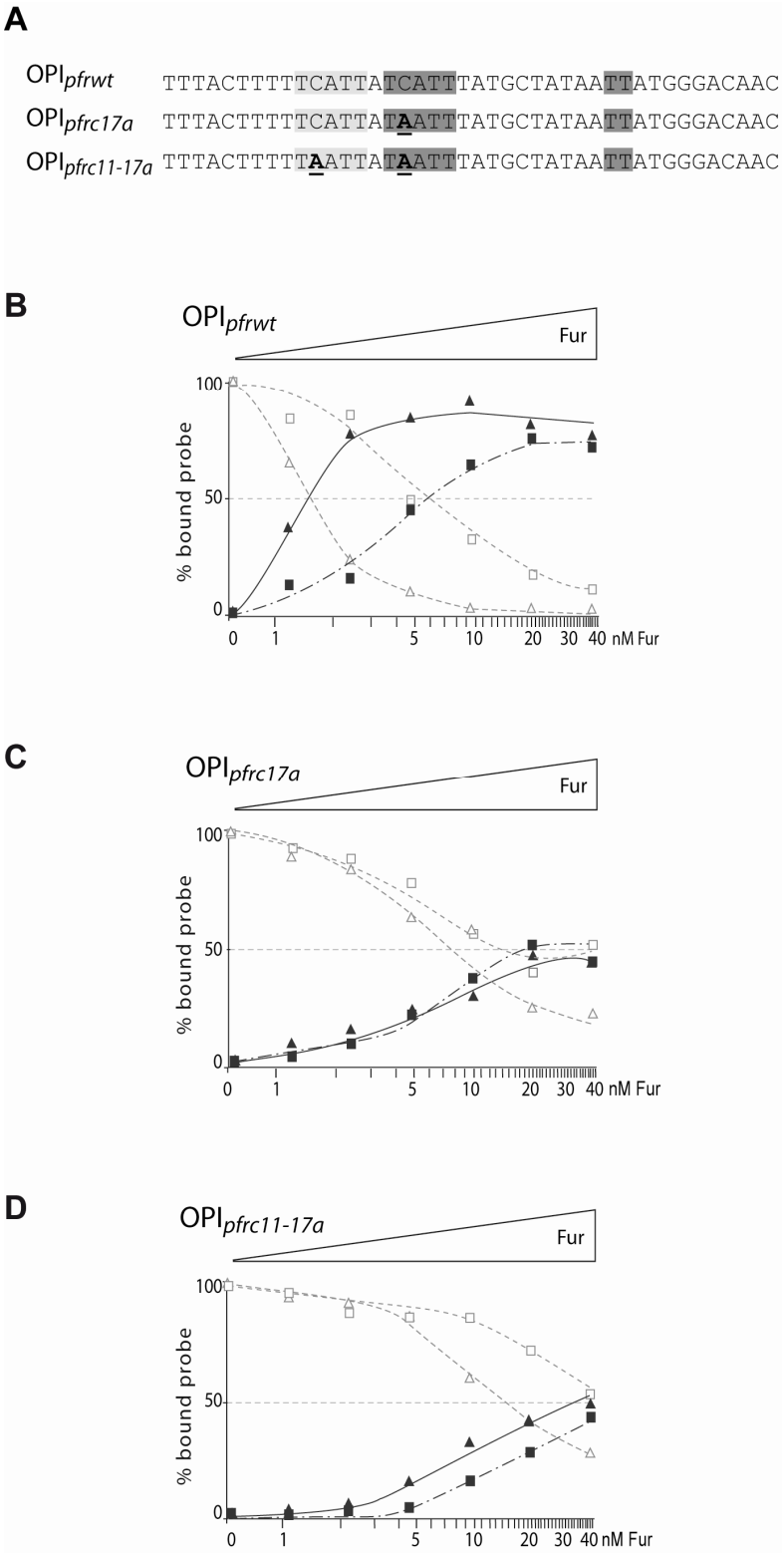

FIG. 14. Role of the TCATT$_{n10}$TT motif in Fur binding. (A) Nucleotide sequence alignment of wild-type OPI$_{pfr}$ and mutants OPI$_{pfrc17a,}$OPI$_{pfrc11-17a}$. The identified consensus TCATT$_{n10}$TT motif, and the additional TCATT element are shaded in dark and light grey respectively. Underlined bold letters indicate the point mutation affecting the TCATT elements. EMSA assays with OPI$_{pfrwt}$ **(B)**, OPI$_{pfrc17a}$ **(C)**, and OPI$_{pfrc17c11a}$ **(D)**. Samples of approximately 0.6 nM of 5'-end-labeled probes were incubated with increasing amount of Fur protein (indicated below each graph) in presence of 150 µM Fe^{2+} (squares) or 150 µM 2,2' dipyridyl (triangles). Affinity of Fur to DNA was calculated by plotting the percentage of both bound (closed triangles and closed squares) and free probe (opened triangles and opened squares) versus protein concentration in presence or absence of iron. The K_D was defined as protein concentration required to shift 50% of the probe.

In contrast, the binding studies reported in Fig. 14C and 14D show that the mutant operators OPI$_{pfrc11a}$ and OPI$_{pfrc11-17a}$ are bound by Fur only at the highest protein concentration employed in the binding reactions (40 nM), both in presence or in absence of iron. Thus, the affinity of Fur decreases significantly for both mutant operators, despite the absence of the metal cofactor in the binding reaction.

This loss of affinity likely reflects the fact that the introduced mutation affects the motif responsible for Fur recognition of this operator, suggesting that an integer TCATT$_{n10}$TT recognition element is needed for high affinity binding of Fur to an *apo*-operator.

8. Helical phasing of TT dimers affects *holo*-Fur binding architecture on an *apo*-operator

The substitution of the C base within the $TCATT_{n10}TT$ motif significantly reduced the metal-dependent Fur binding to OPI_{pfr}, indicating a key role of this element in *apo*-Fur binding. It will be noted that, the two thymine dimers of the $TCATT_{n10}TT$ element are separated by 10 bp, indicating that they are located at the same face of the DNA helix (Fig. 10F). Therefore, we set out to investigate whether the precise helical phasing of thymine dimers of the $TCATT_{n10}TT$ element could also be important for preferential recognition by *apo*-Fur. We constructed a mutant operator, OPI_{pfrsw}, in which the original spacing between TT residues found in OPI_{pfr} was reduced of 5bp, corresponding to half an helix turn, resulting in thymine dimers TT located at opposite faces of the DNA helix (Fig. 15A). Furthermore, the construction of this mutant places a CT dinucleotide in the same position of TT dimer, thus representing also a single T to C base substitution.

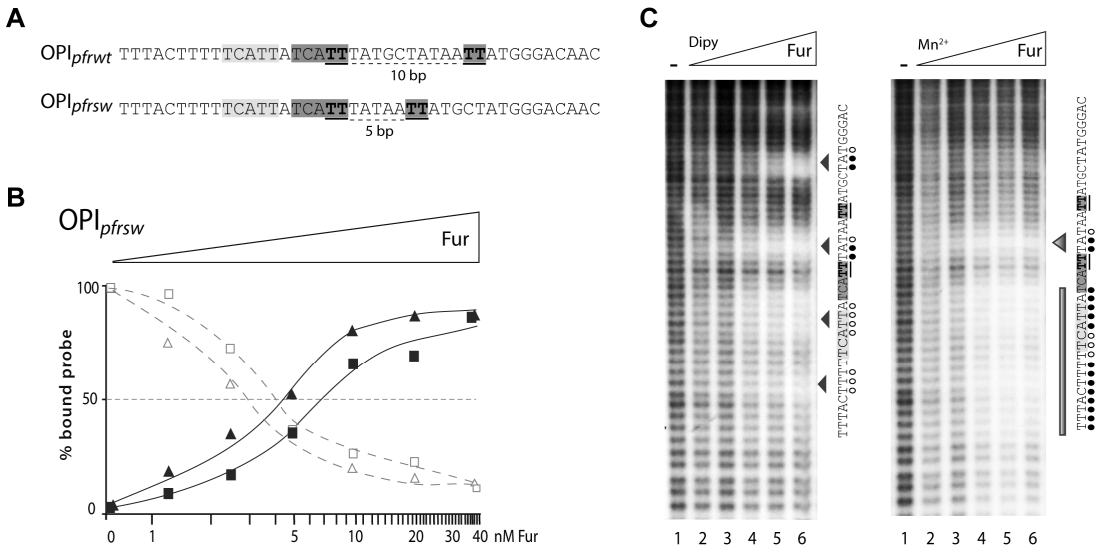

FIG. 15. Fur binding to an apo-recognized operator as a function of helical spacing between TT dimers. (A) Nucleotide sequence alignments of OPI_{pfrwt} and OPI_{pfrsw} display the variation in spacing between TT dimers corresponding to a half helix turn. Thymine dimers are in bold and

underlined. The $TCATT_{n10}TT$ motif is shaded in grey. **(B)** The affinity of Fur for OPI_{pfrsw} was determined by plotting the percentage of shifted probe versus protein concentration in the presence of Fe^2 or 2,2'dipyridyl, marked as closed squares and closed triangles, respectively. The amount of free probe was calculated in presence or absence of iron, indicated as opened squares and opened triangles, respectively. **(C)** Hydroxyl radical footprints of Fur on the OPI_{pfrsw} mutant operator. Arrows to the right of each gel, mark short protected areas from OH* protection, while the grey vertical bar indicates extended region of OH* protection. Open circles indicate bases protected by Fur. Among these, filled circles indicate the strong protected bases. The first lane marked (-) contains the OH* reaction in absence of Fur protein, and subsequent lanes contain reactions with increasing amounts of Fur. Lanes 1 to 6 contained 0, 29, 61, 122, 244 and 490 nM Fur added, respectively.

The effects of this mutation on Fur binding to OPI_{pfrsw} were investigated first by EMSA. As shown in Fig. 15B, 4.5 nM Fur was required to bind 50% of the probe in absence of iron, while 1.5 nM *apo*-Fur was necessary to bind the same fraction of the wild-type OPI_{pfr} operator probe (compare Fig.15B and Fig. 14B). Thus, the affinity of *apo*-Fur decreases 3-fold in this mutant. In contrast, the affinity of *holo*-Fur towards this mutant operator, OPI_{pfrsw}, showed an unaltered K_D (7nM) with respect to the wild-type OPI_{pfr} operator I (compare Fig. 15B and Fig. 14B). Thus, the distance of 10 bp between two intact TT dimers seems to be the key element for the preferential binding of *apo*-Fur on an *apo*-operator.

To verify the binding architecture of Fur on this mutant operator, the protection pattern of Fur binding to the OPI_{pfrsw} was analyzed by OH*footprinting experiments. The results shown in Fig. 15C indicate that the *apo*-Fur binding architecture on OPI_{pfrsw} looks very similar to that observed for OPI_{pfrwt} (compare left panel Fig. 15C with Fig. 10B and Fig. 13C). In fact, Fur still protects short stretches of four nucleotides with an average periodicity close to 10 bp, albeit, in this case, the protein binds mainly two TA nucleotides dimers separated by 10 bp. Accordingly, the affinity of *apo*-Fur is significantly reduced, with protection occurring only at 122 nM protein concentration (compare Fig. 15C; left panel with Fig. 11C) in line with decreased *apo*-Fur affinity observed in EMSA experiments.

Therefore, the binding architecture of *apo*-Fur on OPI_{pfrsw} is unaffected by mutations of TT dimers, while the affinity is affected. In contrast, in presence of metal ions, Fur binds just one TA nucleotides dimer and starts to extend its protection toward a

downstream region of about 15 bp, displaying a partial extended protection pattern (Fig. 15C; right panel). Hence, for the first time, a differentiation in Fur binding architecture on the same operator was observed in response to the presence of divalent metal ions.

9. Reconstitution of the TCATT$_{n10}$TT motif within an *holo*-operator changes the *holo*-Fur operator into an *apo*-Fur recognized operator

Taking into account that the *holo*-Fur-box of *H. pylori* appear as an AT-rich region with inverted repeats of AAT triplets (see Fig.13 and Merrell *et al.*, 2003) we reasoned that the well-defined TCATT$_{n10}$TT motif could be critical to allow Fur to correctly discriminate between *apo*- and *holo*-operators. To verify this hypothesis, the TCATT$_{n10}$TT motif was reconstituted in the *holo*-Fur recognized *frpB* operator I (OPI$_{frpB}$) by substitution of solely four bases within the native OPI$_{frpB}$ nucleotide sequence. Thereby, a motif similar to that found in the *apo*-Fur recognized operator OPI$_{pfr}$ was created (Fig. 16A).

Once again, the binding affinity of Fur to the wild-type (OPI$_{frpBwt}$) and mutant *frpB* operator (OPI$_{frpBsw}$) was tested by EMSA in presence of either 150 μM Fe^{2+} or 150 μM 2,2' dipyridyl. The binding affinity curves of Fur to OPI$_{frpBwt}$ and OPI$_{frpBsw}$ operators are shown in Fig. 16B. The K_D of Fur towards OPI$_{frpBwt}$ in presence of iron was calculated as 11 nM Fur, while the K_D after iron chelation with 2,2' dipyridyl, was 27 nM (Fig. 16B, left panel). Therefore, *holo*-Fur binds with higher affinity than *apo*-Fur to OPI$_{frpBwt}$, providing further evidence that the *frpB* operator I exhibits higher affinity for the *holo*-protein.

On the contrary, 5 nM Fur was sufficient to shift 50% of the OPI$_{frpBsw}$ mutant probe when iron was chelated, whereas the K_D of OPI$_{frpBsw}$ binding remained unaltered in the presence of iron with respect to OPI$_{frpBwt}$ (11 nM; Fig. 16B, right panel). Thus, *apo*-Fur exhibits a twofold increase of affinity to OPI$_{frpBsw}$ over *holo*-Fur, which instead binds both OPI$_{frpBsw}$ and OPI$_{frpBwt}$ with the same affinity (Fig. 16B; see curves with closed square). In addition, *apo*-Fur affinity for OPI$_{frpBsw}$ is 4.5 fold higher than that for OPI$_{frpBwt}$ (K_D= 5 nM and 27 nM for OPI$_{frpBsw}$ and OPI$_{frpBwt}$ respectively).

This indicates that Fur binds to OPI$_{frpBsw}$ with higher affinity in its *apo*-form, providing the first evidence of a swap in the metal responsive binding affinity of the Fur protein. Based on this finding, we conclude that the reconstitution of the TCATT$_{n10}$TT motif in an *holo*-Fur operator swaps the iron responsive binding of the Fur protein.

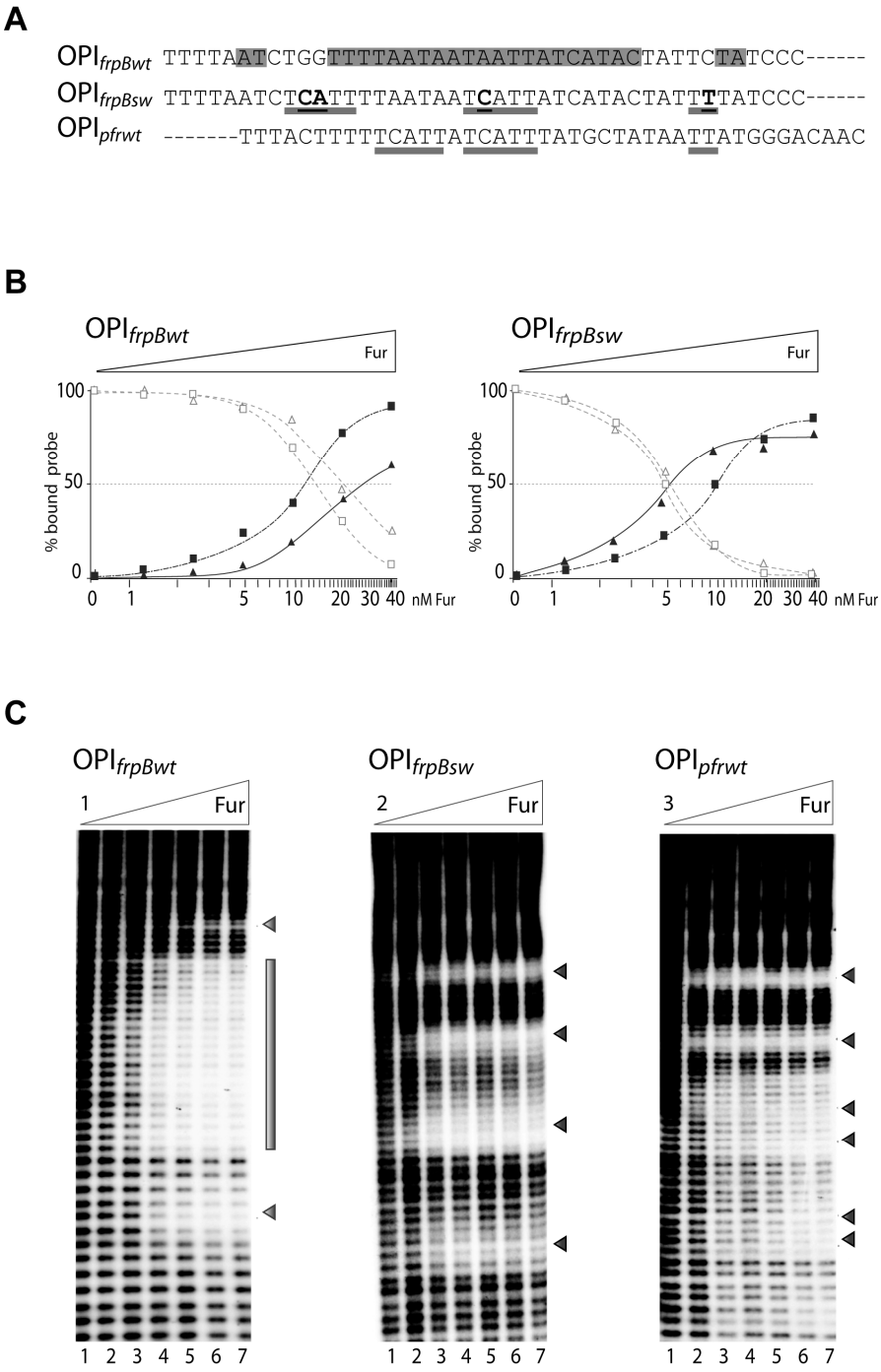

FIG. 16. Feature binding swap of Fur from an *holo*-Fur to an *apo*-Fur recognized operator. (A) Sequence alignments of OPI_{frpBwt}, OPI_{pfrwt} and derived mutant OPI_{frpBsw}, illustrating the reconstitution of the $TCATT_{n10}TT$ element in an *holo*-Fur recognized operator. The extended protection pattern of Fur on an *holo*-operator is shaded in grey. Horizontal bars mark the TCATT elements and TT dimers. Underlined bold nucleotides indicate substitutions from the wild type *frpB* operator I. **(B)** EMSA and **(C)** OH*Footprinting assays on OPI_{frpBwt}, OPI_{frpBsw} and OPI_{pfrwt}. Symbols have been previously described in legend for Fig. 14.

Next, OH* footprinting were performed to investigate whether the $TCATT_{n10}TT$ motif within the swapped mutant OPI_{frpBsw} could also impair the binding architecture of Fur. Remarkably, the binding architecture turned from the typical extended protection pattern distinctive of an *holo*-operator (Fig. 16C, left panel) to a periodic pattern of four protected regions separated by approximately ten OH* sensitive base pairs (Fig. 16C, middle panel). This pattern is very similar to the well-characterized protection pattern, found in operators recognized with higher affinity by the *apo*-protein (Fig. 16C, left panel). Consistently, Fur binds mainly the thymine dimers separated by 10 bp of the $TCATT_{n10}TT$ element reconstituted in OPI_{frpBsw} (data not shown), as previously shown for the *apo*-operator $OPI_{pfr.}$ (Fig. 10B and 10D). Again metal chelation or repletion had no effects on the Fur binding architecture (data not shown). Thus, the reconstitution of the $TCATT_{n10}TT$ motif in an *holo*-Fur operator affects also the Fur binding architecture, changing the protection pattern of Fur.

Taken together these data confirm the feature binding swap of Fur form an *holo*-Fur to an *apo*-Fur recognized operator and confirms that the $TCATT_{n10}TT$ consensus motif is the distinctive element of the *apo*-operators needed for high affinity *apo*-Fur binding. This demonstrates that the specific operators sequence dictates the mode of binding of Fur to DNA, which implies the distinctions between the *holo*- and *apo*-operator as two different operator typologies.

10. Reconstitution of the TCATT$_{n10}$TT motif within an *holo*-operator affects Fur-regulation *in vivo*

In order to verify the role of different operators typologies on the iron-dependent regulation of Fur *in vivo*, two transcriptional fusions were constructed. The wild-type and swapped *frpB* operators, OPI$_{frpBwt}$ and OPI$_{frpBsw}$ (Fig. 16A), encompassing the *frpB* promoter elements, were cloned upstream of a promoterless *lacZ* gene (OPI$_{frpBwt}$-*lacZ* and OPI$_{frpBsw}$-*LacZ*; see Material and Methods). Both transcriptional fusions were inserted by homologous recombination in the *vacA* locus of wild-type and *fur* knockdown mutant strains (*H. pylori* G27 and G27*fur*, respectively).

Fur- and iron-dependent regulation of the transcriptional fusions was monitored by primer extensions analyses on total RNA extracted from exponentially growing *H. pylori* cultures treated for 15 min with 1mM Fe^{2+} or 150 μM 2,2'dipyridyl in parallel with results shown in Fig. 17. In the parental G27 background, transcription of OPI$_{frpBwt}$-*lacZ* fusion is almost completely repressed by Fe^{2+} treatment (Fig. 17A lane 1). Iron chelation leads to a marked de-repression of the transcriptional fusion (Fig. 17A, lane 2) while in the G27*fur* background transcription of OPI$_{frpBwt}$-*lacZ* is constitutively derepressed (Fig. 17B, lanes 1 and 2).

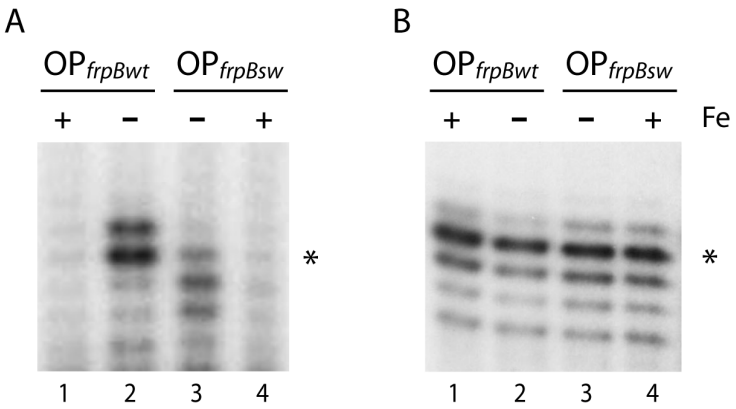

Fig. 17. Primer extension with total RNA extracted at mid-log growth phase from a recombinant G27 wild-type **(A)** and G27*fur* **(B)** strains, harboring the OPI$_{frpB}$-*lacZ* transcriptional fusions with wild-type OPI$_{frpBwt}$ and mutated OPI$_{frpBsw}$ operator I in response to different environmental iron conditions: 1mM $(NH_4)_2Fe(SO_4)_2$; or 150 μM 2,2'-dipyridyl (marked + or –, respectively). The elongated primer is marked with an asterisk.

This provides compelling evidence that the OPI_{frpBwt} *holo*-operator, encompassing the native -10 box, retains the molecular determinant responsible for the correct iron-dependent Fur regulation, in *cis*. On the other hand, transcription of the OPI_{frpBsw}-*LacZ* fusion, bearing the swapped *frpB* operator, is similarly repressed by iron and constitutively derepressed in a Δ*fur* background. However, the de-repressive effect of iron-chelation is significantly reduced in the parental G27 strain (Fig. 17A and B lanes 3-4). Thus, the presence of the $TCATT_{n10}TT$ element, characteristic of *apo*-Fur repressed operators, within OPI_{frpBsw}, does not affect the iron-dependent repression (compare lanes 1 and 4 of Fig.17A) but rather impairs the de-repressive effect of iron chelation (compare lanes 2 and 3 Fig. 17A).

These data demonstrate that the $TCATT_{n10}TT$ element confers *apo*-repression features to Fur. This is consistent with the in vitro data, which showed that the presence of the $TCATT_{n10}TT$ had no effects on the *holo*-Fur binding affinity but confers higher affinity to the *apo*-protein towards OPI_{frpBsw} containing the $TCATT_{n10}TT$

11. Recognition of either minor or major groove DNA establishes Fur binding to the *holo*- and *apo*-operators.

Fur binding to *apo*-operators occurs on two TT dimers on the same face of the DNA helix. By contrast, the binding of Fur to *holo*-operators occurs on continuous stretch of AT nucleotides arranged in AAT triplets (Fig. 10).

It has been reported that AT-rich tracts, defined as three or more As or Ts that not contain the flexible TpA step, have a strong tendency to narrow the minor groove (Burkhoff *et al.*, 1988, Crothers *et al.*, 1999, Haran *et al.*, 2009). This structural feature is exploited by some families of DNA binding proteins [Hox protein SCR (Joshi *et al.*, 2007), POU homeodomains (Remenyi *et al.*, 2001), MATα1-Matα2 (Li *et al.*, 1998)] to recognize the enhanced electrostatic potential induced by narrowing of the minor groove (Rohs *et al.*, 2009, Tullius, 2009). Accordingly, we hypothesized that a similar requirement for Fur binding to the *holo*-operators, could rely on the direct recognition of the minor groove width or structure, rather than to the readout of a specific nucleotide sequence.

In order to verify this hypothesis, we set out to implement (DNA-binding) interference experiments with the minor groove binding drug Distamycin A. With a crescent-shaped structure composed of planar aromatic groups joined by amide bonds (Fig. 18A), distamycin A binds deeply within minor groove at AT-rich sequences (Fig. 18B).

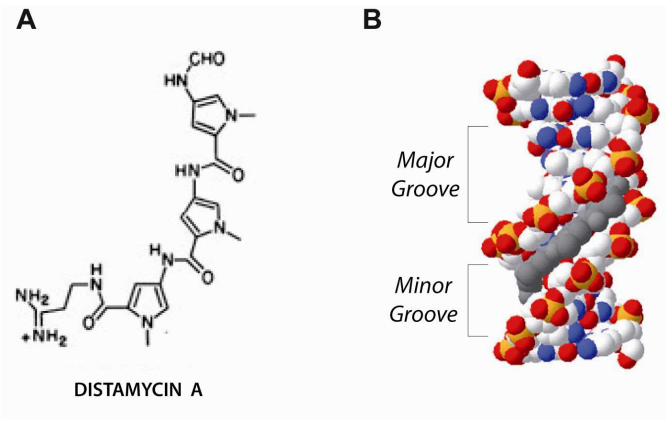

Fig. 18. (A) Structure of Distamycin A**; (B)** van der Waals diagram of the DNA-Distamycin complex. Distamycin is colored in grey, whereas DNA follows typical CPK color assignments.

The binding specificity for AT-rich regions in DNA is probably due to better van der Waals contacts between the drug and groove walls in this region, since A/T regions are narrower than G/C groove regions and also because of the steric hindrance in the latter, presented by the C2 amino group of the guanine base (Coll *et al.*, 1987, Churchill *et al.*, 1990, Van Dyke *et al.*, 1982).

To determine whether the drug would be useful to interfere with Fur binding to both the *holo*- and *apo*-operator OPI_{frpB} and OPI_{pfr}., the binding sites for distamycin were first characterized by hydroxyl radical footprinting (Fig. 19). Specific protections were detected within the same regions protected by Fur on both OPI_{frpB} and OPI_{pfr}. The length of protection, 4-5bp in size, is consistent with the length previously reported in distamycin OH* footprints (Churchill *et al.*, 1990).

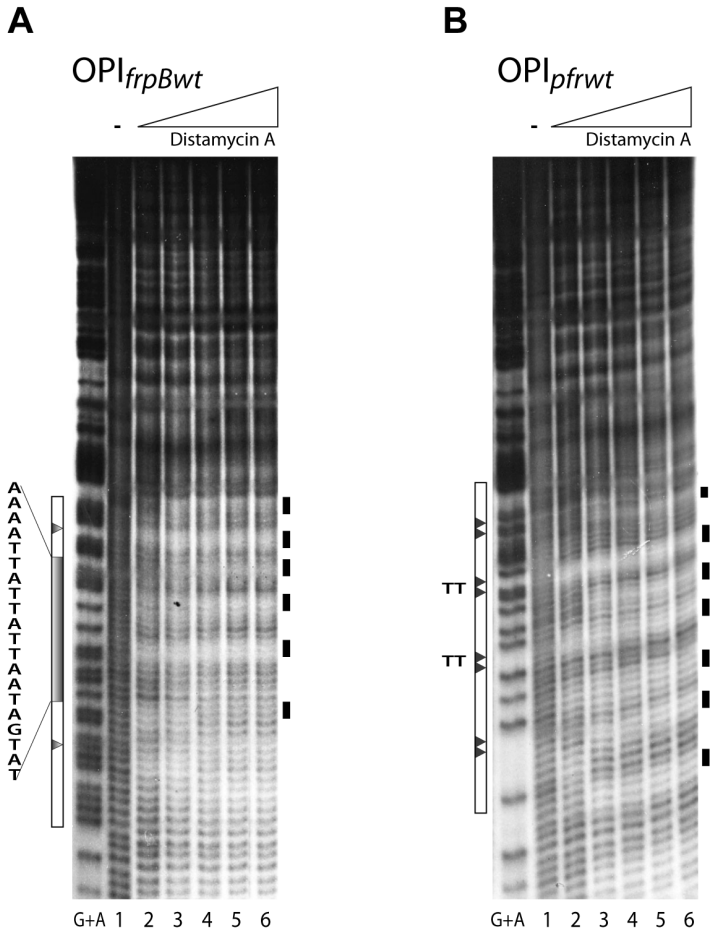

Fig. 19. Hydroxyl radical footprints of Distamycin A on OPI_{frpBwt} and OPI_{pfrwt}. Specific DNA probes for OPI_{frpBwt} **(A)** OPI_{pfrwt} **(B),** end labeled at their coding strands, were incubated with

increasing amount of minor groove binder Distamycin A and subjected to OH* cleavage. Lanes 1 to 6; 62.5, 125, 250, 500, 1000 mM Distamycin, respectively. On the left of each panel, open boxes define the operator region. The grey box and arrowheads within the open boxes indicate the regions protected by Fur as previously identified by OH*footprinting analysis (see Fig. 10). On the right of each panel, small dark boxes map Distamycin binding sites.

The overlapping Fur and distamycin binding patterns permitted to ask whether distamycin binding in the minor groove could interfere with binding of Fur. We used EMSAs to determine the effect of distamycin on Fur binding to both the *holo*- (OPI_{frpB}) and *apo*-operators (OPI_{pfr}). The assays were performed by preincubating operator probes with increasing amounts of distamycin followed by the addiction of purified Fur protein. (Fig. 20).

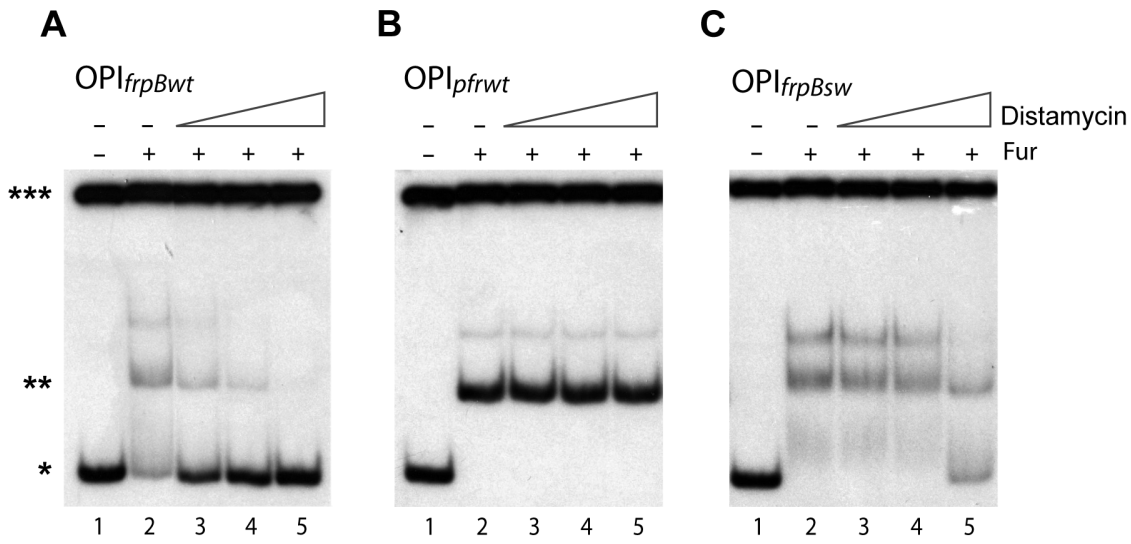

Fig. 20. Competition of minor groove binding drug Distamycin A with Fur binding to the OPI_{frpBwt} (A), OPI_{pfrwt} (B) and OPI_{frpBsw} (C). Incubation of labelled DNA fragments with Distamycin A preceded the addition of Fur protein. Complexes were separated from free DNA on native polyacrylamide gel followed by autoradiography. Fur concentration employed in each binding reaction is 40 nM. Lane 1 indicates DNA control. Lane 2 represents Fur DNA complexes with no drug treatment. Lanes 3-5 denoted addiction of Distamycin A at concentration of 1.2, 2.4 and 4.8 nM respectively. Single asterisk indicates free probe, double asterisks Fur DNA complexes and three asterisks pBluescript KS used as non specific competitor in binding reactions.

Although Fur binds to OPI_{frpB} with lower affinity than OPI_{pfr} (compare lanes 2 in Fig. 20A and B), as little as 1.2 nM distamycin is sufficient to start to prevent Fur binding to the *holo*-operator OPI_{frpB} (lane 3, Fig. 20A). At 2.4 nM distamycin half maximal Fur-OPI_{frpB} complex formation is inhibited, while at higher drug concentration a complete inhibition of complex formation is observed (lane 5, Fig. 20A). Conversely, at the same distamycin concentrations, binding to the OPI_{pfr} *apo*-operator is totally unaffected (Fig. 20B). These results show that distamycin outcompetes Fur binding to OPI_{frpB} but not to OPI_{pfr}. This is a strong indication that Fur binds *holo*-operators trough the minor groove, while the recognition of *apo*-operators occurs through the major groove of the DNA as a result of a direct readout of a specific nucleotide sequence ($TCATT_{n10}TT$). Accordingly, the binding of Fur to the mutated (swapped) *holo*-operator, encompassing the $TCATT_{n10}TT$ motif (OPI_{frpBsw}) is less sensitive to distamycin and is only partially inhibited at the maximum drug concentration, [that instead has been shown to totally hinder the Fur binding at the wild type *holo*-operator OPI_{frpB} (compare lanes 5 Fig. 20 A-C).]

These results provide strong evidences that the requirement for Fur binding to the *holo*- and the *apo*-operator is reliant on a different mechanism of recognition of the DNA helix. Thus, Fur binding to the *apo*-operators occurs primarily in the major groove, through the direct readout of the specific TCATT element, whereas the recognition of the *holo*-operators occurs mainly through protein binding into the minor groove.

12. Stoichiometry of Fur-DNA complexes within the *holo*- and the *apo*-operators

To gather information on the stoichiometry of Fur binding to operator sequences we carried out EMSA experiment on both operators, OPI_{frpB} and OPI_{pfr}, with the purified recombinant Fur protein in the presence and absence of iron-cofactor. EMSA experiments showed a difference in mobility among complexes formed in presence or absence of iron (Fig. 21A and 21B). While *apo*-Fur bound on both OPI_{frpB} and OPI_{pfr}, forms a single higher-mobility complex HMC (Fig. 21A), *holo*-Fur forms preferentially two additional lower-mobility complexes, LMC and LMC2 (Fig. 21B). Moreover, size exclusion chromatography indicated that Fur is a dimer in solution and that is able to multimerize in presence of divalent metal ions (data not shown).

In order to determine the number of Fur dimers within the various gel shifted species, the Ferguson method was used (Orchard *et al.*, 1993, Ferguson, 1964). Fur-operator complexes were run along with molecular weight markers on a series of nondenaturating gels of various acrylamide concentrations. The molecular mass of Fur-operator complexes was then determined by interpolation of the titration curve of the molecular weight standards (Fig. 21C and 21D).

For both OPI_{pfrwt} and OPI_{frpBwt} operators the molecular mass of HMC was estimated as 85 kDa, which is comparable to the expected mass of 76 kDa calculated for a dimer of Fur bound to the 64 bp probe (since OPI_{pfr} and OPI_{frpB} are 42.2 kDa and one Fur dimer is 34 kDa). In contrast, the LMC complex had an apparent molecular mass of 118 kDa, in close agreement with the expected mass of 110 kDa calculated for two dimers of Fur bound to the DNA operators. Finally, the LMC2 is a complex of 228 kDa; this molecular mass is close to the predicted value of 220 kDa for two Fur tetramers, each bound to an operator probe. In all cases, the estimated molecular weight of the Fur-DNA complexes was somewhat higher than the predicted values, perhaps due to the fact that the protein-DNA complexes have different shape than the globular protein standards employed (Baichoo *et al.*, 2002a). Similar, an 8-kDa overestimate was also obtained when the stoichiometry of the Lrp-DNA complexes was determined by this method (Cui *et al.*, 1996).

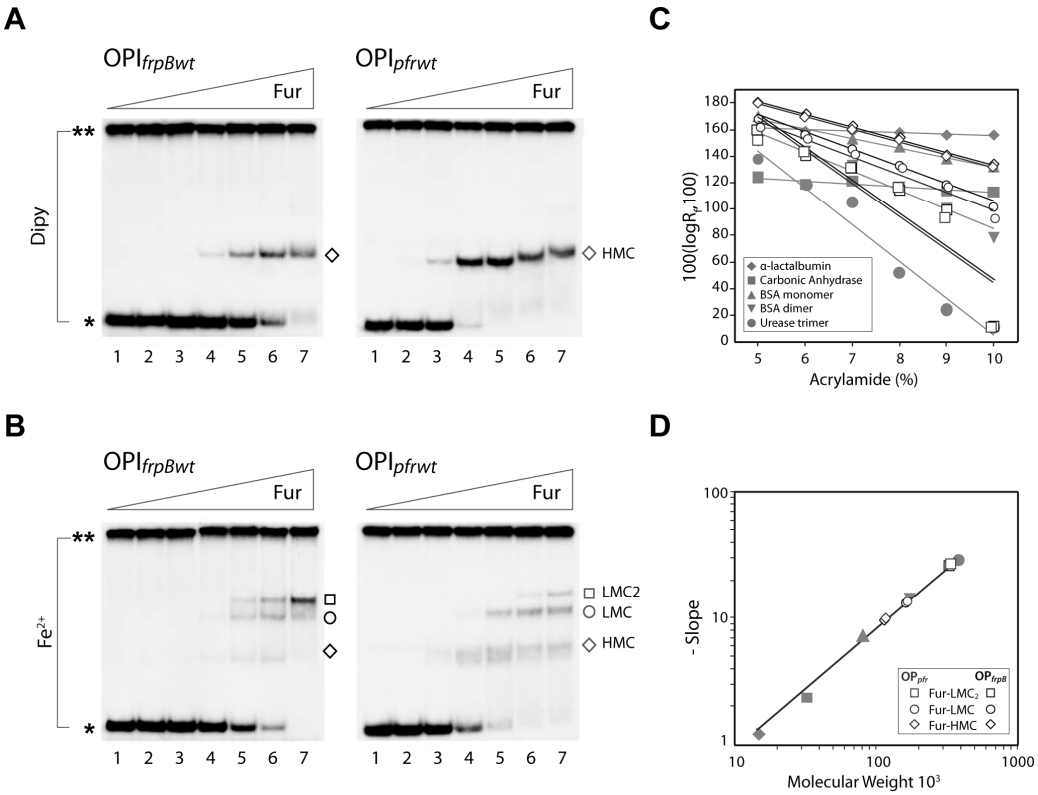

FIG. 21. Determination of the stoichiometry of Fur-DNA complexes by native PAGE. Representative gel shifts with OPI_{frpBwt} and OPI_{pfrwt} used as an example of an holo- and apo-Fur recognized operators. Increasing amounts of Fur protein were incubated with end-labeled probes in presence of 150 µM 2,2 dipyridyl **(A)** and 150 µM Fe^{2+} **(B).** Lane 1 to 7; 0, 1.2, 2.4, 4.8, 9.6, 18, 39 nM Fur added respectively. Single asterisks indicate free probe, while double asterisks indicate pBluescript KS used as non specific competitor in binding reactions. HMC and LMC denote the high mobility complex and the low mobility complex, respectively, formed in a metal-dependent manner. **(C)** Logarithm of the relative mobilities of Fur-DNA complexes and marker proteins as function of gel concentration. **(B)** Determination of apparent molecular weights of HMC, LMC, LMC2 Fur complexes. The negative slopes of the mobility lines in panel C were plotted against the molecular weights of the protein standards on double-log graph. The apparent mass of Fur-DNA complexes were determined by interpolation. The legend for the protein markers and Fur complexes are shown inside each graph.

These results indicates that *apo*-Fur binds DNA as a dimer, while *holo*-Fur is able to tetramerize (on DNA), and the two *holo*-Fur tetramers can interacts with each

other without losing contacts to the bound operators. Together this data support the idea that the metal ions determine the stoichiometry of Fur binding to DNA, regardless of the operator typology specifically recognized by the protein.

DISCUSSION

The *H. pylori* Fur protein is a transcriptional repressor involved in metal ion homeostasis and virulence. Classically, it is activated to bind DNA by the iron co-repressor. However, it has been shown that the *Hp*Fur binds DNA also in the absence of the iron regulatory cofactor. These two modes of Fur regulation have been termed *holo*- and *apo*- repression respectively, and rely on opposite effects of the regulatory metal ion on the affinity of Fur towards specific operator elements (Delany *et al.*, 2001b) (Fig. 9). This feature distinguishes *Hp*Fur from all other members of the Fur-family, which have not been shown to be able to bind DNA in the *apo*-form, to date (Carpenter *et al.*, 2009b).

Nevertheless, very little is understood about the molecular determinants that underlie Fur-dependent transcriptional regulation of iron-induced and -repressed genes. In *H.pylori*, the Fur-box consensus is still ill defined, and the nucleotide sequence of known Fur operators diverges significantly from that of *E. coli* and other bacteria. Even among *Hp*Fur target genes, the operators sequences are poorly conserved. An operator consensus sequence for the *apo*-repressed genes is lacking, due to little sequence homology between the only two known *apo*-Fur regulated genes, *pfr* and *sodB* (Delany *et al.*, 2001b, Ernst *et al.*, 2005b), while the consensus element for *holo*-Fur repression has been repeatedly reinterpreted based only on computational analysis of Fur bound operators sequences (Baichoo *et al.*, 2002a, de Lorenzo *et al.*, 1987, Escolar *et al.*, 1998b, Gao *et al.*, 2008). A common feature of Fur-boxes is the high number of A/T nucleotides. Thus it is not surprising that in silico definition of the Fur-box in *H. pylori* has been somewhat hindered by the AT-rich genome of this bacterium, considering also the lack of knowledge on the exact bases that are contacted by the protein. Recent reviews indicate this black box as one of the most intriguing puzzles in the wide field of Fur regulation.

Using OH* footprinting, electrophoretic mobility shift assays, and mutational analyses, we identify for the first time a specific Fur box consensus motif ($TCATT_{n10}TT$) for the *apo*-Fur operators (Fig. 13B), to which Fur is recruited with a characteristic binding architecture (Fig. 10 and Fig. 11). This finding led to unravel key molecular determinants responsible for the iron-responsive Fur regulation in *H. pylori*,

which ultimately involves: i) the nucleotide sequence of the operator element associated with the binding architecture of the regulator; ii) possible conformational changes of the protein induced by the metal ion cofactor; and iii) the ability of Fur to bind with different affinity distinct operator elements, carried within different grooves of the DNA helix.

In particular, we demonstrate the existence of two binding architectures of Fur to DNA, distinctive of the operator typology recognized with higher affinity by either the *holo*- or *apo*-regulator. The determinants, characterizing *holo*- and *apo*-operators, are carried in cis, within the operator sequences, and are represented by distinct nucleotide sequences important for *holo*- or *apo*-Fur binding. We have been able to identify a $TCATT_{n10}TT$ consensus motif responsible for discriminative binding of Fur to *apo*-operators. Fur binding to this element resulted insensitive to the minor groove binding drug distamycin A. On the contrary, Fur binding to *holo*-operators, characterized by extensive protein wrapping on AT-rich DNA elements, result to be distamycin-sensitive. Thus, the *apo*- and *holo*-Fur repression mechanisms apparently rely on two distinctive modes of operator-recognition, involving respectively the readout of a specific nucleotide consensus motif in the major groove for *apo*-operators, and the recognition of AT-rich stretches in the minor groove for *holo*-operators.

The shape of the DNA minor groove varies depending on the nucleotide sequence in a segment of DNA. TpA dinucleotide steps tend to widen the minor groove (Burkhoff *et al.*, 1988, Stefl *et al.*, 2004), enabling recognition by transcription factors such as TBP complexed to the TATA box (Kim *et al.*, 1993a, Kim *et al.*, 1993b). Instead, short runs of adenine nucleotides (called A-tracts) followed by a T residue, have the strong tendency to narrow the minor groove, leading to a cleft with enhanced negative electrostatic potential, which can be recognized by proteins bearing arginine residues (that offer a complementary set of positive charges) in their DNA binding domains (Rohs *et al.*, 2009, Tullius, 2009). Accordingly, the AAT repeats found within the extended protection region on *holo*-operators (Fig. 10C), may influence the minor groove width in such a way that it can serve as site for specific recognition by Fur. Interestingly, the *H. pylori* Fur protein encompasses a unique RLR amino acid motif within the recognition helix H1 in the N-terminal winged helix-turn-helix DNA-

binding domain (Fig. 5), not found in Fur orthologues of other bacterial species. Moreover, *Hp*Fur bears an additional short N-terminal sequence, rich in positive amino acid residues, predicted to fold in an α-helix secondary structure (Fig 5). This may contribute to confer affinity to Fur for negatively charged clefts predicted to form in the minor groove of the *holo*-operators as a consequence of contiguous repeats of ATT triplets.

On the contrary, *apo*-operators are characterized by a consensus $TCATT_{n10}TT$ motif, in which two thymine dimers, separated 10 bp one from another, are directly contacted by the DNA binding domain of Fur. This is indicative of Fur binding to one side of the DNA helix. In addition, binding to the *apo*-operators in not out-competed by distamycin in EMSA experiments (Fig. 20B), suggesting that recognition of these operators does not occur in the minor groove. EMSA experiments performed with cytosine substitutions of thymines (and consequential inosine substitutions of adenines) in the $TCATT_{n10}TT$ element, indicated that the affinity of Fur is significantly reduced (data not shown), suggesting indeed a specific readout of consensus motif in the major groove, in the case of *apo*-operators. Therefore, the binding affinity of Fur to *apo*- and *holo*-operators appears to depend on specific recognition of determinants in the major and minor groove, respectively. As a consequence, it will be noted that the *apo*- and *holo*- recognition elements are not mutually exclusive, but may coexist within the same operator. Evidence for this is provided by the reconstitution of the $TCATT_{n10}TT$ motif within the *holo*-operator *frpB* I (OPI_{frpBsw}), which confers *apo*-repression features to Fur *in vivo*, leaving the *holo*-repression unaltered (Fig. 17A). The *in vivo* data correlate with the results gathered in vitro, which indicate that the reconstitution of the $TCATT_{n10}TT$ element in a *holo*-operator has little effect of *holo*-Fur binding affinity, but confers a higher affinity to the *apo*-protein (Fig. 16). In addition, the presence of the $TCATT_{n10}TT$ motif within OPI_{frpBsw} resulted in lower sensitivity to distamycin A (compare the wild-type and mutant *frpB* operator in Fig. 20A and 20C), further strengthening the concept that *apo*- and *holo*-regulation molecular determinants are biochemically distinct and located on different grooves, but can be concurrently encompassed within the same operator sequence. A similar situation is found at the native operator I of the autoregulated *fur* promoter, which is recognized with the same affinity by *holo*- as well as *apo*-Fur (Delany *et al.*, 2003). Strikingly, this operator

encompasses both a perfectly conserved TCATT$_{n10}$TT motif, which could serve as high affinity *apo*-Fur recognition element, as well as short AT-rich tracts, which may recruit *holo*-Fur through narrowing of the minor groove.

Based on these evidences, we propose a schematic model that allows to explain the relationship between the distinctive binding architecture of Fur, the recognition of either the major or the minor groove, and the opposite regulatory effect of iron on *apo*- and *holo*-Fur repressed promoters in *H. pylori* (Fig. 22). The model postulates that the nucleotide sequences of the *holo*- and *apo*-operators dictate a specific binding architecture of Fur, which is not influenced by the regulatory iron ion. However, the metal ion plays a fundamental role in modulating the affinity of Fur to the different operator typologies, through allosteric conformational changes, supported by the evidence of different multimerization states of the regulator. In fact, it has been proposed that the DNA binding activity of Fur is activated by iron, which complexes to the regulatory metal binding site and changes the conformation of the protein (Coy *et al.*, 1991, Gonzalez de Peredo *et al.*, 2001). It is possible that once a dimer binds DNA, additional dimers are readily recruited to cooperatively bind *holo*-operators in response to the metal ions. This is consistent with the observation that Fur has the ability to multimerize on its binding sites through protein-protein interactions generating helical arrays spiraling around the DNA helix (Bagg *et al.*, 1987, Lavrrar *et al.*, 2002, Le Cam *et al.*, 1994).

In the case of *H. pylori* Fur, only the *holo*-protein is able to multimerize on DNA, while the *apo*-protein preferentially binds DNA as a dimer (Fig. 21). In particular, in the absence of iron, an *apo*-Fur dimer is prompted to bind with higher affinity to the OPI$_{pfr}$ *apo*-operator in the major groove, through a direct readout of nucleotides encompassed in the TCATT$_{n10}$TT consensus element (Fig. 22; upper left panel). By contrast, the affinity of the *apo*-Fur dimer for the OPI$_{frpB}$ *holo*-operator is significantly reduced, likely because the *apo*-recognition element TCATT$_{n10}$TT is missing in the major groove, while the structural conformation of the regulator poorly fits within the minor groove the DNA on the *holo*-operator in absence of iron (Fig. 22; upper right panel). Thus, under iron-deplete conditions, Fur gains affinity for *apo*-operators, enabling to repress transcription of iron-induced genes, while *holo*-Fur controlled promoters (iron-repressed) are derepressed. Accordingly, when an *apo*-recognition element (TCATT$_{n10}$TT) is inserted into an *holo*-operator sequence overlapping the promoter

elements, the derepression under iron-deplete conditions is less pronounced (Fig. 17A), as Fur gains the ability to bind to OPI_{frpBsw} also in its *apo*-form, contributing to its repression.

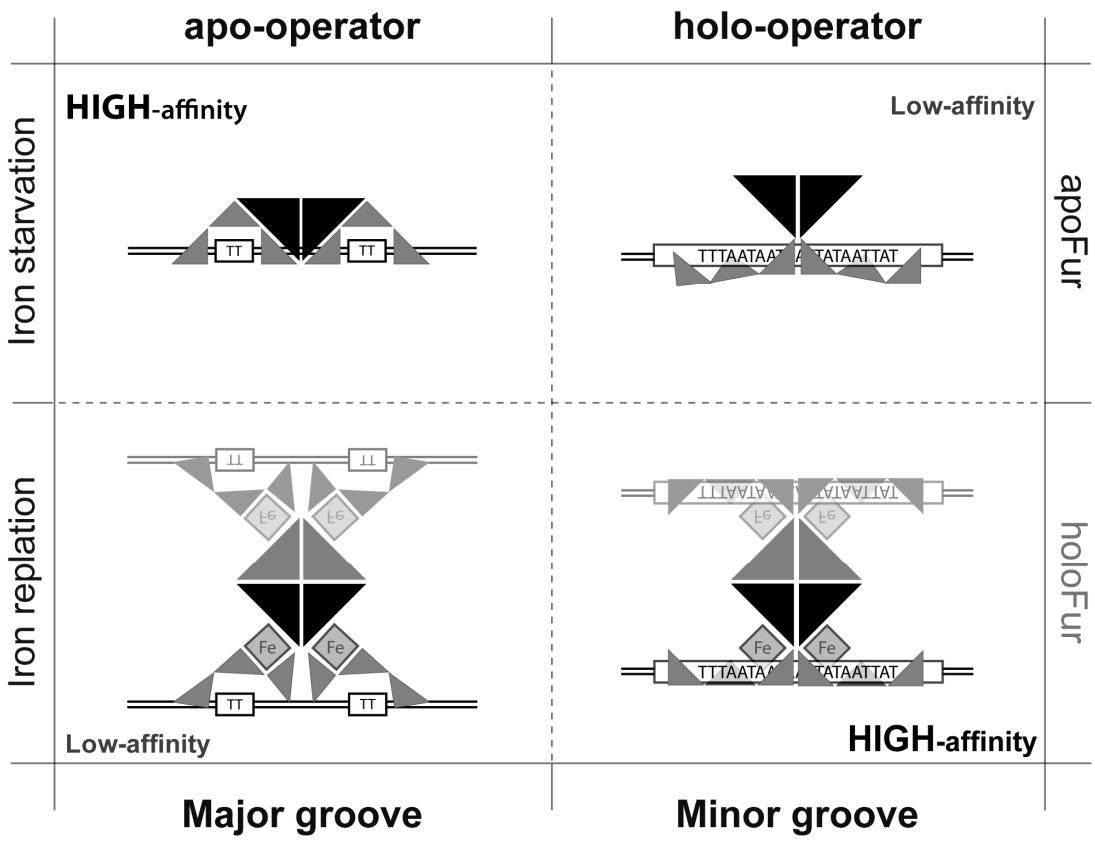

FIG.22 Schematic representation of proposed mode of action of *holo*- and *apo*-Fur binding on target operators. Fur protein recognized the *apo*- and *holo*-operator with differential affinity, binding into the major and minor groove of DNA respectively, exhibiting a distinctive binding architecture. The iron cofactor induces Fur oligomerization and may stabilize protein structure modulating protein affinity. Black triangles represent the dimerization domain of Fur dimer. Grey small triangles represent α-helices in the DNA-binding domain.

Conversely, under iron replete conditions, metal-dependent conformational changes in protein structure, accompanied by tetramerization or multimerization of the

regulator, allow the allosteric activation responsible for correct fitting of the DNA binding domain into the narrower minor groove of the AT-rich OPI_{frpB} *holo*-operator (Fig. 22; lower right panel). This results in increased affinity of *holo*-Fur to this operator and transcriptional repression of the *frpB* promoter. Concomitantly, the affinity for the OPI_{pfr} apo-operators decreases, in virtue of a regulator conformation less favorable to recognize the thymine dimers of the $TCATT_{n10}TT$ *apo*-element (Fig. 22; lower left panel). A key factor supporting this model, is that holo-Fur continues to bind OPI_{pfr} with the same binding architecture (specificity) characteristic of *apo*-Fur recognized *apo*-operators, but with decreased affinity (Fig.10B). This strongly suggests that the holo-regulator loses affinity for the readout of specific nucleotide pairs in the major groove. This loss of affinity is not compensated by a gain of affinity for the minor groove as the *apo*-operator lacks the AAT stretches or other determinants that are responsible for narrowing of the minor groove.

In conclusion, we propose that the principal molecular determinant governing the iron-dependent and iron-sensitive regulation of Fur resides in *cis*, within the operator sequence. Importantly, the nucleotide sequence of the operator determines the specificity of recognition, reflected in different binding architectures, while the affinity is controlled through metal-dependent shaping of the protein structure in order to match preferentially the major or the minor groove. Base-specific contacts in the minor groove of AT-rich DNA sequence have been demonstrated for a number of other DNA-binding proteins [MogR repressor of *Listeria monocytogenes* (Shen *et al.*, 2009); the nucleoid-associated protein Lsr2 of *Mycobacterium tuberculosis* (Gordon *et al.*, 2010) and α-subunit of RNA polymerase (Ross *et al.*, 2001)]. Frequently, these interactions are made by short peptide motifs containing arginine residues that contact bases in the minor groove. [e.g., AT-hooks in the chromatin-associated protein HMG-I(Y) (Huth *et al.*, 1997), and extended arm sequences in the Hin recombinase (Feng *et al.*, 1994) and in homeodomains (Kissinger *et al.*, 1990)]. Some of these proteins interact with DNA exclusively through the minor groove [e.g. TATA-box binding protein, integration host factor IHF, high mobility group I (Y) (HMG I) and the HMG-box- containing SRY and LEF-1(Bewley *et al.*, 1998)], while others are able to bind both the minor and the major groove of the DNA (MogR repressor of *L. Monocytogenes* (Shen *et al.*, 2009), Hin recombinase (Feng *et al.*, 1994), and THAP proteins (Sabogal *et al.*, 2010)]. *H. pylori* Fur adds to list of regulators able to bind both the major and the minor groove. To our

knowledge, the *Hp*Fur represents the first prokaryotic protein that is able to take advantage of the specific recognition of either the minor or the major groove to regulate gene expression in response to a specific environmental stimulus. This stunning evidence is consistent with the paucity of transcriptional regulators in *H. pylori* (Scarlato *et al.*, 2001, Tomb *et al.*, 1997) and the large number of Fur gene targets in the genome (Danielli *et al.*, 2006). The bacterium may have evolved a regulatory mechanism to control transcription of AT-rich loci, exploiting Fur to recognize structural features of the minor DNA groove imposed by recurrent AT-tracts.

To our knowledge, this is the first evidence of a prokaryotic transcription factor binding alternatively either the major or minor groove of the DNA in response to a specific environmental stimulus.

MATERIALS and METHODS

13. Bacterial strains, plasmids and growth conditions

The bacterial strain and plasmids used for this study are listed in Table 1. *H. pylori* strains were recovered from frozen stocks on Columbia or Brucella agar plates containing respectively 5% horse blood (Oxoid) or 5% fetal calf serum (Oxoid), 0.2% cyclodextrin and Dent's or Skirrow's antibiotic supplement. Bacteria were grown at 37°C under microaerophilic conditions in a water-jacketed thermal incubator or in an anaerobe jar by using Campygen gas pack (Oxoid). Liquid cultures were grown in brucella broth (BB) (Difco) containing 5% fetal calf serum and Dent's or Skirrow's antibiotic supplement under gentle agitation in a microaerobic environment. To monitor the iron-dependent transcriptional responses, a master culture (30 ml) of *H. pylori* strains were grown to an OD_{600} of 0.5-0.6, divided into aliquots of 5 ml and treated for 15 min with freshly made 1mM $(NH_4)_2Fe(SO_4)_2 \cdot 6H_2O$ [Fe^+] or 100 μM 2,2'-dipyridyl [Fe^-] prior to RNA extraction. For transformation, 5-10 μg of plasmid DNA was added to spotted O.N. cultures of naturally competent *H. pylori* and incubated overnight. Transformants were then selected on plates containing chloramphenicol (30 μg ml^{-1}), and single colonies were selected for further analysis.

E. coli strains DH5α and BL21 (D3) were growth on Luria-Bertani (LB) agar or in LB broth at 37°C. When required, ampicillin, kanamycin and chloramphenicol were added at final concentration of 100 μg ml^{-1}, 25 μg ml^{-1}, and 30 μg ml^{-1}, respectively.

14. DNA manipulations

Standard molecular biology techniques for DNA purification, PCR analyses, restriction digestion, and cloning were performed according to published protocols (Sambrook *et al.*, 1989). All constructs were confirmed by sequencing. Restriction and modification enzymes were purchased by New England Biolabs (NEB). Small- and large-scale plasmid DNA preparations were carried out using QIAprep Spin Mini-Kit (Qiagen) and NucleoBond Xtra-Midi (Macherey-Nagel) respectively, according to manufacturer's instructions.

Table 1. Strains and plasmids and used in this study

Strains or Plasmid	Genotype or Description[a]	Source or reference
E. coli strains		
DH5α	*supE44 ΔlacU169 (ϕ80 lacZΔM15) hsdR17 recA1 endA1 gyrA96 thi-1 relA1ß*	(Hanahan, 1983)
BL21 (DE3)	*hsdS gal (λcIts857 ind1 Sam7 nin5 lacUV5-T7 gene 1)*	(Studier *et al.*, 1986)
H. pylori strains		
G27	Clinical isolated, wild type	(Xiang *et al.*, 1995)
G27*fur* (Δ*fur*::Km)	G27 derivative in which 462 bp of the Fur gene has been deleted and replaced by a kanamycin cassette, *fur*$^-$, Km^r	(Delany *et al.*, 2001a)
G27 *vac*::OPI$_{frpBwt}$-*lacZ*	G27 derivative containing the wild-type OPI P$_{frpB}$-*lacZ* fusion in the *vacA* locus; Km^r, Cp^r	This study
G27 *vac*::OPI$_{frpBsw}$-*lacZ*	G27 derivative containing the mutant OPI P$_{frpB}$ -*lacZ* fusion in the *vacA* locus; Km^r, Cp^r	This study
G27*fur vac*::OPI$_{frpBwt}$-*lacZ*	G27*fur* derivative containing the wild-type OPI P$_{frpB}$-*lacZ* fusion in the *vacA* locus; Km^r, Cp^r	This study
G27*fur vac*::OPI$_{frpBsw}$-*lacZ*	G27*fur* derivative containing the mutant OPI P$_{frpB}$ -*lacZ* fusion in the *vacA* locus; Km^r, Cp^r	This study
Plasmids		
pET15b	IPTG-inducible vector over-expressing N-terminally His$_6$-tagged recombinant protein; Amp^r	Novagene
pET15b*fur*	pET15b derivative containing the *fur* coding sequence cloned in frame within *Nde*I/*Xho*I restriction sites	(Delany *et al.*, 2001b)
pGEM-T	Cloning vector for PCR products; Amp^r	Promega
pGEMpfr	Derivative of pGEM-T containing a 390 bp of *pfr* promoter region amplified by PCR with primers PFR-f and PFR-r	(Delany *et al.*, 2001b)
pGEM3-z	General cloning vector, Amp^r	Promega
pGEMK-F	Derivative of pGEM3-z containing a 470 bp of *frpB* promoter region amplified with primers 0875-L and 0875-R	(Delany *et al.*, 2001a)

[a] IPTG, isopropyl-β-D-thiogalactopyranoside

pGEMT-P_{fecA1}	pGEM-T Easy derivative containing 402 bp of *fecA1* promoter region, amplified by PCR with primers A1F and A1R	(Danielli *et al.*, 2009)
pGEMT-P_{fecA2}	pGEM-T easy derivative containing 380 bp of *fecA2* promoter region, amplified by PCR with primers A2F and A2R	(Danielli *et al.*, 2009)
pBluescript II KS	General cloning vector; Amp^r	Stratagene
pBS-OPI_{pfrwt}	pBluescript derivative containing operator I from *pfr* promoter region obtained by annealing of complementary primers PFRI-f and PFRI-r	This study
pBS-$OPII_{pfrwt}$	pBluescript derivative containing operator II from *pfr* promoter region obtained by annealing of complementary primers PFRII-f and PFRII-r	This study
pBS-$OPIII_{pfrwt}$	pBluescript derivative containing operator III from *pfr* promoter region obtained by annealing of complementary primers PFRIII-f and PFRIII-r	This study
pBS-OPI_{pfrsw}	pBluescript derivative containing mutant operator I from *pfr* promoter region obtained by annealing of complementary primers PFRS-f and PFRS-r	This study
pBS-$OP_{pfrc17a}$	pBluescript derivative containing mutant operator I from *pfr* promoter region obtained by annealing of complementary primers PFRC-f and PFRC-r	This study
pBS-$OP_{pfrc11\text{-}17a}$	pBluescript derivative containing mutant operator I from *pfr* promoter region obtained by annealing of complementary primers PFRC1-f and PFRC1-r	This study
pBS-OPI_{frpBwt}	pBluescript derivative containing operator I from *frpB* promoter region obtained by annealing of complementary primers FRPI-f and FRPI-r	This study
pBS-$OPII_{frpBwt}$	pBluescript derivative containing operator II from *frpB* promoter region obtained by annealing of complementary primers FRPII-f and FRPII-r	This study
pBS-OPI_{frpBsw}	pBluescript derivative containing mutant operator I from *frpB* promoter region obtained by annealing of complementary primers FRPS-f and FRPS-r	This study
pVac::Km	pGEMZ derivative containing kanamycin cassette	(Delany *et al.*, 2002b)
pVac::OPI_{frpBwt}LacZ	pVac::derivative containing the transcriptional fusion OP-I wild-type P_{frpB} –*lacZ*; Km^r, Cp^r	This study

15. Cloning of Fur operator regions

The Fur operator regions used in this study, were generated by annealing complementary oligonucleotides containing both wild-type and mutated operator regions of P_{pfr} and P_{frpB} promoters. The OPI_{frpB} and $OPII_{frpB}$ operators contain regions spanning positions -1 to -42 and 57 to – 91 of the *frpB* promoter, whereas the OPI_{pfr}, $OPII_{pfr}$ and $OPIII_{pfr}$ operators comprises regions spanning positions +5 to -36, -49 to -85, and -110 to -148 of the *pfr* promoter respectively (Delany *et al.*, 2001b). Oligonucleotides used are listed in Table 2. Equimolar amounts of complementary oligonucleotides were incubated at 94°C for 10 min in annealing buffer (50 mM $NaCl_2$, 10 mM Tris-HCl, 1 mM EDTA, pH 8.0) and then allowed to cool at room temperature over a 5-h period. The resulting double stranded DNA products were cloned as blunt-end fragments at the *Hinc*II site in pBlueScript (Stratagene) vector to generate the plasmids listed in Table 1.

The pBlueScript derivatives, bearing the various Fur binding operators, were used to obtain DNA probes used in Electrophoretic Mobility Shift Assays, Hydroxyl radical footprinting and Ferguson analysis.

16. Purification of *H. pylori* Fur protein

Expression and purification of Fur protein was done as described by Delany et al. 2001. The protocol was modified as follows. Over-expression of recombinant Fur was induced in cells at mid-log phase by the addiction of 0.4mM IPTG and then incubating at 30°C for 4hs. The recombinant His-Fur protein was purified under native conditions by Ni-NTA (Qiagen) affinity chromatography according to manufacturer's instructions. The His-tag was cleaved by adding 10 U of thrombin protease (Amersham, GE Healthcare) per mg of purified protein and incubating for 2 hours at room temperature and subsequently at 4°C overnight. To remove the His-tag and exchange the protein storage buffer, the purified untagged protein was subjected to gel filtration using PD SpinTrap G-25 (GE Healthcare). After determination of the protein

concentration by the Bradford method (Bio-Rad), protein fractions were aliquoted and stored at -80°C in EMSA or footprinting buffer for the subsequent assays. Fur concentrations indicated through this work refer to the protein dimer.

Table 2. Primers used for cloning of Fur binding sites

Operator	Primers	Sequence (5'-3')[a]
OPI_{pfr}	PFRI-f	GTTGTCCCATAATTATAGCATAAATGATAATGAAAAAGTAA
	PFRI-r	TTACTTTTTCATTATCATTTATGCTATAATTATGGGACAAC
$OPII_{pfr}$	PFRII-f	AAATTTTTAAAAATTTACAAAAATGAGAAAGAACACC
	PFRII-r	GGTGTTCTTTCTCATTTTTGTAAATTTTTAAAAATTT
$OPIII_{pfr}$	PFRIII-f	ATTTTATCATAAAAATCTATTTAATGAGAATTAGGTAAA
	PFRIII-r	TTTACCTAATTCTCATTAAATAGATTTTTATGATAAAAT
OPI_{pfrsw}	PFRS-f	GTTGTCCCATAGCATAA*TTATA*AATGATAATGAAAAAGTAA
	PFRS-r	TTACTTTTTCATTATCATT*TATAA*TTATGCTATGGGACAAC
$OPI_{pfrc17a}$	PFRC-f	GTTGTCCCATAATTATAGCATAAAT*T*ATAATGAAAAAGTAA
	PFRC-r	TTACTTTTTCATTAT*A*ATTTATGCTATAATTATGGGACAAC
$OPI_{pfrc11-17a}$	PFRC1-f	GTTGTCCCATAATTATAGCATAAAT*T*ATAAT*T*AAAAAGTAA
	PFRC1-r	TTACTTTTT*A*ATTAT*A*ATTTATGCTATAATTATGGGACAAC
OPI_{frpB}	FRPI-f	TTTTAATCTGGTTTTAATAATAATTATCATACTATTCTATCCC
	FRPI-r	GAAAAGGATAGAATAGTATGATAATTATTATTAAAACCAGATT
$OPII_{frpB}$	FRPII-f	CTATTCGTAACAATTAATGAAAATAAGAAAGATTAA
	FRPII-r	TTAATCTTTCTTATTTTCATTAATTGTTACGAATAG
OPI_{frpBsw}	FRPS-f	TTTTAATCT*CA*TTTTAATAAT*C*ATTATCATACTATT*T*TATCCC
	FRPS-r	GGGATA*A*AATAGTATGATAAT*G*ATTATTAAAA*TG*AGATTAAAA

[a] Bases underlined and in italics represent introduced mutations

17. Electrophoretic Mobility Shift Assay (EMSA)

EMSAs were used to assays the *holo*- or *apo*-Fur binding to DNA. DNA probes for gel retardation assays were isolated as 64 bp fragments, containing only the operators under study surrounded by unrelated sequence, from *Hind*III and *Xho*I

digestion of pBlueScript-derived plasmids described above (Table 2). Following double restriction digestion, both the DNA fragments and the pBS vector were dephosphorylated with calf intestinal phosphatase and labeled at both ends with T4 polynucleotide kinase and [γ-^{32}P] ATP (Perkin Elmer); unincorporated radiolabeled nucleotide was removed with a G-50 microspin column (GE Healthcare).

The binding reaction was carried out for 15 min, at room temperature, in EMSA buffer (50 mM NaCl; 10 mM Tris pH 8.0; 10 mM KCl; 0.01% IGEPAL; 10% glycerol; 0.1 mM DTT) in presence of vector used as an unspecific competitor. Approximately 0.6 nM of radiolabeled target DNA and increasing concentrations of Fur, ranging from 0 to 40 nM, were incubated in a final volume of 15 µl in presence of 5 mM DTT. Depending on the effect analyzed the buffer was supplemented 150 µM $(NH_4)_2Fe(SO_4)_2 \cdot 6H_2O$ or 150 µM 2,2'-dipyridyl as indicated in figure legends. Binding reactions were resolved on native 6% polyacrylamide [19:1] gel and electrophoresed in 1X Tris-borate (TB) buffer (60 mM Tris, 240 mM boric acid, pH 8.0). The gels were prerun at 50 V for 30 min prior to loading and then run at 150 V for 2 h at room temperature, dried and autoradiographed. The binding pattern was examined by exposing the gel to Kodak XAR film.

To determine the apparent dissociation constant (K_D) for each operators, gels were expose to a phosphorimager screen. The image was scanned into a Storm 840 scanner and the intensity of the individual bands was measured with ImageQuant 5.2 software (Molecular Dynamics). By comparing relative signal intensities and analyzing them with Excel Microsoft, percent DNA bound versus unbound fragments was calculated for each Fur concentration. One hundred percent represents the association of all DNA in the sample with Fur. Also the remaining unbound DNA in each binding reaction was estimated with the respect to the band area corresponding to free DNA control taken as 100%. Apparent K_D is defined as the concentration of protein at which 50% of DNA is bound.

18. Probe preparation and Hydroxyl radical footprinting

Hydroxyl-radical footprinting was carried out to determine the bases directly contacted by *holo*- and *apo*-Fur and their relative binding architecture on target operators or promoter regions.

The pBlueScript derivatives pBS-OPI$_{pfr}$, pBS-OPI$_{frpB}$ and their mutants (Table 1) were digested with *Bam*HI or *Acc*56I for labeling of the top or the bottom strand, respectively. The linearized vectors were dephosphorylated with calf intestinal phosphatase (NEB) and 5'end-labelled with [γ-32]-P ATP (5,000 Ci/mmol; PerkinElmer) and T4 polynucleotides kinase (NEB).

The labeled DNA probes were further digested with *Pvu*II (top strand) or *Pvu*I (bottom strand) and products were separated by native polyacrylamide gel electrophoresis and purified as described previously (Delany *et al.*, 2001b).

The P$_{pfr}$ and P$_{frpB}$ promoter regions were obtained from pGEMpfr and pGEMK-F plasmids (Table 1). Probe preparation was carried out as previously described with some modifications (Delany *et al.*, 2001b). A 390 bp *BamH1*/*NcoI*-digested *pfr* promoter fragment was isolated from pGEMpfr and 5'end-labelled with T4 PNK at the site *BamH1* (for labeling of the non coding strand) or *NcoI* (for labeling of the coding strand). A 447 bp *HindIII*/*EcoRI*-digested *frpB* promoter fragment was isolated from pGEMK-F and 5'end-labelled with T4 PNK at the site *HindIII* or *EcoRI* for labeling of the non coding strand and the coding strand respectively. Probe preparation for P$_{fecA1}$ and P$_{fecA2}$ promoters was carried out as previously described (Danielli *et al.*, 2009).

The OH*-footprinting assay used in this study is a modified version of that described previously by (Tullius *et al.*, 1986). Approximately 0.6 nM of labelled probe was incubated with increasing concentration of Fur in footprinting buffer (50 mM NaCl,10 mM KCl, 10 mM Tris-HCl pH 8.0, 0.01% Igepal CA-630, 0.1mM DTT) at room temperature for 15 min using 300 ng of salmon sperm DNA (Invitrogen) as non specific competitor in a final volume of 30 µl. Glycerol was omitted in the footprinting buffers as it is a radical scavenger. An excess of $MnCl_2$ (150µM) or 2,2'-dipyridyl (150 µM) was added where indicated. Mn^{2+} was used in place of Fe^{2+} to avoid interference with the reaction generating OH* formation. The cutting reaction was carried out by the addition of 2 µl each of the following solutions: 125mM Fe $(NH_4)_2(SO_4)_2$-250 mM

EDTA, 1% H_2O_2 and 0.1 M DTT. The stock solution of iron(II)-EDTA was prepared immediately before use by mixing equal volumes of freshly prepared 125 mM ammonium iron (II) sulfate hexahydrate [Sigma $(NH_4)_2Fe(SO_4)_2 \cdot 6H_2O$)] and 250 mM EDTA. After 2 min at room temperature the reaction was quenched by the addition of 25 µl of OH-stop buffer (4% glycerol, 0.6 M sodium acetate pH 5.2, 100 ng μl^{-1} 100 µg ml^{-1} sonicated salmon sperm DNA), extracted once with an equal volume of phenol-chloroform isoamyl alcohol (25:24:1), and ethanol precipitated. Sample were resuspended in 6 µl of formamide loading buffer, denaturated at 92°C for 2 min, separated on 8 M urea-8,5% acrylamide sequencing gels and autoradiographed. A modified G+A sequencing ladder protocol (Liu *et al.*, 1998) was employed to map the bases directly involved in either *holo*- or *apo*-Fur DNA interactions.

19. Distamycin A interference assays.

Distamycin A, a minor groove DNA binding drug, (Churchill *et al.*, 1990) was purchased from Chemper (Prato, CO Italy), resuspended in distilled water at final concentration of 10 mM, and stored at – 20°C.

Hydroxyl radical footprinting were implemented to detect distamycin binding sites on OPI_{frpBwt}, $OPI_{pfrwt,}$ and OPI_{frpBsw}. End-labeled fragment containing *frpB* and *pfr* operator regions was incubated at 22° C for 15 minute with 0.62-1 µM distamycin in 50 mM NaCl,10 mM KCl, 10 mM Tris-HCl pH 8.0, 0.01% Igepal CA-630, 0.1mM DTT and 300 ng salmon sperm DNA (Invitrogen). OH* cleavage and gel electrophoresis was carried out as described previously.

EMSA assays were performed to study the effects of the minor groove binder distamycin A on Fur binding to DNA operators. DNA probes (0,6 nM) was preincubated for 15 min at 22°C with 1.2, 2.4, 4.8 nM distamycin A in 10 µl of EMSA buffer. Then, 39 nM Fur was added to the reaction for additional 15–min incubation.

Samples were analyzed on 6% native gel and the binding pattern was examined by exposing gel to Kodak XAR film.

20. Determination of Fur oligomerization by Native PAGE (Ferguson analysis)

An EMSA-based method for determining the molecular weights of Fur-DNA complexes was done by performing native PAGE as described by Orchard and May (Orchard *et al.*, 1993) and using a native PAGE molecular weight marker kit (SIGMA MW ND 500). Briefly, EMSA reactions, along with molecular weight markers, were analyzed on a series of nondenaturating gels (5 to 10% polyacrylamide, 19:1) and electrophoresed until the bromophenol blu bands in flanking samples lanes just reached the bottom of the gels. The gels were stained in Coomassie blue, destained, incubated in 7% acetic acid, dried and exposed to Kodak XAR film. To determine the relative mobilities (R_f) (of the protein-DNA complexes and protein markers), the distance from the top of the gel to the complexes or protein standards were measured and divided by the distance migrated by bromophenol blue band for each gel. The logarithm of the R_f was plotted against the gel concentration for each complex and protein standard, and best-fit lines were obtained. The negative slopes of these lines were the plotted against the molecular weight of the protein standards on a double-logarithmic scale, and titration curve was obtained. Interpolation of this curve by using the slopes of the lines from the protein DNA-complexes was used to deduce the approximate molecular weights of the complexes.

21. Construction of *lacZ* transcriptional fusions and integration into the *vacA* locus of *H. pylori*

Transcriptional fusions of the wild-type and mutant *frpB* operators I (OPI_{frpBwt} and OPI_{frpBsw}, respectively) to a promoterless *LacZ* was constructed as previously described (Danielli *et al.*, 2009).

OPI_{frpBwt} and OPI_{frpBsw} were cloned blunt at *Hinc*II site in pBluescript II KS (Table 1) to have transcriptional fusions with the *lacZ 3'* region carried in the plasmid vector. These constructs were then excised from the pBluescript derivatives (pBS-OPI_{frpBwt} and pBS-

OPI$_{frpBsw}$) as *Xho*I-*Pvu*II segments, blunted and cloned into the pVac::Km transformation vector (Delany *et al.*, 2002b) by exploiting a unique *Hinc*II site. The transcriptional fusions were inserted into the *vacA* locus on the chromosome of both wild-type and *Δfur H. pylori* strains by homologous recombination; positive colonies on agar plates were selected according to the antibiotic resistance phenotype. The integrations were confirmed by PCR amplifications using primers FRPI-f (Table 2) and A3Z2 (GTTTTCCCAGTCACGACGTTG).

22. RNA isolation and Primer extension analysis

Total RNA was extracted by a hot-phenol procedure as described previously (Danielli *et al.*, 2006); RNA integrity and purity were ensured by electrophoresis on 1% agarose gels. Primers BZ9 (CCCCCGGGCTGCAGGAATTC) and BZ10 (GCTGCAGGAATTCGATATC) were used for primers extension experiments. The primer (5pmol) was 5' end labelled using 6 pmol [γ-^{32}P]-ATP (Perkin Elmer) with T4 polynucleotide kinase (NEB) at 37°C for 45 min. Unincorporated radiolabeled nucleotide was removed with a G-50 microspin column (GE Healthcare).

Labelled primer (0.1 pmol) was then added to 18 μg of total RNA, 2 μl of 2mM dNTPs and 2 μl of 5X AMV reverse transcriptase buffer (Promega) to make up a final volume of 9 μl. The reaction mixture was incubated at 100°C for 3 min, cooled to 42°C, before addition of reverse transcriptase. 1 μl of AMV reverse transcriptase (10 U μl^{-1}, Promega) was added, and incubation continued at 42°C for a further 45 min. After cDNA synthesis, samples were incubated for 10 min at room temperature with 1 ml of RNase A (10mg ml^{-1}), extracted once with an equal volume of phenol–chloroform (1:1), ethanol precipitated and resuspended in 6 μl of sequence loading buffer (Sambrook *et al.*, 1989). After denaturation at 100°C for 2 min, samples were subjected to electrophoresis on 6% urea–polyacrylamide gels at 1500 V, dried and autoradiographed. For sequencing ladders, sequencing reaction was carried out by the same set of primers employed in the primer extension, using a T7 Sequencing kit (USB Corp).

REFERENCES

Ahn, B.E., Cha, J., Lee, E.J., Han, A.R., Thompson, C.J. and Roe, J.H. (2006). Nur, a nickel-responsive regulator of the Fur family, regulates superoxide dismutases and nickel transport in Streptomyces coelicolor. *Mol Microbiol* **59,** 1848-1858.

Akada, J.K., Shirai, M., Takeuchi, H., Tsuda, M. and Nakazawa, T. (2000). Identification of the urease operon in Helicobacter pylori and its control by mRNA decay in response to pH. *Mol Microbiol* **36,** 1071-1084.

Alamuri, P., Mehta, N., Burk, A. and Maier, R.J. (2006). Regulation of the Helicobacter pylori Fe-S cluster synthesis protein NifS by iron, oxidative stress conditions, and fur. *J Bacteriol* **188,** 5325-5330.

Alm, R.A., Ling, L.S., Moir, D.T., King, B.L., Brown, E.D., Doig, P.C., *et al.* (1999). Genomic-sequence comparison of two unrelated isolates of the human gastric pathogen Helicobacter pylori. *Nature* **397,** 176-180.

Bagg, A. and Neilands, J.B. (1987). Ferric uptake regulation protein acts as a repressor, employing iron (II) as a cofactor to bind the operator of an iron transport operon in Escherichia coli. *Biochemistry* **26,** 5471-5477.

Baichoo, N. and Helmann, J.D. (2002a). Recognition of DNA by Fur: a reinterpretation of the Fur box consensus sequence. *J Bacteriol* **184,** 5826-5832.

Baichoo, N., Wang, T., Ye, R. and Helmann, J.D. (2002b). Global analysis of the Bacillus subtilis Fur regulon and the iron starvation stimulon. *Mol Microbiol* **45,** 1613-1629.

Balazsi, G. and Oltvai, Z.N. (2005). Sensing your surroundings: how transcription-regulatory networks of the cell discern environmental signals. *Sci STKE* **2005,** pe20.

Baltrus, D.A., Amieva, M.R., Covacci, A., Lowe, T.M., Merrell, D.S., Ottemann, K.M., *et al.* (2009). The complete genome sequence of Helicobacter pylori strain G27. *J Bacteriol* **191,** 447-448.

Bereswill, S., Greiner, S., van Vliet, A.H., Waidner, B., Fassbinder, F., Schiltz, E., *et al.* (2000). Regulation of ferritin-mediated cytoplasmic iron storage by the ferric uptake regulator homolog (Fur) of Helicobacter pylori. *J Bacteriol* **182,** 5948-5953.

Bereswill, S., Lichte, F., Greiner, S., Waidner, B., Fassbinder, F. and Kist, M. (1999). The ferric uptake regulator (Fur) homologue of Helicobacter pylori: functional analysis of the coding gene and controlled production of the recombinant protein in Escherichia coli. *Med Microbiol Immunol* **188,** 31-40.

Bereswill, S., Lichte, F., Vey, T., Fassbinder, F. and Kist, M. (1998). Cloning and characterization of the fur gene from Helicobacter pylori. *FEMS Microbiol Lett* **159,** 193-200.

Berg, D.E., Hoffman, P.S., Appelmelk, B.J. and Kusters, J.G. (1997). The Helicobacter pylori genome sequence: genetic factors for long life in the gastric mucosa. *Trends Microbiol* **5,** 468-474.

Berg, G., Bode, G., Blettner, M., Boeing, H. and Brenner, H. (2001). Helicobacter pylori infection and serum ferritin: A population-based study among 1806 adults in Germany. *Am J Gastroenterol* **96,** 1014-1018.

Bewley, C.A., Gronenborn, A.M. and Clore, G.M. (1998). Minor groove-binding architectural proteins: structure, function, and DNA recognition. *Annu Rev Biophys Biomol Struct* **27,** 105-131.

Bijlsma, J.J., Waidner, B., Vliet, A.H., Hughes, N.J., Hag, S., Bereswill, S., *et al.* (2002). The Helicobacter pylori homologue of the ferric uptake regulator is involved in acid resistance. *Infect Immun* **70,** 606-611.

Blaser, M.J. (1990). Helicobacter pylori and the pathogenesis of gastroduodenal inflammation. *J Infect Dis* **161,** 626-633.

Blencowe, D.K. and Morby, A.P. (2003). Zn(II) metabolism in prokaryotes. *FEMS Microbiol Rev* **27,** 291-311.

Bouvard, V., Baan, R., Straif, K., Grosse, Y., Secretan, B., El Ghissassi, F., *et al.* (2009). A review of human carcinogens--Part B: biological agents. *Lancet Oncol* **10,** 321-322.

Braun, V. (2005). Bacterial iron transport related to virulence. *Contrib Microbiol* **12,** 210-233.

Braun, V., Hantke, K. and Koster, W. (1998). Bacterial iron transport: mechanisms, genetics, and regulation. *Met Ions Biol Syst* **35,** 67-145.

Braun, V. and Killmann, H. (1999). Bacterial solutions to the iron-supply problem. *Trends Biochem Sci* **24,** 104-109.

Bsat, N., Herbig, A., Casillas-Martinez, L., Setlow, P. and Helmann, J.D. (1998). Bacillus subtilis contains multiple Fur homologues: identification of the iron uptake (Fur) and peroxide regulon (PerR) repressors. *Mol Microbiol* **29,** 189-198.

Burkhoff, A.M. and Tullius, T.D. (1988). Structural details of an adenine tract that does not cause DNA to bend. *Nature* **331,** 455-457.

Bury-Mone, S., Thiberge, J.M., Contreras, M., Maitournam, A., Labigne, A. and De Reuse, H. (2004). Responsiveness to acidity via metal ion regulators mediates virulence in the gastric pathogen Helicobacter pylori. *Mol Microbiol* **53,** 623-638.

Carpenter, B.M., Gancz, H., Gonzalez-Nieves, R.P., West, A.L., Whitmire, J.M., Michel, S.L. and Merrell, D.S. (2009a). A single nucleotide change affects fur-dependent regulation of sodB in H. pylori. *PLoS One* **4,** e5369.

Carpenter, B.M., Whitmire, J.M. and Merrell, D.S. (2009b). This is not your mother's repressor: the complex role of fur in pathogenesis. *Infect Immun* **77,** 2590-2601.

Churchill, M.E., Hayes, J.J. and Tullius, T.D. (1990). Detection of drug binding to DNA by hydroxyl radical footprinting. Relationship of distamycin binding sites to DNA structure and positioned nucleosomes on 5S RNA genes of Xenopus. *Biochemistry* **29,** 6043-6050.

Coll, M., Frederick, C.A., Wang, A.H. and Rich, A. (1987). A bifurcated hydrogen-bonded conformation in the d(A.T) base pairs of the DNA dodecamer d(CGCAAATTTGCG) and its complex with distamycin. *Proc Natl Acad Sci U S A* **84,** 8385-8389.

Covacci, A., Censini, S., Bugnoli, M., Petracca, R., Burroni, D., Macchia, G., *et al.* (1993). Molecular characterization of the 128-kDa immunodominant antigen of Helicobacter pylori associated with cytotoxicity and duodenal ulcer. *Proc Natl Acad Sci U S A* **90,** 5791-5795.

Cover, T.L., Tummuru, M.K., Cao, P., Thompson, S.A. and Blaser, M.J. (1994). Divergence of genetic sequences for the vacuolating cytotoxin among Helicobacter pylori strains. *J Biol Chem* **269,** 10566-10573.

Coy, M. and Neilands, J.B. (1991). Structural dynamics and functional domains of the fur protein. *Biochemistry* **30,** 8201-8210.

Crosa, J.H. (1997). Signal transduction and transcriptional and posttranscriptional control of iron-regulated genes in bacteria. *Microbiol Mol Biol Rev* **61,** 319-336.

Crothers, D.M. and Shakked, Z. (1999) Oxford Handbook of Nucleic Acid Srtucture, Oxford University Press.

Cui, Y., Midkiff, M.A., Wang, Q. and Calvo, J.M. (1996). The leucine-responsive regulatory protein (Lrp) from Escherichia coli. Stoichiometry and minimal requirements for binding to DNA. *J Biol Chem* **271,** 6611-6617.

Cussac, V., Ferrero, R.L. and Labigne, A. (1992). Expression of Helicobacter pylori urease genes in Escherichia coli grown under nitrogen-limiting conditions. *J Bacteriol* **174,** 2466-2473.

Danielli, A., Amore, G. and Scarlato, V. (2010). Built Shallow to mantain homeostasis and persisten infection: Insight into the Trascriptional Regulatory Network of the gastric human pathogen *Helicobacter pylori*. *Plos Pathogens* **in press**.

Danielli, A., Romagnoli, S., Roncarati, D., Costantino, L., Delany, I. and Scarlato, V. (2009). Growth phase and metal-dependent transcriptional regulation of the fecA genes in Helicobacter pylori. *J Bacteriol* **191,** 3717-3725.

Danielli, A., Roncarati, D., Delany, I., Chiarini, V., Rappuoli, R. and Scarlato, V. (2006). In vivo dissection of the Helicobacter pylori Fur regulatory circuit by genome-wide location analysis. *J Bacteriol* **188,** 4654-4662.

De Lorenzo, V., Herrero, M., Giovannini, F. and Neilands, J.B. (1988). Fur (ferric uptake regulation) protein and CAP (catabolite-activator protein) modulate transcription of fur gene in Escherichia coli. *Eur J Biochem* **173,** 537-546.

de Lorenzo, V., Wee, S., Herrero, M. and Neilands, J.B. (1987). Operator sequences of the aerobactin operon of plasmid ColV-K30 binding the ferric uptake regulation (fur) repressor. *J Bacteriol* **169,** 2624-2630.

de Reuse, H. and Bereswill, S. (2007). Ten years after the first Helicobacter pylori genome: comparative and functional genomics provide new insights in the variability and adaptability of a persistent pathogen. *FEMS Immunol Med Microbiol* **50,** 165-176.

Delany, I., Ieva, R., Soragni, A., Hilleringmann, M., Rappuoli, R. and Scarlato, V. (2005). In vitro analysis of protein-operator interactions of the NikR and fur metal-responsive regulators of coregulated genes in Helicobacter pylori. *J Bacteriol* **187,** 7703-7715.

Delany, I., Pacheco, A.B., Spohn, G., Rappuoli, R. and Scarlato, V. (2001a). Iron-dependent transcription of the frpB gene of Helicobacter pylori is controlled by the Fur repressor protein. *J Bacteriol* **183,** 4932-4937.

Delany, I., Spohn, G., Pacheco, A.B., Ieva, R., Alaimo, C., Rappuoli, R. and Scarlato, V. (2002a). Autoregulation of Helicobacter pylori Fur revealed by functional analysis of the iron-binding site. *Mol Microbiol* **46,** 1107-1122.

Delany, I., Spohn, G., Rappuoli, R. and Scarlato, V. (2001b). The Fur repressor controls transcription of iron-activated and -repressed genes in Helicobacter pylori. *Mol Microbiol* **42,** 1297-1309.

Delany, I., Spohn, G., Rappuoli, R. and Scarlato, V. (2002b). Growth phase-dependent regulation of target gene promoters for binding of the essential orphan response regulator HP1043 of Helicobacter pylori. *J Bacteriol* **184,** 4800-4810.

Delany, I., Spohn, G., Rappuoli, R. and Scarlato, V. (2003). An anti-repression Fur operator upstream of the promoter is required for iron-mediated transcriptional autoregulation in Helicobacter pylori. *Mol Microbiol* **50,** 1329-1338.

Dhaenens, L., Szczebara, F., Van Nieuwenhuyse, S. and Husson, M.O. (1999). Comparison of iron uptake in different Helicobacter species. *Res Microbiol* **150,** 475-481.

Diaz-Mireles, E., Wexler, M., Sawers, G., Bellini, D., Todd, J.D. and Johnston, A.W. (2004). The Fur-like protein Mur of Rhizobium leguminosarum is a Mn(2+)-responsive transcriptional regulator. *Microbiology* **150,** 1447-1456.

Du, M.Q. and Isaccson, P.G. (2002). Gastric MALT lymphoma: from aetiology to treatment. *Lancet Oncol* **3,** 97-104.

Dubrac, S. and Touati, D. (2000). Fur positive regulation of iron superoxide dismutase in Escherichia coli: functional analysis of the sodB promoter. *J Bacteriol* **182,** 3802-3808.

Dunn, B.E., Cohen, H. and Blaser, M.J. (1997). Helicobacter pylori. *Clin Microbiol Rev* **10,** 720-741.

Ernst, F.D., Bereswill, S., Waidner, B., Stoof, J., Mader, U., Kusters, J.G., *et al.* (2005a). Transcriptional profiling of Helicobacter pylori Fur- and iron-regulated gene expression. *Microbiology* **151,** 533-546.

Ernst, F.D., Homuth, G., Stoof, J., Mader, U., Waidner, B., Kuipers, E.J., *et al.* (2005b). Iron-responsive regulation of the Helicobacter pylori iron-cofactored superoxide dismutase SodB is mediated by Fur. *J Bacteriol* **187,** 3687-3692.

Escolar, L., de Lorenzo, V. and Perez-Martin, J. (1997). Metalloregulation in vitro of the aerobactin promoter of Escherichia coli by the Fur (ferric uptake regulation) protein. *Mol Microbiol* **26,** 799-808.

Escolar, L., Perez-Martin, J. and de Lorenzo, V. (1998a). Binding of the fur (ferric uptake regulator) repressor of Escherichia coli to arrays of the GATAAT sequence. *J Mol Biol* **283,** 537-547.

Escolar, L., Perez-Martin, J. and de Lorenzo, V. (1998b). Coordinated repression in vitro of the divergent fepA-fes promoters of Escherichia coli by the iron uptake regulation (Fur) protein. *J Bacteriol* **180,** 2579-2582.

Escolar, L., Perez-Martin, J. and de Lorenzo, V. (1999). Opening the iron box: transcriptional metalloregulation by the Fur protein. *J Bacteriol* **181,** 6223-6229.

Escolar, L., Perez-Martin, J. and de Lorenzo, V. (2000). Evidence of an unusually long operator for the fur repressor in the aerobactin promoter of Escherichia coli. *J Biol Chem* **275,** 24709-24714.

Fassbinder, F., van Vliet, A.H., Gimmel, V., Kusters, J.G., Kist, M. and Bereswill, S. (2000). Identification of iron-regulated genes of Helicobacter pylori by a modified fur titration assay (FURTA-Hp). *FEMS Microbiol Lett* **184,** 225-229.

Feng, J.A., Johnson, R.C. and Dickerson, R.E. (1994). Hin recombinase bound to DNA: the origin of specificity in major and minor groove interactions. *Science* **263,** 348-355.

Ferguson, K.A. (1964). Starch-Gel Electrophoresis--Application to the Classification of Pituitary Proteins and Polypeptides. *Metabolism* **13,** SUPPL:985-1002.

Fuangthong, M., Herbig, A.F., Bsat, N. and Helmann, J.D. (2002). Regulation of the Bacillus subtilis fur and perR genes by PerR: not all members of the PerR regulon are peroxide inducible. *J Bacteriol* **184,** 3276-3286.

Gaballa, A. and Helmann, J.D. (1998). Identification of a zinc-specific metalloregulatory protein, Zur, controlling zinc transport operons in Bacillus subtilis. *J Bacteriol* **180,** 5815-5821.

Gancz, H., Censini, S. and Merrell, D.S. (2006). Iron and pH homeostasis intersect at the level of Fur regulation in the gastric pathogen Helicobacter pylori. *Infect Immun* **74,** 602-614.

Gao, H., Zhou, D., Li, Y., Guo, Z., Han, Y., Song, Y., *et al.* (2008). The iron-responsive Fur regulon in Yersinia pestis. *J Bacteriol* **190,** 3063-3075.

Gerrits, M.M., van Vliet, A.H., Kuipers, E.J. and Kusters, J.G. (2006). Helicobacter pylori and antimicrobial resistance: molecular mechanisms and clinical implications. *Lancet Infect Dis* **6,** 699-709.

Gonzalez de Peredo, A., Saint-Pierre, C., Latour, J.M., Michaud-Soret, I. and Forest, E. (2001). Conformational changes of the ferric uptake regulation protein upon metal activation and DNA binding; first evidence of structural homologies with the diphtheria toxin repressor. *J Mol Biol* **310,** 83-91.

Gordon, B.R., Li, Y., Wang, L., Sintsova, A., van Bakel, H., Tian, S., *et al.* (2010). Lsr2 is a nucleoid-associated protein that targets AT-rich sequences and virulence genes in Mycobacterium tuberculosis. *Proc Natl Acad Sci U S A.*

Grifantini, R., Sebastian, S., Frigimelica, E., Draghi, M., Bartolini, E., Muzzi, A., *et al.* (2003). Identification of iron-activated and -repressed Fur-dependent genes by transcriptome analysis of Neisseria meningitidis group B. *Proc Natl Acad Sci U S A* **100,** 9542-9547.

Hanahan, D. (1983). Studies on transformation of Escherichia coli with plasmids. *J Mol Biol* **166,** 557-580.

Hantke, K. (1981). Regulation of ferric iron transport in Escherichia coli K12: isolation of a constitutive mutant. *Mol Gen Genet* **182,** 288-292.

Hantke, K. (2001). Iron and metal regulation in bacteria. *Curr Opin Microbiol* **4,** 172-177.

Haran, T.E. and Mohanty, U. (2009). The unique structure of A-tracts and intrinsic DNA bending. *Q Rev Biophys* **42,** 41-81.

Husson, M.O., Legrand, D., Spik, G. and Leclerc, H. (1993). Iron acquisition by Helicobacter pylori: importance of human lactoferrin. *Infect Immun* **61,** 2694-2697.

Huth, J.R., Bewley, C.A., Nissen, M.S., Evans, J.N., Reeves, R., Gronenborn, A.M. and Clore, G.M. (1997). The solution structure of an HMG-I(Y)-DNA complex defines a new architectural minor groove binding motif. *Nat Struct Biol* **4,** 657-665.

Illingworth, D.S., Walter, K.S., Griffiths, P.L. and Barclay, R. (1993). Siderophore production and iron-regulated envelope proteins of Helicobacter pylori. *Zentralbl Bakteriol* **280,** 113-119.

Imlay, J.A., Chin, S.M. and Linn, S. (1988). Toxic DNA damage by hydrogen peroxide through the Fenton reaction in vivo and in vitro. *Science* **240,** 640-642.

Jacquamet, L., Aberdam, D., Adrait, A., Hazemann, J.L., Latour, J.M. and Michaud-Soret, I. (1998). X-ray absorption spectroscopy of a new zinc site in the fur protein from Escherichia coli. *Biochemistry* **37,** 2564-2571.

Jacquamet, L., Traore, D.A., Ferrer, J.L., Proux, O., Testemale, D., Hazemann, J.L., *et al.* (2009). Structural characterization of the active form of PerR: insights into the metal-induced activation of PerR and Fur proteins for DNA binding. *Mol Microbiol* **73,** 20-31.

Josenhans, C., Beier, D., Linz, B., Meyer, T.F. and Suerbaum, S. (2007). Pathogenomics of helicobacter. *Int J Med Microbiol* **297,** 589-600.

Joshi, R., Passner, J.M., Rohs, R., Jain, R., Sosinsky, A., Crickmore, M.A., *et al.* (2007). Functional specificity of a Hox protein mediated by the recognition of minor groove structure. *Cell* **131,** 530-543.

Joyce, E.A., Gilbert, J.V., Eaton, K.A., Plaut, A. and Wright, A. (2001). Differential gene expression from two transcriptional units in the cag pathogenicity island of Helicobacter pylori. *Infect Immun* **69,** 4202-4209.

Kim, J.L., Nikolov, D.B. and Burley, S.K. (1993a). Co-crystal structure of TBP recognizing the minor groove of a TATA element. *Nature* **365,** 520-527.

Kim, Y., Geiger, J.H., Hahn, S. and Sigler, P.B. (1993b). Crystal structure of a yeast TBP/TATA-box complex. *Nature* **365,** 512-520.

Kissinger, C.R., Liu, B.S., Martin-Blanco, E., Kornberg, T.B. and Pabo, C.O. (1990). Crystal structure of an engrailed homeodomain-DNA complex at 2.8 A resolution: a framework for understanding homeodomain-DNA interactions. *Cell* **63,** 579-590.

Larkin, M.A., Blackshields, G., Brown, N.P., Chenna, R., McGettigan, P.A., McWilliam, H., *et al.* (2007). Clustal W and Clustal X version 2.0. *Bioinformatics* **23,** 2947-2948.

Laub, M.T., McAdams, H.H., Feldblyum, T., Fraser, C.M. and Shapiro, L. (2000). Global analysis of the genetic network controlling a bacterial cell cycle. *Science* **290,** 2144-2148.

Lavrrar, J.L., Christoffersen, C.A. and McIntosh, M.A. (2002). Fur-DNA interactions at the bidirectional fepDGC-entS promoter region in Escherichia coli. *J Mol Biol* **322,** 983-995.

Lavrrar, J.L. and McIntosh, M.A. (2003). Architecture of a fur binding site: a comparative analysis. *J Bacteriol* **185,** 2194-2202.

Le Cam, E., Frechon, D., Barray, M., Fourcade, A. and Delain, E. (1994). Observation of binding and polymerization of Fur repressor onto operator-containing DNA with electron and atomic force microscopes. *Proc Natl Acad Sci U S A* **91,** 11816-11820.

Ledala, N., Pearson, S.L., Wilkinson, B.J. and Jayaswal, R.K. (2007). Molecular characterization of the Fur protein of Listeria monocytogenes. *Microbiology* **153,** 1103-1111.

Lee, H.J., Bang, S.H., Lee, K.H. and Park, S.J. (2007a). Positive regulation of fur gene expression via direct interaction of fur in a pathogenic bacterium, Vibrio vulnificus. *J Bacteriol* **189,** 2629-2636.

Lee, J.W. and Helmann, J.D. (2006a). Biochemical characterization of the structural Zn2+ site in the Bacillus subtilis peroxide sensor PerR. *J Biol Chem* **281,** 23567-23578.

Lee, J.W. and Helmann, J.D. (2006b). The PerR transcription factor senses H2O2 by metal-catalysed histidine oxidation. *Nature* **440,** 363-367.

Lee, J.W. and Helmann, J.D. (2007b). Functional specialization within the Fur family of metalloregulators. *Biometals* **20,** 485-499.

Li, T., Jin, Y., Vershon, A.K. and Wolberger, C. (1998). Crystal structure of the MATa1/MATalpha2 homeodomain heterodimer in complex with DNA containing an A-tract. *Nucleic Acids Res* **26,** 5707-5718.

Litwin, C.M. and Calderwood, S.B. (1993). Role of iron in regulation of virulence genes. *Clin Microbiol Rev* **6,** 137-149.

Liu, S.T. and Hong, G.F. (1998). Three-minute G + A specific reaction for DNA sequencing. *Anal Biochem* **255,** 158-159.

Madan Babu, M., Teichmann, S.A. and Aravind, L. (2006). Evolutionary dynamics of prokaryotic transcriptional regulatory networks. *J Mol Biol* **358,** 614-633.

Maier, R.J., Fu, C., Gilbert, J., Moshiri, F., Olson, J. and Plaut, A.G. (1996). Hydrogen uptake hydrogenase in Helicobacter pylori. *FEMS Microbiol Lett* **141,** 71-76.

Marais, A., Mendz, G.L., Hazell, S.L. and Megraud, F. (1999). Metabolism and genetics of Helicobacter pylori: the genome era. *Microbiol Mol Biol Rev* **63,** 642-674.

Marshall, B.J. and Warren, J.R. (1984). Unidentified curved bacilli in the stomach of patients with gastritis and peptic ulceration. *Lancet* **1,** 1311-1315.

Masse, E., Salvail, H., Desnoyers, G. and Arguin, M. (2007). Small RNAs controlling iron metabolism. *Curr Opin Microbiol* **10,** 140-145.

Megraud, F. and Lamouliatte, H. (2003). Review article: the treatment of refractory Helicobacter pylori infection. *Aliment Pharmacol Ther* **17,** 1333-1343.

Mehta, N., Olson, J.W. and Maier, R.J. (2003). Characterization of Helicobacter pylori nickel metabolism accessory proteins needed for maturation of both urease and hydrogenase. *J Bacteriol* **185,** 726-734.

Merrell, D.S., Thompson, L.J., Kim, C.C., Mitchell, H., Tompkins, L.S., Lee, A. and Falkow, S. (2003). Growth phase-dependent response of Helicobacter pylori to iron starvation. *Infect Immun* **71,** 6510-6525.

Mobley, H.L.T., Mendz, G.L. and Hazell, S.L. (2001) Helicobacter pylori: Physiology and Genetics, ASM Press, pp. 626.

Muhsen, K. and Cohen, D. (2008). Helicobacter pylori infection and iron stores: a systematic review and meta-analysis. *Helicobacter* **13,** 323-340.

Nomura, A., Stemmermann, G.N., Chyou, P.H., Perez-Perez, G.I. and Blaser, M.J. (1994). Helicobacter pylori infection and the risk for duodenal and gastric ulceration. *Ann Intern Med* **120,** 977-981.

Oh, J.D., Kling-Backhed, H., Giannakis, M., Xu, J., Fulton, R.S., Fulton, L.A., *et al.* (2006). The complete genome sequence of a chronic atrophic gastritis Helicobacter pylori strain: evolution during disease progression. *Proc Natl Acad Sci U S A* **103,** 9999-10004.

Olson, J.W. and Maier, R.J. (2002). Molecular hydrogen as an energy source for Helicobacter pylori. *Science* **298,** 1788-1790.

Orchard, K. and May, G.E. (1993). An EMSA-based method for determining the molecular weight of a protein--DNA complex. *Nucleic Acids Res* **21,** 3335-3336.

Panina, E.M., Mironov, A.A. and Gelfand, M.S. (2001). Comparative analysis of FUR regulons in gamma-proteobacteria. *Nucleic Acids Res* **29,** 5195-5206.

Parsonnet, J., Hansen, S., Rodriguez, L., Gelb, A.B., Warnke, R.A., Jellum, E., *et al.* (1994). Helicobacter pylori infection and gastric lymphoma. *N Engl J Med* **330,** 1267-1271.

Patzer, S.I. and Hantke, K. (1998). The ZnuABC high-affinity zinc uptake system and its regulator Zur in Escherichia coli. *Mol Microbiol* **28,** 1199-1210.

Pecqueur, L., D'Autreaux, B., Dupuy, J., Nicolet, Y., Jacquamet, L., Brutscher, B., *et al.* (2006). Structural changes of Escherichia coli ferric uptake regulator during metal-dependent dimerization and activation explored by NMR and X-ray crystallography. *J Biol Chem* **281,** 21286-21295.

Peek, R.M., Jr. and Blaser, M.J. (2002). Helicobacter pylori and gastrointestinal tract adenocarcinomas. *Nat Rev Cancer* **2,** 28-37.

Pennella, M.A. and Giedroc, D.P. (2005). Structural determinants of metal selectivity in prokaryotic metal-responsive transcriptional regulators. *Biometals* **18,** 413-428.

Pohl, E., Haller, J.C., Mijovilovich, A., Meyer-Klaucke, W., Garman, E. and Vasil, M.L. (2003). Architecture of a protein central to iron homeostasis: crystal structure and spectroscopic analysis of the ferric uptake regulator. *Mol Microbiol* **47,** 903-915.

Remenyi, A., Tomilin, A., Pohl, E., Lins, K., Philippsen, A., Reinbold, R., *et al.* (2001). Differential dimer activities of the transcription factor Oct-1 by DNA-induced interface swapping. *Mol Cell* **8,** 569-580.

Rohs, R., West, S.M., Sosinsky, A., Liu, P., Mann, R.S. and Honig, B. (2009). The role of DNA shape in protein-DNA recognition. *Nature* **461,** 1248-1253.

Ross, W., Ernst, A. and Gourse, R.L. (2001). Fine structure of E. coli RNA polymerase-promoter interactions: alpha subunit binding to the UP element minor groove. *Genes Dev* **15,** 491-506.

Sabogal, A., Lyubimov, A.Y., Corn, J.E., Berger, J.M. and Rio, D.C. (2010). THAP proteins target specific DNA sites through bipartite recognition of adjacent major and minor grooves. *Nat Struct Mol Biol* **17,** 117-123.

Sachs, G., Weeks, D.L., Melchers, K. and Scott, D.R. (2003). The gastric biology of Helicobacter pylori. *Annu Rev Physiol* **65,** 349-369.

Sambrook, J., Fritsch, E.F. and Maniatis, T. (1989) Molecular Cloning: A Laboratory Manual Cold Spring Harbour, New York, USA, Cold Spring Harbor Laboratory Press.

Scarlato, V., Delany, I., Spohn, G. and Beier, D. (2001). Regulation of transcription in Helicobacter pylori: simple systems or complex circuits? *Int J Med Microbiol* **291,** 107-117.

Schneider, B.D. and Leibold, E.A. (2000). Regulation of mammalian iron homeostasis. *Curr Opin Clin Nutr Metab Care* **3,** 267-273.

Sharma, C.M., Hoffmann, S., Darfeuille, F., Reignier, J., Findeiss, S., Sittka, A., *et al.* (2010). The primary transcriptome of the major human pathogen Helicobacter pylori. *Nature*.

Shen, A., Higgins, D.E. and Panne, D. (2009). Recognition of AT-rich DNA binding sites by the MogR repressor. *Structure* **17,** 769-777.

Silver, S. and Phung, L.T. (1996). Bacterial heavy metal resistance: new surprises. *Annu Rev Microbiol* **50,** 753-789.

Stefl, R., Wu, H., Ravindranathan, S., Sklenar, V. and Feigon, J. (2004). DNA A-tract bending in three dimensions: solving the dA4T4 vs. dT4A4 conundrum. *Proc Natl Acad Sci U S A* **101,** 1177-1182.

Studier, F.W. and Moffatt, B.A. (1986). Use of bacteriophage T7 RNA polymerase to direct selective high-level expression of cloned genes. *J Mol Biol* **189,** 113-130.

Suerbaum, S., Josenhans, C. and Labigne, A. (1993). Cloning and genetic characterization of the Helicobacter pylori and Helicobacter mustelae flaB flagellin genes and construction of H. pylori flaA- and flaB-negative mutants by electroporation-mediated allelic exchange. *J Bacteriol* **175,** 3278-3288.

Telford, J.L., Ghiara, P., Dell'Orco, M., Comanducci, M., Burroni, D., Bugnoli, M., *et al.* (1994). Gene structure of the Helicobacter pylori cytotoxin and evidence of its key role in gastric disease. *J Exp Med* **179,** 1653-1658.

Thompson, J.D., Higgins, D.G. and Gibson, T.J. (1994). CLUSTAL W: improving the sensitivity of progressive multiple sequence alignment through sequence weighting, position-specific gap penalties and weight matrix choice. *Nucleic Acids Res* **22,** 4673-4680.

Tiss, A., Barre, O., Michaud-Soret, I. and Forest, E. (2005). Characterization of the DNA-binding site in the ferric uptake regulator protein from Escherichia coli by UV crosslinking and mass spectrometry. *FEBS Lett* **579,** 5454-5460.

Tomb, J.F., White, O., Kerlavage, A.R., Clayton, R.A., Sutton, G.G., Fleischmann, R.D., *et al.* (1997). The complete genome sequence of the gastric pathogen Helicobacter pylori. *Nature* **388,** 539-547.

Tsuda, M., Karita, M., Morshed, M.G., Okita, K. and Nakazawa, T. (1994). A urease-negative mutant of Helicobacter pylori constructed by allelic exchange mutagenesis lacks the ability to colonize the nude mouse stomach. *Infect Immun* **62,** 3586-3589.

Tullius, T. (2009). Structural biology: DNA binding shapes up. *Nature* **461,** 1225-1226.

Tullius, T.D. and Dombroski, B.A. (1986). Hydroxyl radical "footprinting": high-resolution information about DNA-protein contacts and application to lambda repressor and Cro protein. *Proc Natl Acad Sci U S A* **83,** 5469-5473.

Tullius, T.D., Dombroski, B.A., Churchill, M.E. and Kam, L. (1987). Hydroxyl radical footprinting: a high-resolution method for mapping protein-DNA contacts. *Methods Enzymol* **155,** 537-558.

Van Dyke, M.W., Hertzberg, R.P. and Dervan, P.B. (1982). Map of distamycin, netropsin, and actinomycin binding sites on heterogeneous DNA: DNA cleavage-inhibition patterns with methidiumpropyl-EDTA.Fe(II). *Proc Natl Acad Sci U S A* **79,** 5470-5474.

van Vliet, A., Bereswill, S. and Kusters, J.G. (2001a) Ion metabolism and trasport. In *Helicobacter pylori: Physiology and genetics*, H.L. Mobley, G.L. Mendz, S.L. Hazell (eds.). Washington DC, ASM Press.

van Vliet, A.H., Kuipers, E.J., Stoof, J., Poppelaars, S.W. and Kusters, J.G. (2004). Acid-responsive gene induction of ammonia-producing enzymes in Helicobacter pylori is mediated via a metal-responsive repressor cascade. *Infect Immun* **72,** 766-773.

van Vliet, A.H., Kuipers, E.J., Waidner, B., Davies, B.J., de Vries, N., Penn, C.W., *et al.* (2001b). Nickel-responsive induction of urease expression in Helicobacter pylori is mediated at the transcriptional level. *Infect Immun* **69,** 4891-4897.

van Vliet, A.H., Stoof, J., Poppelaars, S.W., Bereswill, S., Homuth, G., Kist, M., *et al.* (2003). Differential regulation of amidase- and formamidase-mediated ammonia production by the Helicobacter pylori fur repressor. *J Biol Chem* **278,** 9052-9057.

van Vliet, A.H., Stoof, J., Vlasblom, R., Wainwright, S.A., Hughes, N.J., Kelly, D.J., *et al.* (2002). The role of the Ferric Uptake Regulator (Fur) in regulation of Helicobacter pylori iron uptake. *Helicobacter* **7,** 237-244.

Vitale, S., Fauquant, C., Lascoux, D., Schauer, K., Saint-Pierre, C. and Michaud-Soret, I. (2009). A ZnS(4) structural zinc site in the Helicobacter pylori ferric uptake regulator. *Biochemistry* **48,** 5582-5591.

Weinberg, E.D. (1978). Iron and infection. *Microbiol Rev* **42,** 45-66.

Worst, D.J., Maaskant, J., Vandenbroucke-Grauls, C.M. and Kusters, J.G. (1999). Multiple haem-utilization loci in Helicobacter pylori. *Microbiology* **145 (Pt 3),** 681-688.

Xiang, Z., Censini, S., Bayeli, P.F., Telford, J.L., Figura, N., Rappuoli, R. and Covacci, A. (1995). Analysis of expression of CagA and VacA virulence factors in 43 strains of Helicobacter pylori reveals that clinical isolates can be divided into

two major types and that CagA is not necessary for expression of the vacuolating cytotoxin. *Infect Immun* **63,** 94-98.

Xiao, B., Li, W., Guo, G., Li, B., Liu, Z., Jia, K., *et al.* (2009a). Identification of small noncoding RNAs in Helicobacter pylori by a bioinformatics-based approach. *Curr Microbiol* **58,** 258-263.

Xiao, B., Li, W., Guo, G., Li, B.S., Liu, Z., Tang, B., *et al.* (2009b). Screening and identification of natural antisense transcripts in Helicobacter pylori by a novel approach based on RNase I protection assay. *Mol Biol Rep* **36,** 1853-1858.

Xiong, A., Singh, V.K., Cabrera, G. and Jayaswal, R.K. (2000). Molecular characterization of the ferric-uptake regulator, fur, from Staphylococcus aureus. *Microbiology* **146 (Pt 3),** 659-668.